UNIVERSITY OF CYPRUS

FACULTY OF PURE AND APPLIED SCIENCES

DEPARTMENT OF BIOLOGICAL SCIENCES

EMBRYOLOGY/DEVELOPMENTAL GENETICS AND STEM CELL LABORATORY

A NEW ROLE FOR TROPHOBLAST AND THE GENE *Ets2* IN EMBRYO GASTRULATION.

POLYDOROU CHRISTIANA

Ph.D. THESIS

May 2013

ΠΑΝΕΠΙΣΤΗΜΙΟ ΚΥΠΡΟΥ

ΣΧΟΛΗ ΘΕΤΙΚΩΝ ΚΑΙ ΕΦΑΡΜΟΣΜΕΝΩΝ ΕΠΙΣΤΗΜΩΝ

ΤΜΗΜΑ ΒΙΟΛΟΓΙΚΩΝ ΕΠΙΣΤΗΜΩΝ

ΕΡΓΑΣΤΗΡΙΟ ΕΜΒΡΥΟΛΟΓΙΑΣ/ΑΝΑΠΤΥΞΙΑΚΗΣ ΓΕΝΕΤΙΚΗΣ ΚΑΙ ΒΛΑΣΤΟΚΥΤΤΑΡΩΝ

ΝΕΟΙ ΡΟΛΟΙ ΤΗΣ ΤΡΟΦΟΒΛΑΣΤΗΣ ΚΑΙ ΤΟΥ ΓΟΝΙΔΙΟΥ *Ets2* ΚΑΤΑ ΤΗΝ ΓΑΣΤΡΙΔΙΩΣΗ ΤΩΝ ΕΜΒΡΥΩΝ ΠΟΝΤΙΚΟΥ.

ΠΟΛΥΔΩΡΟΥ ΧΡΙΣΤΙΑΝΑ

ΔΙΔΑΚΤΟΡΙΚΗ ΔΙΑΤΡΙΒΗ

Μάιος 2013

Περίληψη

Η γαστριδίωση, η οποία προηγείται της οργανογένεσης είναι μια από τις πιο σημαντικές διαδικασίες κατά την εμβρυογένεση. Ξεκινά με την δημιουργία της αρχικής λωρίδας (primitive streak, PS) κατά την εμβρυονική μέρα 6.5 προκειμένου να δημιουργηθούν οι τρεις εμβρυονικές στοιβάδες: το μεσόδερμα, το ενδόδερμα και το εξώδερμα. Για την έναρξη της γαστριδίωσης χρειάζονται σήματα τα οποία προέρχονται από τους δύο εξωεμβρυονικούς ιστούς: το σπλαχνικό ενδόδερμα (visceral endoderm) το οποίο αποτελεί πρόγονο ιστό του αμνιακού σάκου και συμβάλλει στη δημιουργία του ενδοδέρματος και το εξτραεμβρυονικό εκτόδερμα (EXE) το οποίο είναι ο πρόγονος ιστός του μεγαλύτερου τμήματος του πλακούντα που ονομάζεται τροφοβλάστη. Παρόλο που έχει δειχθεί ότι σήματα τα οποία προέρχονται από το εξτραεμβρυονικό εκτόδερμα χρειάζονται για την έναρξη της γαστριδίωσης, παραμένει άγνωστο κατά πόσο αυτά τα σήματα επηρεάζουν την πορεία της γαστριδίωσης. Ο κύριος στόχος αυτής της διατριβής είναι η χρησιμοποίηση knockout ποντικών για το γονίδιο *Ets2*, τα ονομαζόμενα *Ets2* type-II mutant έμβρυα για τον προσδιορισμό νέων επιδράσεων του EXE στις διαδικασίες τις γαστριδίωσης μετά την έναρξη της. Τα αποτελέσματα μας έχουν δείξει για πρώτη φορά ότι ότι τα σήματα που προέρχονται από το EXE χρειάζονται για την συνέχιση της γαστριδίωσης στα έμβρυα αφού επηρεάζει: την επιμύκηνση του PS, την ολοκλήρωση της μετατροπής των PS επιθηλιακών κυττάρων σε μεσεγχυματικά (EMT), καθώς και την ανάπτυξη παραγώγων του PS όπως για παράδειγμα του node. Παρουσιάζονται αποδείξεις και προτείνουμε ένα μοντέλο το οποίο παρέχει μια γενετική εξήγηση για το πώς η έκφραση του *Ets2* στο EXE, ρυθμίζει αυτά τα γεγονότα.

ABSTRACT

Gastrulation, a prerequisite for organogenesis, is one of the most fundamental aspects of embryogenesis. During gastrulation the initially amorphous one-layered and unpatterned epiblast transforms into a fully patterned three-layered entity that allows correct organogenesis to take place. Gastrulation begins with the formation of the Primitive Streak (PS), at the posterior side of the epiblast, which in mice starts 6.5 days after fertilization (E6.5). Mammalian gastrulation requires signals from two extraembryonic tissues: the visceral endoderm (which is the progenitor of yolk-sac endoderm and also contributes to the formation of the definitive endoderm) and the extraembryonic ectoderm (EXE) trophoblast (progenitor of placental trophoblast). Although EXE trophoblast signals the embryo for PS initiation, it is unknown whether it also signals for the progression of gastrulation after PS initiation. The main focus of this project was to use homozygous gene knockout mice for the transcription factor *Ets2* (the *Ets2* type-II mutants) as an *in vivo* model for discovering, new fundamental gastrulation events after gastrulation initiation that require EXE trophoblast signaling. We show for the first time that trophoblast signalling is required *in vivo* for fundamental events during gastrulation such as: PS elongation, completion of intraembryonic mesoderm epithelial–mesenchymal transition (EMT) and the development of anterior primitive streak derivatives such as the node. We present evidence and propose a model that provides a genetic explanation as to how *Ets2*-dependent EXE trophoblast signaling mediates these events within the epiblast.

MEMBERS OF THE EXAMINING COMMITTEE

Dr. Georgiades Pantelis, Assistant Professor, Department of Biological Sciences (Research Advisor), University of Cyprus.

Dr. Paris Skourides, Assistant Professor, Department of Biological Sciences, University of Cyprus.

Dr. Kallayanee Chawengsaksophak, Head of Embryogenesis Unit, Insitute of Molecular Genetics ASCR, Prague, Czech Rebublic.

Dr. Stavros Malas, Head, Developmental and Functional Genetics Group, Cyprus Institute of Neurology and Genetics.

Dr. Katerina Strati, Lecturer, Department of Biological Sciences, University of Cyprus.

Acknowledgements

At first and foremost I would like to thank my advisor Dr. Pantelis Georgiades for giving me the opportunity to achieve one of my major goals. I appreciate all his guidance, his valuable advices and I am thankful helping me during the writing of my thesis. I would like to thank all the members of the examining committee; Dr. Kallayanne Chawengsaksophak, Dr. Stavros Malas, Dr.Paris Skourides, Dr. Katerina Strati and Dr. Pantelis Georgiades for their time, insightful question and evaluation of my PhD thesis. I owe a huge thank to all members of Pantelis Georgiades laboratory especially Christophoros Odiatis, Katerina Drakou, Stavros Nikolaou for their excellent collaboration, understanding and support as without their help the completion of my doctoral thesis would be an impossible feat. Also, I would like to thank Dr. Paris Skourides and his lab members especially Dr. Panayiota Stylianou and Dr. Andriani Ioannou for helping me with fluorescent and confocal microscopy. Dr..Panos Papageorgis for his advices for the Real Time PCR epxreriments and Dr. Antonis Kirmizis. Also, I would like to thank the University of Cyprus and the Cyprus Research Promotion Foundation Organization (ΠΕΝΕΚ/0609/89) for funding. I would also like to thank my friends for their understanding and especially their patience. Last but not least, I am extremely thankful to my family and especially my parents who supported and encouraged me in every way possible.

TABLE OF CONTENTS

A. List of tables.

B. List of figures.

Abbreviations

A-P: Anterior-Posterior axis.

AME: Anterior Mesendoderm.

AN: Anterior Notochord.

APS: Anterior Primitive Streak.

AVE: Anterior Visceral Endoderm.

DE: Defenitive Endoderm

DVE: Distal Visceral Endoderm.

E6.75: Embryonic day 6.75 (6.75 days after fertilization).

Early-PS: Early Primitive Streak stage, E6.5.

EE: Embryonic Ectoderm (Epiblast).

EGO: Early Gartula Organizer.

EMT: Epithelial-to-mesenchymal transition.

EPC: Ectoplacenta Cone.

ES cells: Embryonic stem cells.

EXE: Extraembryonic ectoderm.

MET: Mesechymal to epithelial trasition.

MGO: Mid Gastrula Organizer.

Mid-PS: Mid Primitive Streak stage, E6.75-E7.0.

mTE: Mural trophectoderm.

Late PS: Late Primitive Streak stage, E7.5-E7.75.

PBS: Phosphate buffered saline.

P-D: Proximal-Distal.

PrE: Primitive Endoderm.

pTE: Polar trophectoderm

PP: Prechordal plate.

PS: Primitive Streak.

PPT: Pre-placenta trophoblast.

RNA ISH: RNA *in-situ* hybridization.

TE: Trophectoderm.

TGCs: Trophoblast Giant cells.

TS cells: Trophoblast Stem Cells

VE: Visceral Endoderm.

wt embryos: Wild-type embryos.

Chapter 1

INTRODUCTION

1.1 Overview of early mouse embryo development.

In mice, the gestation period is about 19.5 days. After fertilization of the oocyte, the fertilized mouse egg reaches the eight-cell stage after three rounds of cell divisions, where it is at the morula stage. At embryonic day (E) E3.5, the morula transforms into a blastocyst, which consists of two distinct lineages: the inner cell mass (ICM) and the trophectoderm (TE) (*Fig.1*). After implantation, the polar TE (that part of TE in contact with the ICM) gives rise to the extraembryonic ectoderm (EXE) [which, together with its first derivative, the ectoplacental cone (EPC) constitute the progenitors of the major tissue of the definitive placenta called the trophoblast], whilst the ICM generates the rest of the tissues of the conceptus (*Tam and Behringer 1997; Stern 2004; Tam and Loebel 2007*)

By E4.5 the ICM initially differentiates into the primitive ectoderm (a multilayered cuboidal epithelium) and the primitive endoderm (PrE) and by E4.75 the mouse blastocyst implants into the uterus. At E5.0 the primitive ectoderm, undergoes cavitation and generates the proamniotic cavity. This cavitation transforms the primitive ectoderm into a single-cell-thick columnar epithelium called the epiblast which is the tissue from which three embryonic germ layers (ectoderm, mesoderm and endoderm) arise. On the other hand the PrE forms the visceral endoderm (VE) and parietal endoderm which are both extraembryonic tissues *(Tam and Behringer 1997*). Thus, at E5.0 the conceptus contains three tissues: EXE trophoblast at the proximal site of the embryo, the epiblast at the distal site of the embryo and the VE which surrounds both EXE and epiblast (*Perea-Gomez, Rhinn et al. 2001*). The epiblast as mentioned is the tissue that gives rise to the entire fetus whereas the EXE and VE support the intra-uterine development of the mouse embryo and also act as signaling sources during gastrulation (*Rossant and Tam 2009*). At E5.5 the morphology of the conceptus changes further due to the appearance of (a) the EPC from the mesometrial edge of the EXE, and (b) a thickening in the VE region at the distal tip of the embryo, the so-called distal VE (DVE). At this stage the conceptus has a clear proximal-distal (P-D) axis and the DVE is not symmetrically localized at the distal tip, but tilted more to one side, which is the future anterior side of the embryo. This is the first morphological asymmetry within the VE along its Anterior-Posterior (A-P) axis. By E6.5 the DVE becomes displaced anteriorly and when it does, it is known as the anterior VE (AVE) and lies underneath the anterior epiblast (*Thomas and Beddington 1996; Rivera-Perez, Mager et al. 2003; Srinivas, Rodriguez et al. 2004*) (*Fig.2*).

<u>Figure 1:</u> Pre-implantation development of the mouse embryo.

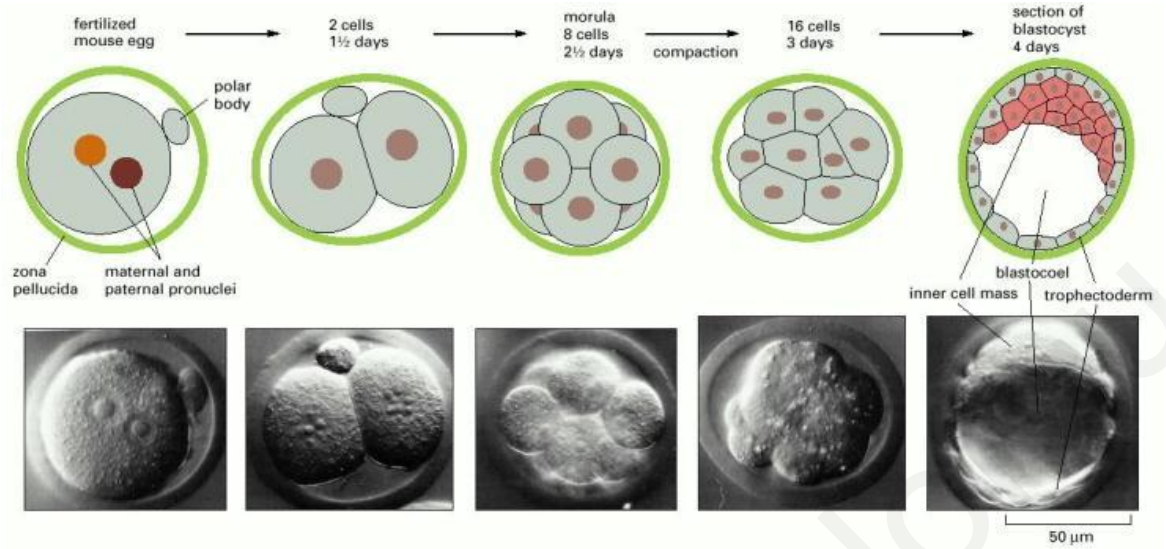

Molecular Biology of the Cell. *4th* edition. *Alberts B, Johnson A, Lewis J, et al.* (2002).

Gastrulation, a prerequisite for organogenesis, is the process during which the initially amorphous one-layered and un-patterned epiblast transforms into a fully patterned three-layered entity is one of the most fundamental aspects of embryogenesis. It begins with the formation of the primitive streak (PS) and PS-derived mesoderm, at the posterior side of the epiblast at E6.5 stage (*Fig.2*). Gastrulation involves morphogenetic movements and cell differentiations for the production of the three embryonic germ layers: ectoderm, mesoderm and endoderm. During gastrulation the epiblast cells at first become specified, then differentiate into specialized cell types and migrate towards their final destinations *(Lawson, Meneses et al. 1991; Tam and Behringer 1997; Tam and Loebel 2007*)

<u>Figure 2</u>: Mouse embryo development from blastocyst to gastrulation initiation (E6.5).

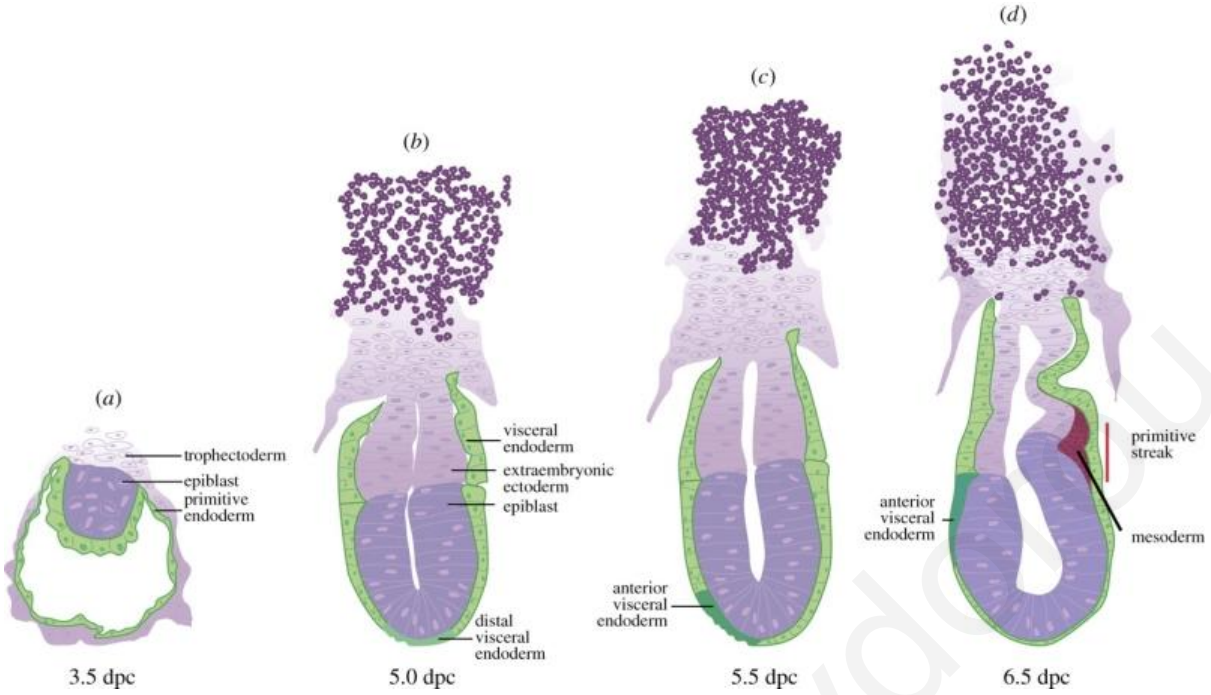

*(a)*The blastocyst consists of the inner cell mass (ICM)/epiblast, the trophectoderm (TE) and the primitive endoderm. (*b*) E5.0 mouse embryo with distal visceral endoderm, and by (c) E5.5 with anterior visceral endoderm. (d) Early-streak embryo at E6.5, with formation of the primitive streak and the nascent mesoderm at the posterior side of the embryo. dpc: days post conception (*Arkell and Tam 2012*)

As the gastrulation proceeds the PS progressively elongates anteriorly so that it becomes fully extended by E7.5 (a stage when the PS reaches the distal tip of the embryo). At this stage, the epiblast PS cells can be divided into three different regions (posterior, middle and anterior PS cells) based on their fate after they exit the PS (*Lawson, Meneses et al. 1991*): the posterior region contains cells destined to form the extraembryonic mesoderm, the middle part contains cells destined for lateral mesoderm, and the anterior part contains anterior axial mesoderm (midline) progenitors. This midline constitutes the mesoderm part of the prechordal plate (PP) and the anterior notochord (AN), which are part of the anterior axial mesendoderm (AME). The definitive endoderm (DE) progenitor cells ingress through the anterior PS at the mid-PS (E6.75-E7.0) stage and are fated to contribute to the epithelium that lines the lumen of the gut and its associated organs such as liver, pancreas and thyroid. The anterior DE and the mesoderm of PP/AN are known as anterior axial mesendoderm (AME) (*Tam and Behringer 1997; Kinder, Tsang et al. 1999; Kinder, Loebel et al. 2001; Robb and Tam 2004; Yamanaka, Tamplin et al. 2007; Kwon, Viotti et al. 2008; Arnold and Robertson 2009*).

Also, by E7.5 stage, at the most anterior part of the PS there is a morphological recognizable structure called the node. The node consists of a two-layered columnar

epithelium and is situated between the most anterior region of PS and the posterior end of the AME, at the distal tip of the embryo (*Fig.3,* 7.5dpc) (*Kinder, Tsang et al. 1999; Kinder, Loebel et al. 2001; Perea-Gomez, Rhinn et al. 2001; Robb and Tam 2004*). Anterior to the node, cells move medially and intercalate in the midline, thereby increasing embryonic length relative to width and hence by E7.5-E7.75 stage, the embryo is becoming wider than it is long. By E8.0-E8.5 stage the mouse embryo undergoes a conformational change leading to ventral closure of the gut, with the PS situated in the caudal part of the embryo, with a distinct anterior neural plate and five pairs of somites (*Copp, Greene et al. 2003*). Finally, by 9 days after fertilization gastrulation is completed.

<u>Figure 3:</u> Mouse embryo development from E6.0 to E7.5 stages.

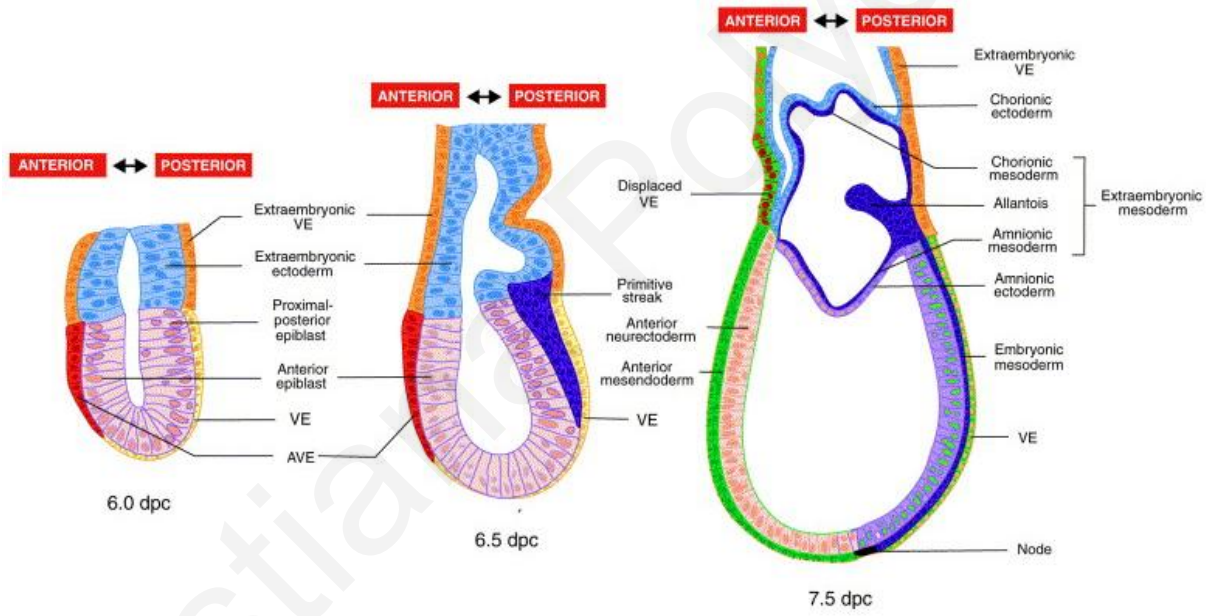

dpc: days post conception *(Lu, Brennan et al. 2001)*

1.2 An Overview of mouse embryo gastrulation: primitive streak (PS) initiation and mesoderm formation.

PS formation, which takes place around E6.5 at the posterior end of the epiblast signifies the beginning of gastrulation. Within the PS, the epiblast cells experience an epithelial-to-mesenchymal transition (EMT), exit the epiblast and form the mesoderm and definitive endoderm (DE) layers whilst the ectoderm is produced from the epiblast cells that do not ingress through the PS (*Lawson, Meneses et al. 1991; Tam and Behringer 1997; Robb and Tam 2004; Arnold and Robertson 2009*). A more recent study using live imaging

analysis showed that the mouse PS forms *in situ* by progressive EMT beginning in the posterior epiblast by E6.5 stage and then the PS elongates anteriorly (*Williams, Burdsal et al. 2012*). They showed that the area in which the EMT starts (and hence where the PS begins) is the area where the epiblast cells lose their basal lamina, become mesenchymal, ingress through the streak and migrate away from it anteriorly to form mesoderm (*Williams, Burdsal et al. 2012*). The mesoderm is expanding laterally from both sides of the PS ("mesodermal wings") and has a distinguishable morphology. The mesodermal cells are large stellate-shaped cells exhibiting many filopodia so as to be able to migrate away from the streak (*Tam, Williams et al. 1993*). As gastrulation proceeds, the mesodermal cells adopt different cell fates depending on the time and the site from which they leave the streak (*Kinder, Tsang et al. 1999*). Fate mapping studies of the PS showed that the first cells exiting from the posterior segment of the streak give rise to extraembryonic mesoderm. The axial and paraxial mesoderm arises from the anterior region of the PS and the lateral mesoderm from the mid-segment of the PS (*Lawson, Meneses et al. 1991; Tam and Behringer 1997; Arnold and Robertson 2009*). The mesoderm germ layer finally produces all mesoderm-derived tissues including the skeletal muscle, the skeleton, the urogenital system, the heart, blood, the kidney, and the spleen.

Gene function studies showed several genes whose expression in the epiblast is required for PS initiation. An example of such a gene is *Nodal*, a secreted factor that is a member of the TGFβ superfamily whose expression is required in the epiblast for the induction of PS and mesoderm (*Conlon, Lyons et al. 1994; Brennan, Lu et al. 2001*). *Nodal* null mutants lack a PS and mesoderm (*Conlon, Lyons et al. 1994; Brennan, Lu et al. 2001*). One other gene that is required in the epiblast for PS initiation is the signalling molecule Cripto, that is a member of the EGF-CFC family and also it regulates *Nodal* expression levels within the epiblast. *Cripto* null mutations showed absence of PS and mesoderm formation and their AVE was remained distal indicating a role for *Cripto* expression within the epiblast for correct formation of the PS and mesoderm (*Ding, Yang et al. 1998*). Another gene that is required in the epiblast for correct PS and mesoderm formation is *Wnt3*, a secreted signaling molecule. Homozygous mutants for *Wnt3* do not form a PS and mesoderm (*Liu, Wakamiya et al. 1999*), suggesting that its expression in the epiblast is required for gastrulation initiation. Double knockout homozygous mutant embryos, for the Wnt co-receptors *Lrp5* and *Lrp6*, showed absence of PS and mesoderm formation. As these defects were very similar to *Wnt3* null phenotype (*Liu, Wakamiya et al. 1999*) it has been suggested that Lrp5/6 function may

be is required for the reception of Wnt3 signaling at the posterior side of the epiblast, so as to be able to form PS and mesoderm (*Kelly, Pinson et al. 2004*).

In order for PS cells to exit the PS and form the mesoderm and definitive endoderm layers, PS epiblast cells have to undergo an epithelial to mesenchymal transition (EMT) which results in the transformation of the epithelial epiblast cells into mesenchymal ones (*Tam and Behringer 1997; Robb and Tam 2004; Arnold and Robertson 2009; Kalluri and Weinberg 2009*). It is known that epithelial cells (including epiblast cells) have an apical-basal polarity with their basal surface being attached to a basement membrane. They are closely attached to each other by (a) adherens junctions which contain E-cadherin (Chd1) in complexes with catenins (b) tight junctions and (c) desmosomes (*Hay 2005*). On the other hand, mesenchymal cells are not closely attached to a basement membrane or to each other and usually contain numerous filopodia, that acquire for migration (*Hay 2005*). In mouse embryos once the epiblast cells enter the PS region they undergo EMT. As a result they loose their apical-basal polarity, detach from the basement membrane and undergo cytoskeletal rearrangements that allow them to migrate away from the PS to reach their destinations (*Arnold and Robertson 2009*). As mentioned above, E-cadherin is an epithelial marker that mediates adhesive interactions between epithelial cells by being a component of adherens junctions. In mouse embryos E-cadherin is expressed in all epiblast cells, but becomes downregulated in those that undergo EMT and is absent from all PS-derived mesenchymal cells. This downregulation is necessary for the completion of PS EMT so as to allow migration of these mesenchymal cells between the epiblast and the VE (*Fig.4*) (*Zohn, Li et al. 2006*). This is consistent with *ex vivo* experiments where disruption of E-cadherin function in mouse epiblast explants was shown to be sufficient to cause EMT (*Burdsal, Damsky et al. 1993*). A signaling cascade that involves the zing-finger transcriptional repressor Snail causes the downregulation of E-cadherin from adherens junctions by binding directly to its promoter to represses its expression (*Arnold, Hofmann et al. 2008*). The *Snail* gene is expressed in epiblast cells undergoing EMT, as well as in the mesoderm cells that migrate away from the PS (*Shook and Keller 2003; Arnold, Hofmann et al. 2008*). Mouse embryos lacking a functional *Snail* fail to complete their EMT: although epiblast cells loose their basal lamina, they fail to downregulate E-Cadherin and do not exit the PS (*Carver, Jiang et al. 2001*). Furthermore *Eomes* (which is expressed in PS epiblast and newly formed mesoderm during early streak mouse embryo) is required in epiblast for complete EMT, as its epiblast-specific knockout results in persistence of E-cadherin in PS epiblast cells and their failure to migrate away from the PS (*Arnold, Hofmann et al. 2008*). On the other hand,

Fgf8 is required in the epiblast for migration of mesoderm cells away from the PS in an EMT-independent way because although PS-derived mesenchymal cells form in *Fgf8* null embryos, they fail to migrate (*Sun, Meyers et al. 1999*). Moreover, epiblast-specific knockout of *Wnt3* (a secreted signaling molecule expressed in the PS and posterior VE) resulted in failure of mesoderm to migrate away from the PS (*Tortelote, Hernandez-Hernandez et al. 2013*). This, taken together with the finding that in embryonic stem (ES) cell-derived embryoid bodies (ES, which are pluripotent stem cells derived from the ICM of the blastocyst and have the ability to differentiate into all derivatives of the three germ layers: ectoderm, endoderm, and mesoderm), *Wnt3* promotes mesoderm EMT by upregulating *Snail* expression and downregulating E-cadherin (*ten Berge, Koole et al. 2008*), suggest that *in vivo* *Wnt3* expression in the PS mediates mesoderm EMT by downregulating E-Cadherin *via* induction and/or maintenance of PS *Snail* expression.

<u>Figure 4:</u> Epithelial to mesenchymal transition.

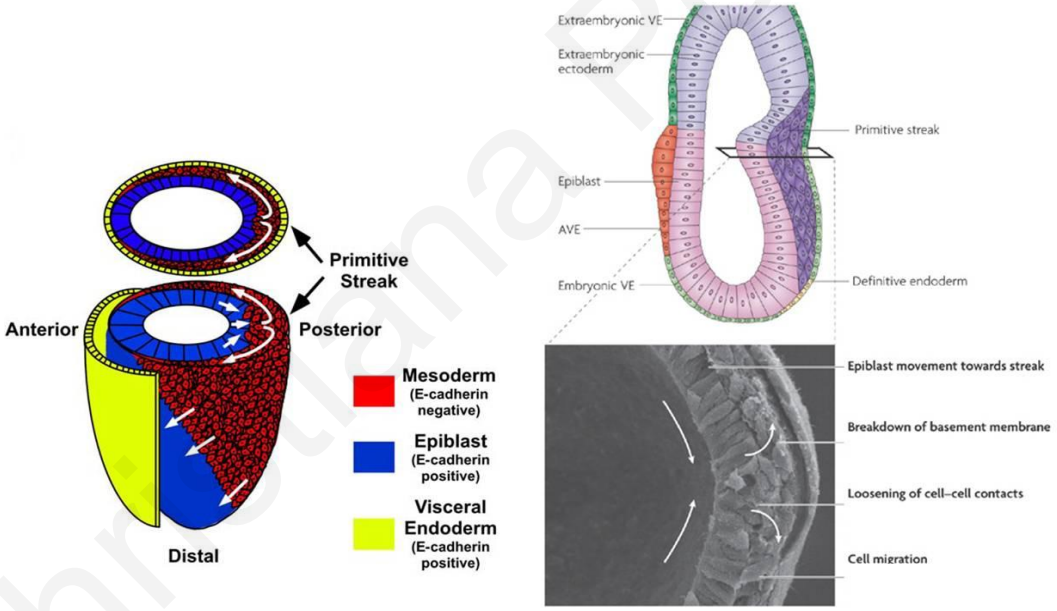

In the left image the small white arrows indicate the epiblast cells that ingress within the PS at the posterior site of the embryo. The big white arrows show the nascent mesoderm which once it exits the streak it migrates anteriorly between the epiblast and the visceral endoderm. Note that the mesodermal cells are e-cadherin negative as in these cells the expression of e-cadherin is downreguled (*Zohn, Li et al. 2006*). The right image also shows the formation of the nascent mesoderm as a result of the EMT and cell migration. The epithelial cells at first detach from the basement membrane, lose their polarity and migrate away from the streak (*Arnold and Robertson 2009*).

1.3 An Overview of mouse gastrulation progression after PS initiation.

Once the PS is formed then is extends anteriorly and by E7.5 when the PS is fully extended it reaches the distal tip of the epiblast. PS cells can be divided into three different regions posterior, middle and anterior PS cells. Fate mapping studies have shown that cells in different regions of the streak display different fates (*Lawson, Meneses et al. 1991*). It was shown that by the late-PS stage the posterior region of the PS contains cells destined to form the extraembryonic mesoderm, the middle part contains cells destined for lateral mesoderm, and the anterior part contains anterior PS derivatives such as anterior definitive endoderm and anterior axial (midline) derivatives such as the node and AME *(Tam and Behringer 1997; Kinder, Tsang et al. 1999; Kinder, Loebel et al. 2001; Robb and Tam 2004; Yamanaka, Tamplin et al. 2007; Kwon, Viotti et al. 2008; Arnold and Robertson 2009*).

At first, in the posterior epiblast of the early streak (~E6.5 stage) mouse embryo, a group of about 40 cells at the posterior midline epiblast was found at a distance of about 50 microns anterior to the newly formed PS, called the early gastrula organizer (EGO). Fate mapping studies showed that the EGO contains a heterogeneous population of progenitor cells of the anterior axial mesendoderm (AME). Transplantation experiments showed that the EGO can induce a secondary neural axis, but this axis is incomplete as it can induce only the formation of posterior neural strucutres (hindbrain and spinal cord) but not the formation of more anterior (forebrain or midbrain) regions (*Kinder, Loebel et al. 2001*). These EGO cells are not moving but as the PS elongates anteriorly, the cells in the posterior region of the EGO are incorporated into the primitive streak and they ingress to join the mesoderm lateral to the anterior end of the primitive streak (*Kinder, Loebel et al. 2001*). On the other hand the cells in the anterior region of the EGO do not ingress the PS and are carried anteriorly to meet the progenitors of the prechordal mesoderm and the head process in the epiblast. The merging of those EGO cells with the anterior end of the PS results in the generation of the Mid Gastrula Organizer (MGO), which contains all the progenitors of the anterior mesendoderm (AME) (*Robb and Tam 2004*). As the MGO cells migrate anteriorly away from the streak to form the anterior axial mesendoderm, the node progenitors constitute the most anterior part of the PS at E7.5 stage (*Kinder, Loebel et al. 2001*). However, when the node (an anterior PS derivative -see below) becomes morphologically distinguishable it is no longer part of the anterior PS.

Gene expression markers such as *Bra* (marks the entire PS), *Cripto* (mesodermal marker) (*Ding, Yang et al. 1998; Arnold and Robertson 2009*) and also *Nodal*, *FoxH1*, *Chordin* and *Foxa2* are required in the epiblast for correct PS elongation and patterning and

also for APS derivatives formation and development (*Ang, Conlon et al. 1994; Sun, Meyers et al. 1999; Bachiller, Klingensmith et al. 2000; Davidson and Tam 2000; Yamamoto, Meno et al. 2001; Anderson, Lawrence et al. 2002; Vincent, Dunn et al. 2003; Dunn, Vincent et al. 2004; Robb and Tam 2004; Yamanaka, Tamplin et al. 2007*). It is also known that PS elongation until E7.0 appears to be necessary for the ingression of the precursors of the PS-derived AME. This is because the AME precursors which are initially localized in the EGO and are marked by *Foxa2* expression, but not *Bra* expression. As the PS elongated, the EGO cells initially become displaced anteriorly and by the mid-PS stage, merge with the anterior end of the PS to generate the MGO (which as mentioned above contains all the precursors of the AME) and expresses *Bra,* in addition to *Foxa2* (*Kinder, Tsang et al. 1999; Kinder, Loebel et al. 2001; Robb and Tam 2004*). MGO is also marked by the expression of the transcription factors *Gsc* and *Foxa2* and these cells are the progenitors of the anterior DE, as well as the precursors of the AME and its derivatives (*Camus, Davidson et al. 2000; Kinder, Tsang et al. 2001; Vincent, Dunn et al. 2003*). Finally, tetraploid embryo chimeras wild type (wt) tetraploid embryo that aggregated with *Cdx2*-/- ES cells, showed that *Cdx2* expression by the late PS stage in the PS-epiblast, has a crucial role in A-P PS patterning as *Cdx2* is necessary for the growth of alantois which is involved in the chorioallantoic fusion and hence the formation of the chorioallantoic placenta (*Chawengsaksophak, de Graaff et al. 2004*).

1.4 Anterior Primitive streak derivatives.

1.4.1 Node.

The node of the mouse embryo is a transient PS-derived structure with organizer activity. It is located at the most anterior end of the PS at the distal area of the gastrulating embryo (E7.5 stage) (*Fig.3*) (*Davidson and Tam 2000*) and as an organizer can induce the formation of an embryo-like structure (formation of a second body axis that lacks anterior neural structures such as for- mid- and hindbrain) when ectopically transplanted into a gastrula embryo (*Beddington 1994; Davidson and Tam 2000*).

Node cells arise from the most anterior PS region (*Kinder, Tsang et al. 2001; Yamanaka, Tamplin et al. 2007; Lee and Anderson 2008*). By the late streak, the mesenchymal node precursor cells accumulate at the anterior PS, between the epithelial layers of the epiblast and the VE. These cells undergo a mesenchymal-to-epithelial (MET)

transition and intercalate into the outer layer of the embryo resulting to the node formation at the distal tip of embryo (*Lee and Anderson 2008*). The mouse node has a unique morphology: it appears as a concave teardrop-shaped pit of cells at the distal tip of the embryo. The node is composed of two small columnar epithelial cell layers: the outer (ventral) layer which faces the yolk sac cavity and the inner (dorsal) layer which faces the PS. The ventral layer is populated by monociliated cells and is adjacent with the endoderm epithelium whilst the inner layer is populated by ectodermal cells and is contiguous with the surrounding epiblast and the PS of the gastrulating embryo (*Sulik, Dehart et al. 1994; Robb and Tam 2004*). Moreover the node pit is surrounded by 20-30 squamous cells called "crown cells" which are adjacent with the endoderm germ layer. Fate mapping studies and live imaging analysis showed that the node give rise to the trunk and tail notochord and floor plate (*Kinder, Tsang et al. 2001; Yamanaka, Tamplin et al. 2007*). Tail notochord cells are derived from the posterior migration of the crown cells of the node *(Yamanaka, Tamplin et al. 2007*).

It was shown that *Nodal* signaling, Noto1, Foxa2 and FoxH1 transcription factors are essential for node cells specification *(Ang and Rossant 1994; Weinstein, Ruiz i Altaba et al. 1994; Hoodless, Pye et al. 2001; Yamanaka, Tamplin et al. 2007*). It has been suggested that the node progenitors expresses *Noto1* (*mNot* which is a homeobox transcription factor). As these cells exit from the streak become at first mesenchymal and then form an epithelium beneath the endoderm layer (*Yamanaka, Tamplin et al. 2007*). During the formation and development of the node there is a unique gene expression pattern encoding several transcription factors as well as signaling ligands. These genes markers include: *Noto1* (m*Not*), *Nodal*, *Bra*, *Sonic hedgehog* (*Shh*), *Chordin* (*Chr*) and *Foxa2* (*Davidson and Tam 2000; Abdelkhalek, Beckers et al. 2004; Dunn, Vincent et al. 2004; Robb and Tam 2004; Blum, Andre et al. 2007; Yamanaka, Tamplin et al. 2007*). Secreted proteins such as *Shh* marks the entire node (*Chiang, Litingtung et al. 1996*), *Nodal* at E7.5 is expressed in the newly formed node but by the head fold stage (E7.5-E7.75) marks only the peripheral crown cells of the node (*Davidson and Tam 2000; Robb and Tam 2004; Blum, Andre et al. 2007*) and *Chordin* marks the entire node (*Davidson and Tam 2000; Robb and Tam 2004*). Transcription factors such as *Foxa2* marks both ventral and dorsal layers (*Dufort, Schwartz et al. 1998*), *Noto1* as mentioned marks the progenitors of the node between mid-to late streak and the pit of cells of the fully formed node by E7.5 until its disappearance (*Abdelkhalek, Beckers et al. 2004; Yamanaka, Tamplin et al. 2007*) and finally *Bra* marks the ventral layer of the node (*Herrmann 1991*). Mutations in several of these genes results in embryos that

lack node formation and its derivatives. For example, null embryos for *Foxa2* or *Noto1* lack a morphological node and notochord (which it is node derivative) (*Ang and Rossant 1994; Weinstein, Ruiz i Altaba et al. 1994; Dufort, Schwartz et al. 1998; Abdelkhalek, Beckers et al. 2004; Beckers, Alten et al. 2007*). Embryos null for *FoxH1,* which is expressed throughout the epiblast and associated VE (*Weisberg, Winnier et al. 1998; Saijoh, Adachi et al. 2000*) and regulates *Nodal* expression levels in the epiblast, lack anterior streak derivatives including the node, because *FoxH1*-dependent maintenance of high levels of *Nodal* fails (*Hoodless, Pye et al. 2001; Yamamoto, Meno et al. 2001*). Furthermore it was shown that low levels of *Nodal* activity in the node result in failure to establish left-right asymmetry in the mouse embryo (*Brennan, Norris et al. 2002*).

1.4.2 Anterior mesendoderm.

By the time when the PS has fully extended to the distal tip and the node is situated at the distal tip, there exists a condensed two-layered stripe of axial (midline) tissue situated underneath the anterior half of the epiblast called the anterior mesendoderm (AME). The part of AME that underlies the future forebrain is called the prechordal plate (PP), whilst the more posterior part is underneath the future mid- and hind-brain regions and is sometimes known as the anterior notochord (AN) (*Robb and Tam 2004; Yamanaka, Tamplin et al. 2007*). As mentioned earlier the progenitors of the AME are initially localized in the anterior part of the EGO, which is located posterior to the newly formed PS epiblast of the early streak mouse embryo. As the PS elongates anteriorly during gastrulation, the AME progenitors within the EGO become displaced anteriorly and by the mid-PS stage, merge with the anterior end of the PS to form the MGO (*Kinder, Tsang et al. 2001*). Once the MGO forms, the precursor cells ingresses through the PS through the most anterior side of the PS and extend along the midline to form the AME (*Fig.3*). The layer of the AME that is closest to the epiblast is anterior axial mesoderm (mesodermal component of the AME), whereas the other AME layer is anterior axial DE (endodermal component of the AME). Both of these are derived from the MGO (*Robb and Tam 2004; Lewis, Khoo et al. 2007; Yamanaka, Tamplin et al. 2007*). Signals from AME are required for correct development of the central nervous system since removal of AME from gastrula embryos suppresses head formation (*Thomas, Brown et al. 1998; Camus, Davidson et al. 2000)*. Useful gene expression markers of the mesodermal component of the AME at E7.5 and E7.75 are the transcription factor Foxa2 and the secreted protein Shh. Also, by E7.5 –E7.75 *Chordin* expression marks the anterior notochord (and also the node) and *Bra* marks the entire PS, node and anterior notochord, but not the

prechordal plate (*Davidson and Tam 2000; Anderson, Lawrence et al. 2002; Dunn, Vincent et al. 2004; Robb and Tam 2004; Yamanaka, Tamplin et al. 2007*). Null mutations for specific genes showed that they are involved in AME formation and development. For example *Cripto* null mutation generated by targeted gene disruption, results in lack of AME based on the absence of *Shh* and *Foxa2* gene expression at E7.5 stage (*Ding, Yang et al. 1998*). Moreover, *Cripto* which is transiently expressed in the precursors of the axial mesoderm and anterior definitive endoderm is essential and necessary in these tissues by mediating *Nodal* signaling (*Chu, Ding et al. 2005*). Nodal signals over a distance to elicit dose-dependent responses (*Ashe and Briscoe 2006*) and the generation of such graded signals is fundamental for anterior patterning and for the specification and formation of anterior primitive structures such as the node and AME (*Shen 2007*). *Nodal* expression within the mouse epiblast with partial loss of *Nodal* function selectively disrupts the specification and the formation of the AME *(Norris, Brennan et al. 2002; Vincent, Dunn et al. 2003; Dunn, Vincent et al. 2004*). Also, maintenance of high *Nodal* expression levels in the epiblast by mid-PS (E6.7) stage are necessary for AME specification, as low levels of its expression in the epiblast showed absence of AME formation (*Yamamoto, Meno et al. 2001; Vincent, Dunn et al. 2003; Shen 2007*). Moreover gene targeting techniques that were used to delete the intronic enhancer of *Nodal* (Anterior Site Element-ASE) which contains binding sites for the FoxH1 transcription factor and controls the early expression of *Nodal* in the epiblast and VE, showed reduced *Nodal* expression in the epiblast. This study suggested that low levels of *Nodal* signaling in the epiblast disrupt A-P PS patterning and anterior primitive streak derivatives formation (*Norris, Brennan et al. 2002*). Also homozygous mutant embryos for *Chordin* showed that this gene is also required for AME formation *(Anderson, Lawrence et al. 2002).*

1.4.3 Definitive Endoderm (DE).

The definitive endoderm (DE) is one of the three embryonic germ layers, which together with the other two (mesoderm and ectoderm) give rise of all cells of the embryo proper. DE is the progenitor cell population of the innermost cellular layer of the fetus and forms the epithelium of the gut tube, lungs and organs including the liver, pancreas and thyroid. The DE emerges 7 to 10 hours after the onset of gastrulation (~E7.0 stage) from the anterior end of the primitive streak (*Lawson, Meneses et al. 1991; Tam and Beddington 1992*). In the mouse, by the completion of gastrulation, the DE forms one cell-thick

squamous epithelium on the outside of the embryo. However, during early organogenesis (~E8.5 stage) the DE becomes positioned as the innermost layer of the conseptus as a result of the embryo body rotation (*Grapin-Botton and Melton 2000; Lewis, Khoo et al. 2007*). Cells that are fated to become DE appear in the anterior PS region from mid to late streak (E7.0-E7.75 stages) *(Lawson, Meneses et al. 1991; Tam and Beddington 1992; Tam and Behringer 1997; Kinder, Loebel et al. 2001; Kinder, Tsang et al. 2001*). It has been shown that when epiblast DE progenitor cells exit the anterior PS (APS), they undergo EMT, become flattened mesenchymal cells and situated between the epiblast and the adjacent VE. These cells then intercalate with the VE layer and at the same time they become epithelial due to acquisition of apical-basal polarity and tight cell junctions The newly-formed DE cells before their intercalation into the VE layer differ from the newly formed mesodermal cells: the latter have a round morphology whereas the former are flattened mesenchymal cells (*Tam and Loebel 2007; Burtscher and Lickert 2009*). Fate mapping studies and time lapse imaging of epiblast cells showed that the epiblast progenitors of the DE cells are localized at the distal area of the epiblast and ingress only through the APS but not at other PS locations (*Lawson and Pedersen 1987; Lawson, Meneses et al. 1991; Tam and Beddington 1992*). Moreover the DE progenitors initially present within the APS (*Burtscher and Lickert 2009*) intercalate within the VE layer and cause the dispersal of the VE epithelium overlying the distal two thirds of the epiblast by E7.5 (*Kwon, Viotti et al. 2008*). Prior to this DE cell intercalation, the VE cells are coherent (closely packed) sheet of cells, but become dispersed upon DE intercalation. This VE cell dispersal can be marked by the downregulation of VE gene markers such as the *Afp* and *Gata4* as downregulation of the levels of these genes was reported to mark the dispersed but not the non-dispersed VE cells (*Dufort, Schwartz et al. 1998; Kwon, Viotti et al. 2008*). Prior to VE spreading, in wt embryos, these genes are expressed throughout the entire VE: the part associated with EXE (VE part that does not experience VE spreading upon DE intercalation because DE cells do not migrate to this region) as well within the VE part associated with the epiblast (VE cells that will experience spreading upon DE intercalation). By E7.75 however (a time when DE intercalation is well under way), *Afp* and *Gata4* expression becomes downregulated within the epiblast-associated, but not the EXE-associated VE (*Dufort, Schwartz et al. 1998; Kwon, Viotti et al. 2008*). Useful DE gene expression markers are *Cer1* (codes for a secreted protein) and *Hex* (codes for a homeobox-containing transcription factor). At the early PS stage (E6.5), both *Cer1* and *Hex* mark the AVE and by the mid streak stages (around E7.0) also mark the population of the DE cells (distal-anterior region of the outer most layer of the embryo). By

the late PS stage (E7.5) *Cer1* marks the anterior DE (ADE) and by early headfold stage (E7.75) *Cer1* expression is restricted to AME *(Shawlot, Deng et al. 1998; Martinez Barbera, Clements et al. 2000; Kinder, Tsang et al. 2001*). On the other hand, by the late PS (E7.5) and early headfold stage (E7.75), *Hex* expression marks the anterior DE, the extraembryonic mesoderm and alantois (*Thomas, Brown et al. 1998; Burtscher and Lickert 2009*).

It has been shown that null mouse conseptuses for *Hex* or epiblast-specific null for *Hex* (upon ES-tertaploid chimera formation) form a DE, but this lacks *Cer1* expression. Importantly, these experiments also showed that *Hex* expression in the DE is required for normal forebrain development because these mutants displayed anterior defects in the forebrain (*Martinez Barbera, Clements et al. 2000*). Moreover, null mutations for other genes have shown that their expression is required for correct DE formation. For example, *Foxa2*, which is expressed in PS epiblast and newly-formed DE cells is required in the epiblast for correct intercalation of DE mesenchymal progenitors within the VE as it promotes an epithelial fate and suppresses a mesenchymal fate (mesenchymal-to-epithelial transition), an event necessary for the DE intercalation within the VE layer (*Burtscher and Lickert 2009*). Also, *Eomes* expression within the epiblast has been demonstrated to be required for DE formation (*Ciruna and Rossant 1999; Arnold, Hofmann et al. 2008*). *FoxH1*, which is expressed in the entire epiblast and its associated VE during gastrulation, was shown to be required in the epiblast for DE formation by mediating high *Nodal* expression levels in the epiblast (*Yamamoto, Meno et al. 2001; Norris, Brennan et al. 2002*). Moreover *Gsc*, which is expressed in the anterior DE of the mid-streak embryo and then its expression is restricted to the prehordal plate of AME, was shown to be required for normal anterior DE and anterior PS derivatives development (*Blum, Gaunt et al. 1992; Lewis, Khoo et al. 2007*).

1.5 Overview of early extraembryonic tissue (visceral endoderm and trophoblast) development.

1.5.1 Visceral endoderm (VE), distal visceral endoderm (DVE) and anterior visceral endoderm (AVE) formation and development.

The visceral endoderm (VE) as mentioned above is a derivative of the primitive endoderm, a transient cell layer that appears along the blastocoelic surface of the primitive ectoderm (the future epiblast) of the implanting blastocyst at E4.5 stage. The primitive endoderm gives rise to two single-layered extraembryonic epithelia: the parietal endoderm and VE. VE cells develop in association with both the epiblast and EXE-have microvilli and contain numerous phagocytic and pinocytic vesicles to allow efficient absorption and digestion of maternal nutrients (*Bielinska, Narita et al. 1999*). VE cells associated with the epiblast exhibit differences in morphology when compared to those associated with EXE. Epiblast-associated VE cells have a squamous morphology, while EXE-associated VE cells are cuboidal (*Bielinska, Narita et al. 1999*). These differences in morphology are accompanied by regional differences in gene expression. For example, gene expression analysis showed that at E5.5 stage, genes such as *Afp* and *Foxa2* are specifically expressed in epiblast-associated VE, whereas genes such as *Gata4*, and *Hnf4* specifically expressed in the VE associated with EXE (*Mesnard, Guzman-Ayala et al. 2006; Pfister, Steiner et al. 2007*).

The first morphological asymmetry within the VE along its A-P axis takes place at around E5.5 and involves the appearance of a thickening within the VE at the distal area of the embryo and it is known as the distal VE (DVE) (*Srinivas, Rodriguez et al. 2004*). From E5.5 onwards, there is polarized movement of DVE cells from the distal tip of the embryo to the region overlying the future anterior part of the embryo (*Srinivas, Rodriguez et al. 2004*). By E6.5, this DVE becomes displaced anteriorly and when it does, it is known as the anterior VE (AVE) and lies underneath the anterior epiblast. The anterior migration of DVE (as well as the AVE) is marked by the expression of genes such as *Hex* and *Cer1* (*Thomas, Brown et al. 1998; Srinivas, Rodriguez et al. 2004*). However, fate mapping and live imaging analysis showed that the DVE and the AVE are descendants from different precursors (*Takaoka and Hamada 2012*). From this study, the DVE was shown to be derived from *Gata6+/Lefty1+* cells that first appear at the blastocysts stage. By contrast, the AVE is derived from *Gata6+/Lefty1–* VE cells that move to the distal tip of the embryo and begin to express *Lefty1* and *Cer1* after E5.5 stage. Examination of the behavior of the entire VE by time-lapse imaging has shown that the DVE guides the migration of the AVE by initiating the movement of VE cells. This was confirmed as ablation of *Lefty1+* DVE cells at E5.5 stage embryos disrupts the movement of the VE cells anteriorly (*Takaoka and Hamada 2012*).

1.5.2 EXE trophoblast, placenta development and trophoblast stem (TS) cells: an introduction.

The mouse blastocyst is composed of two distinct lineages: the inner cell mass (ICM) and the trophectoderm (TE). The trophectoderm contributes to two distinct types: the mural trophectoderm (mTE), which surrounds the blastocyst cavity, and the polar trophectoderm (pTE), which covers the entire ICM. pTE cells proliferate continuously to initially form the EXE, whilst mTE cells differentiate directly to the so-called primary trophoblast 'giant' cells (TGCs). Subsequently, EXE cells proliferate further to form more EXE, whilst also differentiating to form the ectoplacental cone (EPC) trophoblast, by E5.5. Together, EXE and EPC constitute the pre-placental trophoblast (PPT), which is the progenitor of the entire trophoblast compartment of the placenta (*Georgiades and Rossant 2006*). The EPC is located dorsally of the EXE and extends towards the lumen of the uterus. EPC develops rapidly and in later stages becomes part of the placenta as it contains differentiated trophectodermal cells that are thought to form the spongiotrophoblast and secondary TGCs of the definitive mouse placenta (*Tanaka, Kunath et al. 1998*). During gastrulation and as the PS elongates anteriorly the first mesoderm cells that exit the PS are those of the extraembryonic mesoderm. The extra-embryonic mesoderm precursors are located in the posterior/proximal epiblast and migrate (through the streak) to form the allantois, the mesodermal part of the chorion (the chorionic mesoderm) and that of the visceral yolk sac (*Lawson, Meneses et al. 1991; Kinder, Tsang et al. 1999*). The visceral yolk sac is the initial site of vasculogenesis and haematopoiesis and the allantois is the structure that is exclusively derived from the extraembryonic mesoderm. The extraembryonic mesoderm together with part of the EXE produce the posterior amniotic fold, which finally forms a membrane called the amnion by E7.5, which later is necessary for the protection of the mouse embryo and foetus (*Boucher and Pedersen 1996*). Towards the end of gastrulation (E7.5-E8.0 stage), the EXE forms a bilayer with the extraembryonic mesoderm and becomes separated from the epiblast by the exocoelomic cavity. This bilayer is called the chorion. The majority of the chorionic cells are derived from the EXE which then develops into the trophoblast cells of the chorion and in later stages gives rise to the labyrinth zone trophoblast of the definitive placenta. By E8.5 stage the allantois attaches and fuses with the chorion to complete the formation (by E10.5) of the chorioallantoic placenta.

The placenta is an organ that is essential for foeto-maternal nutrient and gaseous exchange which are necessary for the survival/growth of the embryo/foetus whilst preserving the well-being of the pregnant mother (*Boucher and Pedersen 1996*). The mouse placenta

consists of three physiologically and anatomically distinct regions (*Fig.5*). First, is the laregely zygote-derived region known as the labyrinth, where foetal and maternal blood circulate for exchange of oxygen, nutrients and waste products. Second, is the laregely zygote-derived junctional zone or spongiotrophoblast region through which maternal blood enters and exits the labyrinth. This region is flanked by a layer of the so-called 'secondary' TGCs, which are also zygote-derived. The third region of the definitive placenta is the decidua basalis and largely contains maternal cells including maternal endometrium and maternal arteries and veins which are continuous with the arterial and venous channels of the junctional zone (*Georgiades, Ferguson-Smith et al. 2002*)

The derivation and characterization of mouse TS cells provided an invaluable *in vitro* system for studying trophoblast development (*Kunnath et al., 2001*). TS cells can be derived from the polar trophectoderm of the blastocysts stage (E3.5), the extraembryonic ectoderm at E6.5 stage and the chorionic ectoderm at E7.5 stage (*Tanaka, Kunath et al. 1998;Murohashi, Nakamura et al. 2010*; *Kunath et al., 2001*). TS cells are able to self-renew indefinitely *in vitro* in the presence of external factors (*Tanaka, Kunath et al. 1998*). These stem cells are maintained undifferentiated *in vitro* when cultured in 'stem cell medium' which contains several factors such as fibroblast growth factor 4 (Fgf4) and have the potential (when cultured in the absence of these factors) to differentiate into multiple trophoblastic cell types *in vitro* (as well as *in vivo*) including TGCs, spongiotrophoblast, glycogen trophoblast cells and syncytiotrophoblasts (*Cross et al., 2003*). TS cells are the *in vitro* equivalent of EXE and were used in a numerous studies for the detection of several gene interactions. Undifferentiated TS cells, like EXE, express EXE-specific genes such as *Cdx2, Eomes, Bmp4* and *Errb* (*Kunath et al., 2001*). It was shown that *Eomes*, *Cdx2* and *Elf5* are genes that required in these cells for their maintenance and also for EXE character maintenance (*Donnison, Beaton et al. 2005*). *Eomes* is required for EXE trophoblast/TS cells commitment and maintenance (*Kidder and Palmer 2010*) and null mutations for *Elf5* (which also disrupts gastrulation initiation) and *Ets2* are crucial for the maintenance of EXE character (as they cause loss of the EXE character based on gene expression analysis of the specific EXE marker genes) (*Yamamoto, Flannery et al. 1998; Donnison, Beaton et al. 2005; Georgiades and Rossant 2006*). Moreover, *Cdx2* in TS cells to directly regulate *Bmp4* transcription (*Murohashi, Nakamura et al. 2010*) and it is a direct transcription target of *Ets2* in these cells (*Wen, Tynan et al. 2007*). Also, it was shown that knockdown of *Cdx2* or *Ets2* in TS cells in stem cell medium, resulted in downregulation of *Bmp4* expression or *Cdx2, Eomes* and *Esrrb* (both are EXE markers at early gastrulation stages and are required

for EXE and TS cells maintenance), respectively (*Tremblay, Kunath et al. 2001; Niwa, Toyooka et al. 2005; Kidder and Palmer 2010; Odiatis and Georgiades 2010*).

Figure 5*:* **The mouse definitive placenta.**

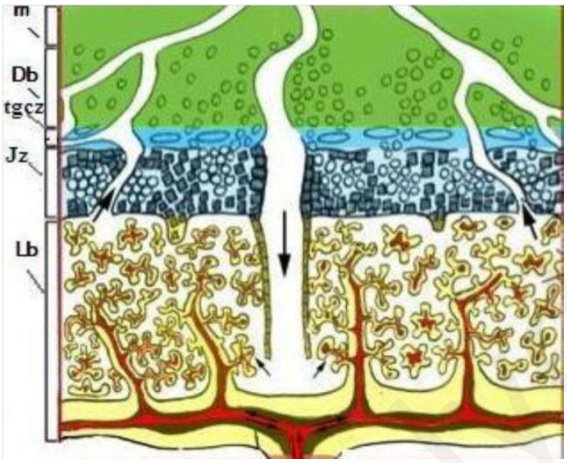

Db-decidua basalis; tgcz-trophoblast giant cells zone; Jz-Junctional zone; Lb-labyrinth; m-myometrium. Labyrinth, junctional zone and trophoblast giant cells zone are exclusively derived from the embryo and specifically from the EXE. The black arrows show the maternal blood that flows into and out of the labyrinth within the maternal arteries and veins (*Georgiades, Ferguson-Smith et al. 2002*).

1.6 Overview of extra embryonic (visceral endoderm and EXE trophoblast) influences on mouse embryo gastrulation.

1.6.1 The role of visceral endoderm in embryo gastrulation.

It is well established that interactions between the epiblast and VE are necessary for correct epiblast A-P patterning. For example, the AVE restricts posterior epiblast character (and hence the formation of the PS and mesoderm) to the posterior site of the embryo due to the suppression of this character in the anterior epiblast by AVE signaling *(Kimura, Yoshinaga et al. 2000*). This was deduced from the phenotype of gene knockout conceptuses whose VE lacks AVE/DVE, as is the case for *Lim1/Foxa2* double mutants whose entire epiblast adopts a posterior character. Moreover, anterior epiblast fragments cultured without, but not with, their associated AVE, expresses posterior genes such as *Bra* indicating that the AVE is required for the suppression of the posterior character in the anterior site of the embryo. Importantly, failure of the anterior DVE shift itself is consistent with this role for DVE/AVE, because mutant conceptuses whose DVE remains distal (such as *Cripto* and *Otx2*

null mutants) fail to posteriorize PS/mesoderm, and as a result display proximal, rather than posterior, PS/mesoderm localization (*Ding, Yang et al. 1998; Dufort, Schwartz et al. 1998; Kimura, Yoshinaga et al. 2000; Perea-Gomez, Rhinn et al. 2001; Acampora, Annino et al. 2005*). Moreover analysis of double mutant embryos for *Cer/Lefty1* which as mentioned are both *Nodal* antagonists has shown that the AVE inhibition of primitive streak formation in the anterior epiblast is *via Nodal* signaling inhibition (*Perea-Gomez, Vella et al. 2002*). Interestingly it was suggested that *Hex*-expressing cells of the AVE are required at E6.5 stage to pattern the anterior PS and also specific subpopulations of this tissue (*Bmp2*-expressing AVE cells) are required for the correct patterning of the posterior side of the embryo (*Stuckey, Di Gregorio et al. 2011*).

In addition to the VE (via the DVE/AVE) signaling being required for restricting PS/mesoderm posteriorly, the VE (*via* its posterior region) is also required for the induction of PS and mesoderm. Specifically, the expression of *Wnt3* in the posterior visceral endoderm is required for PS and mesoderm induction (*Tortelote, Hernandez-Hernandez et al. 2013*).

1.6.2 The role of EXE trophoblast in embryo gastrulation.

Until relatively recently, the EXE was thought to be responsible only for the mediation of feto-maternal interactions for the promotion of embryo growth, but it is now known that it is also essential for PS/mesoderm formation (*Georgiades and Rossant 2006)*. This latter role was shown by several studies. For example, the *Spc1* and *Spc4* genes, which are specifically expressed in the EXE and encode secreted proteases of the subtilisin-like pro-protein convertase (SPC), were shown to be required in EXE for PS and mesoderm formation by maintaining *Nodal* signaling in the epiblast (*Beck, Le Good et al. 2002*). The proposed mechanism how epiblast and EXE signaling leads to the formation of PS mesoderm at the posterior side of the embryo at E6.5 involved *Nodal, Wnt3* and *Bmp4* expression within the epiblast and EXE trophoblast. At first Nodal proprotein (Nodal-Pp) which is expressed in the epiblast, signals to the EXE, which in turn activates the expression of its proprotein convertases Furin and Pace4, as well as *Bmp4* expression in the EXE. The production of the active and mature Nodal in turn induces the expression and the maintenance of *Bmp4* in the EXE (*Beck, Le Good et al. 2002; Ben-Haim, Lu et al. 2006*). The discovery of this EXE role in inducing PS and mesoderm also came from EXE ablation experiments. Specifically, surgical removal of EXE from pre-gastrulation mouse embryos

results in the absence of PS and mesoderm formation (*Rodriguez, Srinivas et al. 2005; Georgiades and Rossant 2006*).

Analysis of *Bmp4* null mice embryos showed that its expression in the EXE is necessary for gastrulation initiation (PS and mesoderm formation) (*Winnier, Blessing et al. 1995; Fujiwara, Dehart et al. 2002*). Also it was shown that *Bmp4* is also required in the EXE for correct PS development during somite stages. Gastrulation in these mutants proceeds normally during presomite stages, but by the early somite stage there was abnormal mesodermal cell accumulation at the posterior PS, there was no formation of allantois and the morphology of the node was abnormal (the overall shape of the ventral surface of the node was flat rather than concave) (*Winnier, Blessing et al. 1995; Fujiwara, Dehart et al. 2002*). Chimaera analysis of this *Bmp4* mutants showed that this gene is required in the EXE (or its derivative, the chorionic ectoderm) for correct posterior PS at the early somite stage, allantois formation and correct node morphology. From this study it is not clear whether the node phenotype is due to defective gastrulation or due to intra-nodal processes occurring after node formation (*Winnier, Blessing et al. 1995; Fujiwara, Dehart et al. 2002*). Another gene required in EXE for correct gastrulation is *Ets2* (see below).

1.7 *Ets2* gene and its role in trophoblast and mouse gastrulation.

1.7.1 *Ets2* gene: an introduction to its structure and expression.

Since this project is based on the role of the *Ets2* gene in gastrulation, this sections deals with an introduction to the structure and expression of this gene. Ets2 *is* a member of the Ets family of transcription factors and was originally identified by its sequence homology to the *v-ets* oncogene of the avian virus E26, which induces both erythroblastic and myeloblastic leukemias in chickens (*Leprince, Gegonne et al. 1983*). The name "Ets" comes from a sequence, called E26 transformation specific sequence. These transcription factors interact with co-regulatory partners to induce gene-specific responses and drive distinct biological processes (*Sharrocks 2001*). The transcription factors of this family can activate or repress transcription on DNA in cooperation with other members of transcription factors and co-factors, and play crucial roles in a variety of cellular functions including growth, apoptosis, development, differentiation and oncogenic transformation (*Sharrocks, Brown et al. 1997; Wasylyk, Hagman et al. 1998*). Examples of the subfamilies within the Ets family are the Ets subfamily (e.g Ets1 and Ets2) and the Elf subfamily (e.g Elf1-5). All the

transcription factors of the Ets family (including Ets2 transcription factor) are characterized by a conserved DNA binding motif called the Ets domain (which is the C-terminal domain). This evolutionarily conserved domain is about 85 amino acids long and mediates binding to purine-rich DNA sequences with a central GGAA/T core consensus (*Papas, Fisher et al. 1989; Wasylyk, Hahn et al. 1993; Wasylyk and Wasylyk 1993*). The Ets domain contains three a-helixes (a1-a3) and four standard-b-sheets (b1-b4) arranged in the order a1-b1-b2-a2-b3-b4 forming a winged helix-turn-helix topology. Moreover the Ets subfamily has the pointed domain (N-terminal domain) whereas the Elf subfamily does not. The pointed domain forms a helix-loop-helix (HLH) for protein-protein interactions and its name is such because it was initially discovered in the *Drosophila* gene *Pointed*. Ets2 is activated both by the calcium signaling pathway (autoinduction) and also by the MAP kinase (MAPK) signaling pathway. Ets2 has a single MAPK phosphorylation site near the pointed domain (*Brunner, Ducker et al. 1994*) and the phosphorylation enhances its ability to activate the transcription by binding to specific sequences called as Ras-responsive elements (RREs) and serum response elements (SREs) which are present in the promoters of many genes.

Ets2 is expressed in many tissues during mouse embryogenesis and plays important roles in cellular proliferation and differentiation during mouse development (*Sharrocks 2001*). During the preimplantation period *Ets2* is not expressed in the blastocyst, but by the early postimplantation period (E5.0) it is specifically expressed in EXE trophoblast and later (E5.5 and E6.75) in EXE and EPC. By E7.75, *Ets2* expression becomes downregulated from the trophoblastic tissues and begins to appear in the PS (*Fig.6*) (*Yamamoto, Flannery et al. 1998;Maroulakou and Bowe 2000; Georgiades and Rossant 2006*). By E8.5 *Ets2* is expressed in the paraxial mesoderm and in the limb buds (*Ristevski et al., 2002*) and during late embryogenesis it is expressed in the central nervous system *(Maroulakou, Papas et al. 1994; Maroulakou and Bowe 2000*). Moreover during organogenesis *Ets2* expression is detected in the kidneys, lungs and gut and its expression is downregulated after bone-formation. In addition, high levels of *Ets2* expression were detected in the cortical region of the thymus and this expression pattern continues throughout adult life (*Maroulakou, Papas et al. 1994; Maroulakou and Bowe 2000*). In the adult mouse, the expression of the *Ets2* is restricted to specific regions of the brain and also is detected in murine mammary glands and the uterine wall. In humans *Ets2* is also expressed during endometrial remodeling (*Kilpatrick, Kola et al. 1999*) and in the ovaries.

<u>Figure 6</u>*: Ets2* gene expression during the early mouse development.

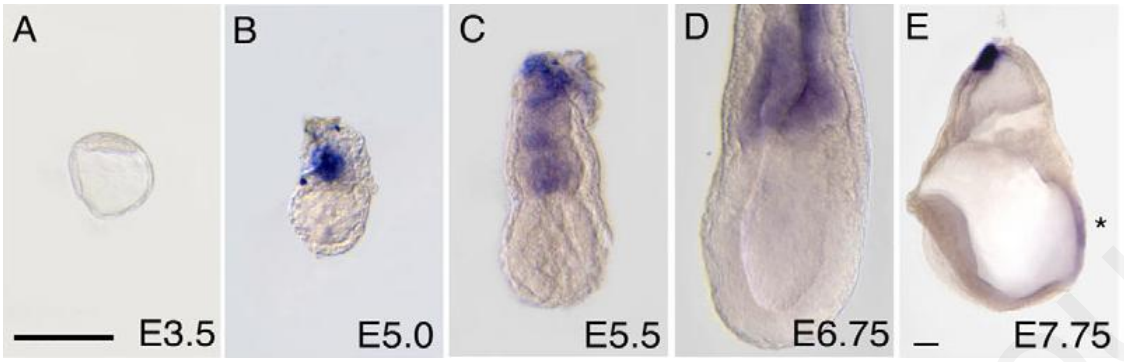

During early gastrulation the *Ets2* is expressed exclusively in the EXE trophoblast and by E7.75 it's expressed also in the PS (*Georgiades and Rossant 2006*).

1.7.2 *Ets2* functions in trophoblast stem (TS) cells.

RNA microarray, quantitative RT-PCR and loss of function studies identified several genes required for TS cell self-renewal including *Ets2*, *Cdx2*, *Eomes* and *Esrrβ* (*Georgiades and Rossant 2006; Okada, Ueshin et al. 2007; Wen, Tynan et al. 2007; Odiatis and Georgiades 2010*). It has been previously shown in our lab that specific *Ets2* knockdown in TS cells was achieved using *lenti-virus.* Using this methodology it was found that *Ets2* knockdown in TS cells cultured under conditions that normally keep them undifferentiated (stem cell conditions), resulted in loss of TS cell self-renewal genes *Cdx2*, *Esrrb* and *Eomes* (which are also EXE markers *in vivo*). This and other TS cell studies concluded that *Ets2* is required in TS cells for their self-renewal, and hence for the maintenance of the EXE/trophoblast character (*Georgiades and Rossant 2006; Okada, Ueshin et al. 2007; Wen, Tynan et al. 2007; Odiatis and Georgiades 2010).* Importantly, TS cell studies support the model that *Ets2* maintains TS cell self-renewal and *Bmp4* expression in TS cells by maintaining the expression of *Cdx2*, a gene required for TS cell self-renewal and *Bmp4* expression (*Cdx2* regulates the expression of both *Elf5*, a TS cell self-renewal gene, and *Bmp4* by directly binding to their promoters) (*Donnison, Beaton et al. 2005; Niwa, Toyooka et al. 2005; Ng, Dean et al. 2008; Murohashi, Nakamura et al. 2010*) through direct binding to its promoter (*Wen, Tynan et al. 2007; Odiatis and Georgiades 2010*). Moreover *Elf5* in TS cells is needed for the maintenance of *Cdx2* and *Eomes* expression, through direct activation of their promoters (*Ng, Dean et al. 2008*).

1.7.3 *In vivo* function of Ets2: *Ets2 null* type-I and type-II mutant embryos.

It has been previously shown that a targeted deletion by homologous recombination replacing the part of the *Ets2* gene that encodes for the conserved DNA binding domain with pMC1NeoA gene, resulted in early embryo death, reduced growth of the EPC and lack the chorion which is a direct derivative of the EXE (*Yamamoto, Flannery et al. 1998*). However from this study it was not examined whether these mutants gastrulate normally. A more recent study showed that *Ets2* homozygous mutant conceptuses display two main types of phenotypes: type-I and type-II (*Fig.7*).

Type-I mutant embryos, based on histology and marker gene expression, fail to form a PS or mesoderm (therefore these mutants do not initiate gastrulation) and their DVE remains distal, (*Georgiades and Rossant 2006*). The finding that *Ets2* is specifically expressed in the trophoblast prior to and during early gastrulation, combined with chimaera analysis (see below) indicates that *Ets2*-mediated signaling from EXE trophoblast is required for the initiation of gastrulation (*Georgiades and Rossant 2006*). Generation of ES cell-tetraploid embryo chimaeras (aggregation of wild-type ES cells with tetraploid *Ets2*-/- embryos), resulted in a subset of these chimaeras displaying a phenotype that was essentially the same as that seen in type-I *Ets2* mutants (*Georgiades and Rossant 2006*). The findings that the trophoblast of type-I mutants lacks EXE character from at least E5.5 (e.g. absence of *Cdx2* and *Bmp4* expression) and that EXE ablation of E5.5 wt conceptuses results in absence of gastrulation initiation, suggests that EXE signaling in general or *Ets2*-dependent EXE signaling in particular (as is the case in type-I mutants), is required around E5.5 for gastrulation initiation (*Georgiades and Rossant 2006*) (*Fig.7*). Taken together, the phenotype of *Ets2* type-I mutants and loss of function studies of *Ets2* in TS cells (see above), suggest that *Ets2* (in the context of the type-I phenotype) is required in EXE from at least E5.5 to maintain EXE character and EXE signalling capability for PS induction (e.g. EXE *Bmp4* expression) by directly maintaining the expression of *Cdx2*, which in turn directly maintains EXE character (by maintaining EXE *Elf5* expression) and EXE *Bmp4* expression.

On the other hand, *Ets2*-/- type-II mutants initiate PS and mesoderm formation (and hence initiate gastrulation), their DVE becomes AVE and have signs of some EXE character around E6.5 (e.g. reduced levels of *Cdx2* expression in their trophoblast) (*Georgiades and Rossant 2006*) (*Fig.7*). However, whether type-II mutants can gastrulate normally after PS/mesoderm initiation is unknown and was the main subject of this project (see below).

Ets2-/- mutant mice (both type-I and type-II phenotypes) are an ideal *in vivo* model for the study of trophoblast signaling influences on embryo development. This is because (a) extraembryonic expression of *Ets2* is confined to the trophoblast, (b) chimaeras generated by aggregation of tetraploid embryos (*Ets2*+/+) with ES cells (*Ets2*-/-), resulted in normal embryonic development to term (i.e all the embryo defects seen in these mutant embryos are because of the absence of *Ets2* expression from the EXE) (*Yamamoto, Flannery et al. 1998; Georgiades and Rossant 2006*), (c) trophoblast-specific *lentivirus-mediated* expression of *Ets2* in *Ets2* null conceptuses from the blastocyst stage onwards resulted in normal development to term (*Okada, Ueshin et al. 2007*).

Figure 7: ***Ets2*** **type-I and type-II mutants.**

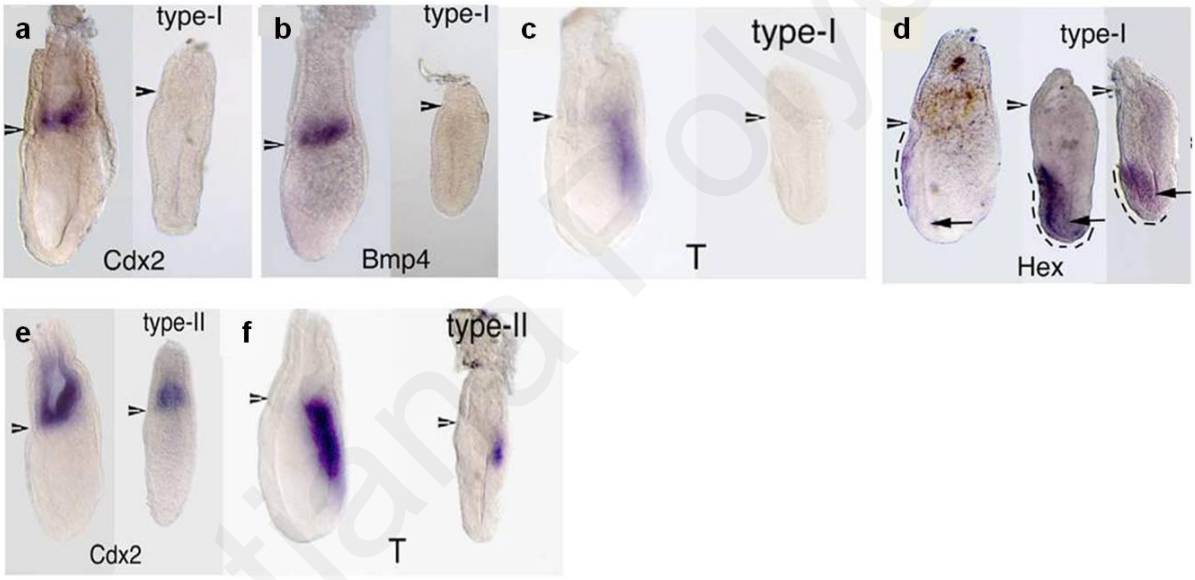

Ets2 type-I mutants lack EXE based on *Cdx2* **(a)** and *Bmp4* **(b)** expression. These mutants do not intiate gastrulation based on T **(c)** expression and the DVE remains distal based on *Hex* expression **(d).** *Ets2* type-II mutants have EXE based on *Cdx2* **(e)** expression and initiates gastrulation based on T **(f)** expression. (*Georgiades and Rossant 2006*)

Chapter 2

AIMS

2.1 General aims of the project.

This project is about discovering new influences for the EXE trophoblast on mouse embryo gastrulation. Until recently, the trophoblast which is the extraembryonic cell type that makes up the majority of placenta tissue was thought to only function for the promotion

of embryo growth and viability *via* promotion of feto-maternal interactions, but not for embryo patterning. Recent work in mice (*Beck, Le Good et al. 2002; Fujiwara, Dehart et al. 2002; Donnison, Beaton et al. 2005; Ben-Haim, Lu et al. 2006; Georgiades and Rossant 2006*) showed that EXE trophoblast signaling is also required for one of the most fundamental patterning events: gastrulation initiation [i.e. initiation of primitive streak (PS) and mesoderm formation]. However, it is currently unknown whether trophoblast signaling is also required for gastrulation progression after PS initiation and this was the main topic of this project.

The main aim of this project was to discover new *in vivo* roles for trophoblast signaling in early embryo patterning by examining whether this signaling is not only required for gastrulation initiation (as shown previously), but also for gastrulation progression after PS initiation, using gene knockout mice for the *Ets2* gene, the so-called type-II *Ets2* mutant phenotype (*Georgiades and Rossant 2006*). This project therefore was set to examine the influence of EXE trophoblast (and the role of *Ets2* in this) in gastrulation progression after PS initiation in type-II *Ets2-/-* mutant embryos, to identify the specific gastrulation processes involved, and to explore (at the genetic and cellular levels) how *Ets2* in trophoblast mediates these events. This is because (a) these mutants can be used as an *in vivo* model for the study of trophoblastic influences on embryo gastrulation (see above), (b) they initiate gastrulation (*Georgiades and Rossant 2006*), (c) it is unknown whether gastrulation progression is normal in these mutants and their trophoblast phenotype is largely unexplored.

Data on which the specific aims of this project were based (generated by P. Georgiades).

Morphological observations from semithin saggital sections of *Ets2* type-II mutants at E7.75 and E8.5 stage (stages when gastrulation is at an advanced stage) indicated that although these mutants initiate a PS and mesoderm, gastrulation progression is severely defective. Specifically, these data suggested that: (a) The PS fails to elongate fully, as judged by the limited anterior-posterior extent of PS-associated mesoderm, which fails to reach the distal tip (*Fig.8b,d*). (b) Intraembryonic mesoderm fails to migrate away from the PS as no anterior mesoderm is observed between the anterior epiblast and the endoderm and also there is a cellular accumulation in the PS region (n=2, *Fig.8b,c,d,i*) (c) There is absence of a morphologically identifiable node (an anterior PS derivative), suggesting defective development of anterior PS derivatives (*Fig.8a,b,e,d*). (d) There is absence of allantois (extraembryonic mesoderm derivative) and amnion and limited extraembryonic mesoderm (probably yolk sac mesoderm) formation (n=2; *Fig.8b,d*). In contrast to the type-II

phenotype, semithin sections of type-I mutants at E6.7 and E7.75 confirmed their previously reported absence of PS and mesoderm (and hence failure to initiate gastrulation) (*Fig.9a,b*).

The above defects observed in type-II mutants were also detected in a subset of chimaeras, thereby confirming that it is the loss of a functional *Ets2* in trophoblast that is responsible for failure of gastrulation to progress normally in the context of the type-II phenotype. Specifically, the generation of E7.75 chimaeric conceptuses (ES cell-tetraploid embryo chimaeras) by aggregating GFP-expressing *Ets2* +/+ ES cells with GFP-negative 4N embryos (either *Ets2* -/-, -/+, or +/+) (*Fig.8g*), showed the following in a subset of these chimaeras where the genotype of 4N embryos was *Ets2*-/-, the so-called '*Ets2* type-II chimaeras': (a) Failure of PS elongation to the distal tip, based on *Bra* (PS marker) expression in whole mounts (*Fig.8h*) and localization of mesoderm in semithin sections (Fig.8i). (b) Failure of intraembryonic mesoderm to migrate away from the PS, absence of a morphological node and limited extraembryonic mesoderm formation (*Fig.8i*). These type-II chimaeras also displayed abnormal GFP positivity localization, suggesting defects in definitive endoderm (DE) formation. That is, in control chimaeras (4N embryo, and hence the trophoblast of these chimaeras, is either *Ets2*-/+ or *Ets2*+/+) where GFP positivity (which marks the epiblast and all its derivatives including DE, which by E7.5 intercalates within the VE layer) extends to the entire epiblast-associated VE layer (*Fig.8j*), indicative of DE formation. However, in type-II chimaeras this VE GFP positivity is either absent (n=2/6) or present, but not localized throughout the entire VE antero-posterior extent (n=4/6). One interpretation of these chimaera results is that in the majority of type-II mutants, DE forms at reduced levels and in a minority it doesn't. On the other hand, the so-called '*Ets2* type-I chimaeras', which were also produced in these experiments never show GFP positivity in their VE, suggesting absence of DE (*Fig.9c,d*), consistent with their previously shown failure to initiate gastrulation (*Georgiades and Rossant 2006*). Taken together, these findings indicate that in the context of the type-II phenotype, *Ets2* in trophoblast is required for gastrulation progression after PS initiation. This novel role for trophoblast in gastrulation involves several fundamental gastrulation events including PS elongation, PS-derived mesoderm migration, and anterior primitive streak derivative development. The specific questions these finding raise were dealt with in the specific aims of this project.

<u>Figure 8:</u> Defective gastrulation progression in *Ets2* type-II mutants and mutant chimeras at E7.75 stage.

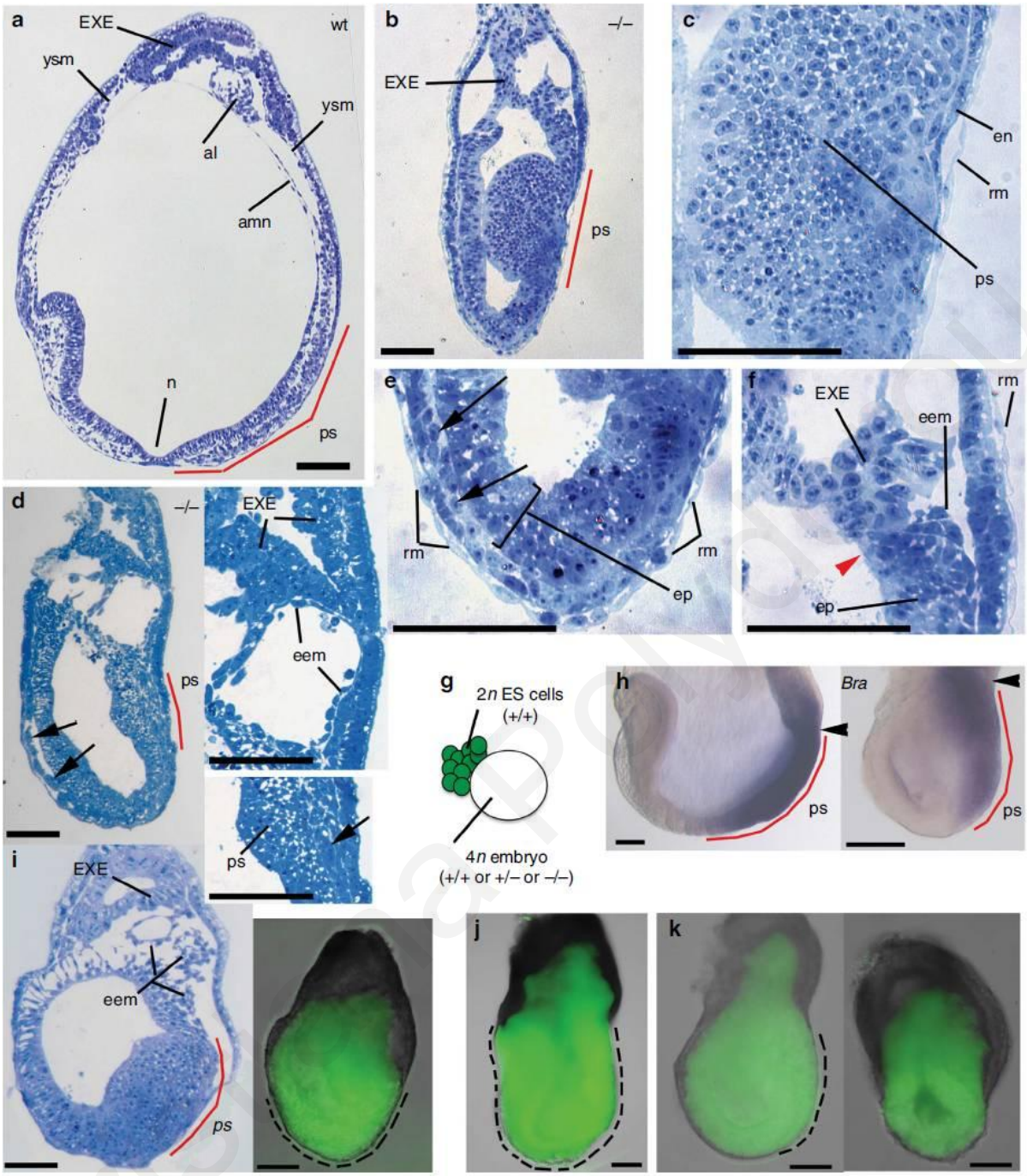

Morphological observations on semithin sections of *Ets2* type-II mutants and their respective chimaeras. Sagittal semithin section of E7.75 stage wild-type (control) **(a)** of type-II mutant at E7.75 in **(b)** and at E8.5 stage in **(d, left image)**. Type-II shows abnormal cellular accumulation of PS-derived cells and absence of anterior mesoderm suggesting a defective EMT. **(c)** High magnification of PS-derived cells shown in b. Note that the mesodermal cells are closely packed and they don't have a stellate morphology. **(e)** High magnification of the distal region of the type-II mutant embryo shown in b. **(f)** High magnification of posterior embryonic-extraembryonic junction (red arrowhead) of the mutant

shown in b. Note the absence of amnion and allantois, but the presence of a few stellate cells indicative of limited extraembryonic mesoderm. The mutants show abnormal cellular accumulation of closely packed and non-stellate cells at the PS at both stages, and absence of mesenchymal cells at E7.75 **(b,c,e,f)** or limited mesenchymal-like cells at E8.75 **(d, right image).** Note the presence of oval cells (arrows) adjacent to the epiblast and the presence of extraembryonic mesoderm (probably yolk-sac mesoderm) at both stages (more abundant at E8.75). Also note that at both stages the mutants lack any morphologically recognizable amnion, allantois, node and anterior intraembryonic mesenchymal cells, and their PS (based on the thickness of posterior epiblast region) appears not to extend to the distal tip. **(g)** Schematic representation of the protocol for generating chimaeric embryos by aggregation of GFP-expressing Ets2+/+ ES cells with a tetraploid embryo derived from a non-GFP expressing embryo whose genotype was either *Ets2*+/+, *Ets2*+/-, or *Ets2*-/-. **(h)** Whole mount *in situ* hybridization for *Bra* expression in E7.75 chimaeras, which in controls (tetraploid embryo ***Ets2*+/+ or -/+; left panel**), but not mutants (tetraploid embryo ***Ets2*-/-; right panel**), extends to the distal tip of the embryo. Arrowheads depict the embryonic-extraembryonic junction. **(i)** Sagittal semithin section **(i, left image)** and wholemount GFP fluorescent (green) view **(i, right image)** of the same E7.75 mutant chimaera. Note, the apparent shortness of the PS and the absence of any recognizable intraembryonic mesenchymal cells, node, allantois and amnion. (**j, k**) Wholemount GFP fluorescent views of control chimaera **(panel j)** and two mutant chimaeras **(panel k).** Taken together with panel I (right image), it is shown that in the majority of mutants (n=4/6), the outermost embryonic layer (the endoderm) is GFP-positive (depicted by dotted lines) to a lesser extent than controls, and in a minority (n=2/6), it is GFP-negative.

In all panels posterior is to the right. Red lines denote apparent PS length.Scale bars in a, b, d, h and i (left image) are 10μm. Scale bars in i (right image), j and k are 20μm. al, allantois; amn, amnion; eem, extraembryonic mesoderm; en, endoderm; ep, epiblast; EXE, extraembryonic ectoderm; m, mesoderm; n, node; ps, primitive streak; rm, Richert's membrane, ysm, yolk-sac mesoderm.

2.2 Specific aims of the project.

<u>Aim 1:</u> Establishment of a morphological and marker gene expression assay for distinguishing between *Ets2* type-I and type-II phenotypes.

This was necessary and crucial for the interpretation of results because the crosses used here to generate the type-II phenotype also produce mutants of the type-I phenotype (*Georgiades and Rossant 2006*). This assay was based on a combination of whole-mount morphology and molecular presence (or absence) of a PS, which forms in type-II, but not type-I, mutants. Moreover, to confirm that type-I mutants also lack definitive endoderm (DE), node and anterior mesendoderm (AME), as would be expected from the lack of PS, simultaneous detection of absence of PS (absence of *Bra* expression) with either the AME/node marker or the staining pattern of *Dolichos biflorus agglutinin* (DBA) lectin, were employed. DBA lectin is specific for D-N-acetylgalactosamine and present in visceral endoderm (VE) cells, but not in DE cells (*Sherwood, Jitianu et al. 2007*). Thus this staining allows the detection of DE indirectly by the presence of discontinuous DBA positivity, indicative of VE spreading to accommodate the incoming DE cells (see below).

<u>Aim 2:</u> Primitive streak development in *Ets2* type-II mutant embryos.

The morphological observations of *Ets2* type-II mutants (see above) suggested that the PS fails to elongate and indicated that (a) intraembryonic mesoderm fails to migrate away from the PS (b) posterior PS derivative formation is defective. The aims here therefore were to: (a) confirm the existence and identify the extent of the PS elongation defect. (b) Examine whether the failure of intraembryonic mesoderm to migrate away from the PS is due to defective epithelial to mesenchymal transition (EMT). (c) Investigate the failure of posterior PS derivatives and patterning of the PS along its posterior-anterior axis.

<u>Figure 9:</u> Type-I phenotype based on morphological and chimera analysis.

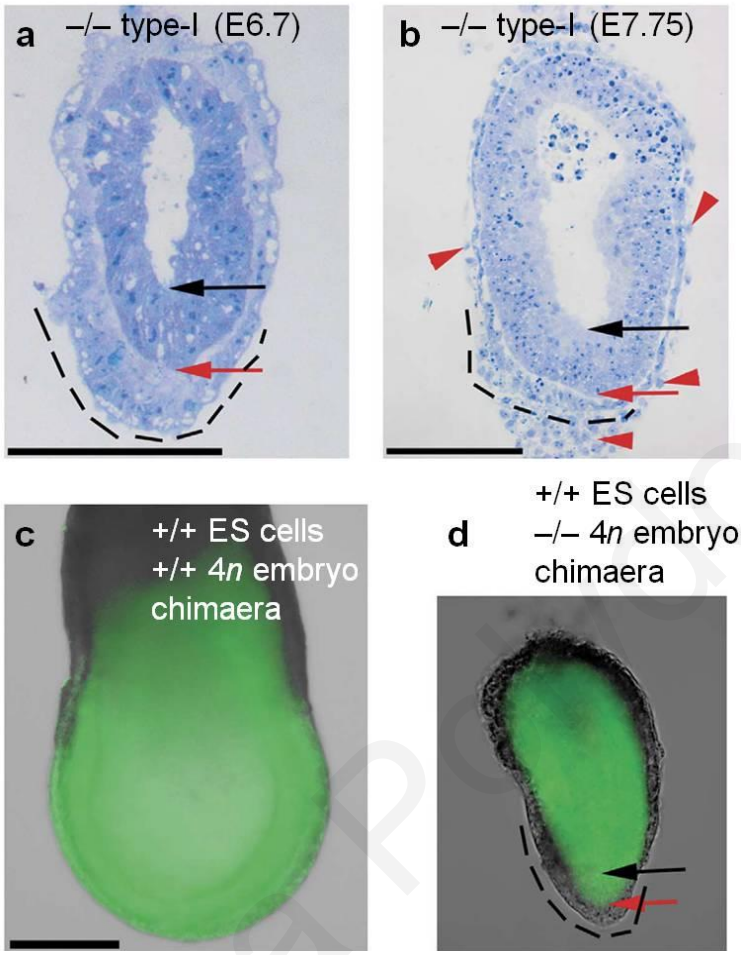

Sagittal semithin sections of type-I mutants at E6.7 **(a)** and E7.75 **(b)**, showing the DVE thickening and the absence of mesoderm or a PS. (**c,d**) E7.5–7.75 chimaeric embryos generated by aggregation of GFP-positive *Ets2*+/+ ES cells with GFP-negative tetraploid (4n) embryos, which are either *Ets2* +/+ **(c)** or *Ets2*-/- **(d).** Note that in contrast to controls, GFP positivity in type-I mutant chimaeras (that is, chimaeras with DVE thickening) does not extend to the outermost layer, indicating absence of DE. The posterior side in all embryos is on the right hand side. Black and red arrows depict the luminal side and outer side of distal tip. Dotted lines depict the localization of DVE/AVE along the anterior-posterior axis. Black arrowheads depict VE cells that experienced spreading, while red arrowheads depict regions of Richert's membrane left attached to the embryo. Scale bars, 100 μm.

<u>Aim 3:</u> Anterior primitive streak derivatives development in *Ets2* type-II mutants.

Morphological examination of *Ets2* type-II mutants showed absence of a morphologically recognizable node (an anterior PS derivative) and investigation of *Ets2* type-II chimaera data suggested reduced or absent DE formation (another anterior PS derivative) (see above). Based on these, the aims here were to: (a) Examine whether node specification occurs in these mutants. (b) Investigate the development of the two other main anterior PS derivatives, DE and AME in type-II mutants.

<u>Aim 4:</u> Regulatory gene expression in type-II mutant epiblast.

The aim here was to understand the genetic basis of the above-mentioned defects in epiblast derived cells of *Ets2* type-II mutants (e.g. PS elongation, intraembryonic mesoderm migration and anterior PS derivative development), by assessing the expression of upstream genes within the epiblast that are required for these processes.

<u>Aim 5:</u> Trophoblast gene expression in *Ets2* type-II mutant embryos.

To explore how *Ets2* gene expression in EXE trophoblast mediates gastrulation progression within the epiblast, the expression of various EXE-expressed genes required for EXE maintenance or EXE signaling were assessed.

<u>Aim 6:</u> Pre-gastrulation examination of type-I and type-II mutants.

The aim here was to assess EXE and epiblast gene expression in type-II mutants at pregastrulation stages in order to investigate the onset of any gene expression defects in these tissues. For comparative purposes, type-I mutants were also examined at equivalent stages.

Chapter 3

MATERIALS AND METHODS

3.1 Mice, embryo collection.

Mice heterozygous for the *Ets2* gene were maintained on an outbred ICR genetic background (*Yamamoto, Flannery et al. 1998; Georgiades and Rossant 2006*). The mice were exposed to light daily between 6:00am and 20:00pm. Assuming that fertilization takes place around midnight, then at noon of the following day (the day on which the vaginal plug is found, (*Fig.10*), the embryos are aged 0.5 day (E0.5). Pregnant females were sacrificed on E6.3-E6.4 (around 8:00-9:00 of the sixth day), E6.5 (around 12:00-13:00 of the sixth day), E6.7 (around 17:00-18:00 of the sixth day), E7.0 (around midnight of the sixth day), E7.5 (around 12:00-13:00 of the seventh day) and E7.75 (around 17:00-18:00 of the seventh day). *Ets2* knockout homozygous type-II embryos were generated by inter-crossing *Ets2* parental heterozygous mice. The conceptuses were dissected out from the decidua using fine tip forceps and the Reichert's membrane was mechanically removed using tungsten needles (*Fig.11*). During dissection the conseptuses were placed in dissection medium containing F12 medium (Gibco, Invitrogen, Cat. No. 31331028), 10% Foetal Bovine Serum, Heat inactivated (FBS, Invitrogen, Cat. No. 10108165) for feeder cells and 1M Hepes (Scharlab, Cat. No. HE0011). The isolated embryos (embryos without the Reichert's membrane) were washed twice in 1XPBS and fixed in 4% paraformaldehyde [(pfa), Sigma-Aldrich Cat. No. P6148) overnight at 4^{o}C. The type-II mutants and their normal littermates (which used as controls), were fixed and then washed with PBT {[1X Phosphate-Buffered Saline (PBS), 7.4 (10X, liquid, Gibco, Cat. No. 70011-044)] with 0.1% TWEEN 20, viscous liquid, Sigma-Aldrich, Cat. No. P1379) for 10 min at Room Temperature (RT), dehydrated through a methanol (Sigma-Aldrich, Cat. No.M0375) series (25%, 50%, and 75% methanol in PBT) for 5 min at RT and stored in 100% methanol at -20^{o}C until used (*Georgiades and Rossant 2006*). Type-II mutants were identified under a dissecting microscope, based on their morphology (*Georgiades and Rossant 2006*). Maximum of 2 homozygous *Ets2* type-II mutants were isolated per litter. During dissection, it was able to distinguish the homozygous mutant embryos (from the wt embryos) because they had a small size and reduced accumulation of maternal blood around their implantation site. Also, the type-II mutants could be distinguished morphologically from type-I mutants based on: (a) the presence of a thickening of VE at the distal tip of the embryo as the (thick) DVE fails to shift anteriorly to form the AVE, (b) the absence of EXE trophoblast and (c) the absence of PS/mesoderm in type-I and not in type-II mutants embryos, at all stages analyzed. However, it should be noted that the heterozygous embryos were indistinguishable from their wt littermates.

<u>Figure 10:</u> Plugged (a, black arrow) compared to unplugged (b, black arrow) female mouse.

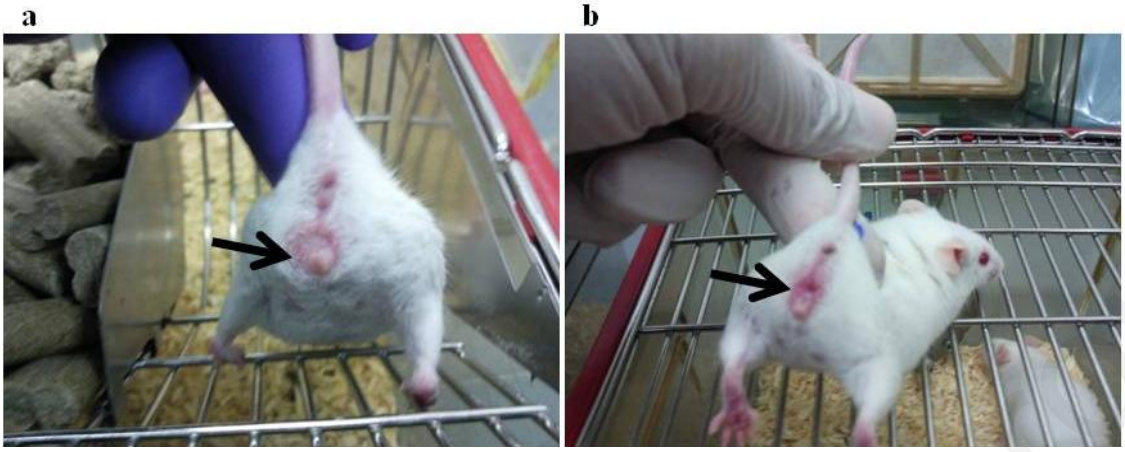

Once the male has successfully mated with the female the excess semen forms a white, 'plug' in her vagina (**a**, black arrow). This plug blocks the entrance to the vagina and prevents other male mice mating with her.

<u>Figure 11</u>: Mouse embryo collection.

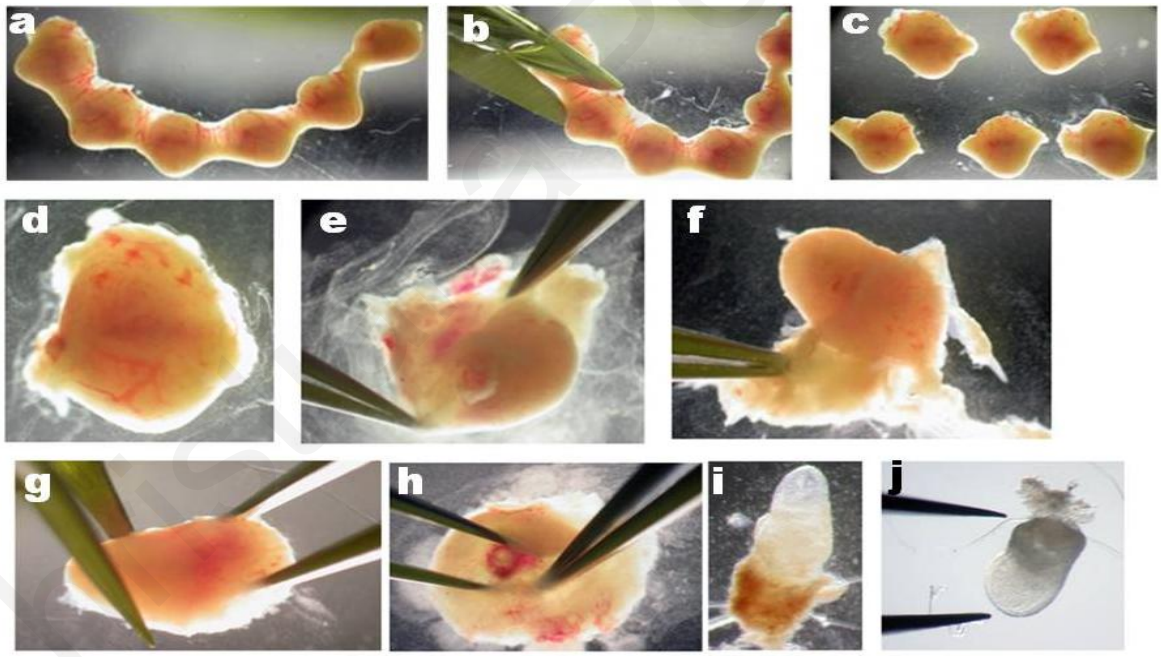

Ar first the uterus was cut along the mesometrium (**a**) and then each embryo (swelling) was seperated by cutting between their implantation sites (**b**). All embryo swellings were placed in a petri dish containing dissection medium (F12, plus 10% FBS and 1M HEPES) (**c,d**). Using fine forceps the endomytrium was removed (by sliding the forceps between the surrounding muscle layer) and then was peeled back, exposing the decidua (**e,f**). The decidua was then cut separated from the embryo. Note that the embryo is at the opposite region of the cutting. (**g,h**). Once the embryo was removed (by pushing it out from the desidua with the forceps), *Reichert's* membrane was still attached to the embryo (**i**). The *Reichert's* membrane was then mechanically removed very carefully using needles and the embryos finaly were isolated (**j**). (*Manipulating the mouse embryo, Nagy 2003*)

3.2 Mouse tails and embryo genotyping.

The heterozygosity of the parent mice was confirmed by PCR analysis of genomic DNA derived from the mouse tails. For genomic DNA extraction from mouse tails were used with the Extract-N-Amp™Tissue PCR Kit (Sigma-Aldrich, Product number: XNAT2). The kit was included the tissue preparation solution which contained Proteinase K, the extraction and the neutralization solutions. Genomic DNA had been extracted from a tail pieces (~ 1 cm) when incubated in 12,5μl tissue preparation solution and 50μl extraction solution (1:4) for 15 minutes at 37^{o}C. Then the samples were heated at 95°C for 3 minutes and then mixed with the neutralization solution (50μl) prior to PCR reaction. Also, embryo genotype was confirmed by PCR analysis of genomic DNA derived from the entire embryo after whole-mount *in situ* hybridization analysis using the same methodology that used for the genomic DNA extraction from mouse tails. Because the embryos were very small in size the concentration of the solutions was reduced 10x (the mixture was contained: 1.25μl Tissue Preparation, 5μl Extraction and 5μl Neutralization solution was added to the samples before the PCR reaction). Two separate PCR reactions were performed using a primer set that produced either the wild-type (220bp) or mutant (200bp) sequences (*Yamamoto, Flannery et al. 1998; Georgiades and Rossant 2006*) were performed. The conditions for both PCR reactions were: 94°C for 3 minutes; 35 cycles of 94°C for 30 seconds, 64°C for 30 seconds and 74°C for 4 seconds; then 72°C for 5 minutes.

For the detection of the wild-type and the mutant DNA sequences, the primers that were used are shown in the **Table 1.**

Table I: Primers for the wt and *Ets2* mutant allele that were used in mouse tails and embryo genotyping (*Georgiades and Rossant 2006*).

	Forward Primer (EtsA)	Reverse Primers
wt	5-CGTCCCTACTGGATGACAGCGG-3	5-TGCTTTGGTCAAATAGGAGCCACTG-3 (EtsB)
Ets2	5-CGTCCCTACTGGATGACAGCGG-3	5-AATGACAAGACGCTGGGCGG-3 (Neo)

The PCR mix for the detection of the **mutant** sequence (10µl reaction) was:

6.5µl H_20 (RNAse and DNAse free, Gibco, Invitrogen, Cat. No.10977-035), 2µl genomic DNA, 1µl enzyme buffer, 0.2µl dNTPs (10mM, Invitrogen), 0.1µl Neo (10mM), 0.1µl EtsA (10mM), 0.1µl Tag Polymerase (Takara, Millipore, 5units/µl).

Also, the PCR mix for the detection of the **wild type** sequence (10µl reaction) was:

6.5µl H_2O, 2µl genomic DNA, 1µl enzyme buffer, 0.2µl dNTPs, 0.1µl EtsA (10mM), 0.1µl EtsB (10mM), 0.1µl Tag Polymerase.

After PCR analysis the samples were run on 1% Agarose (Sigma A0169) in 1X TAE (Life Technologies, Cat. No. 24710-030) gel, at 120 V, for 30-45 min for the detection of the heterozygous *Ets2* mice. Moreover for the detection of the homozygous *Ets2* type-II mutant embryos the samples were run on 1.8% Agarose in 1X TAE gel at 120 V for 30-45 min.

3.3 Whole mount RNA *in situ* Hybridization.

Single-colour and double-colour whole-mount RNA *in situ* hybridization (ISH) was carried out essentially as previously described (*Georgiades and Rossant 2006*). The RNA probes were labeled either with digoxigenin or fluorescein and were detected using alkaline phosphatase-conjugated antibodies that catalyze a chromogenic reaction with different chromogenic substrates, producing blue/purple or red/orange products respectively.

3.3.1 Preparation of RNA probe.

The RNA probe was prepared by *in vitro transcription* (IVT) using RNA polymerase and ribonucleotides one of which the UTP is conjugated with digoxigenin or fluorescein and a cDNA template of a gene of interest which previously cloned within a plasmid vector and flanked by promoter sequence for RNA polymerases either for T3,T7 or Sp6. The polymerase that was used to transcribe the plasmid cDNA template was chosen based on the orientation of the cDNA with respect to the RNA promoters that flank it. For example to transcribe an *anti-sence* probe (to start the transcription from the 3' end of the cDNA) was used an RNA polymerase that is close to the 3' end of the cDNA was utilized. For whole-mount RNA ISH were used *anti-sense* probes for the detection of the gene of interest. This is because the endogenous RNA that will be detected with the probe is transcribed in the *sense* orientation. For this project the probes that were used for the detection of *Bra, Nodal, Hex, Cer1, Bmp4, Foxh1, Cdx2, Cripto, Wnt3,Elf5, Esrrb, Pace4* (*Spc4*),*Chrd, Noto, Shh, Eomes, Gsc, Snail and Foxa2* were as bacterial stocks stored at -80^{o}C (*Georgiades and Rossant 2006*). From these bacterial stocks at first the plasmid DNA templates were purified using Midi-Prep preparation, then were linearized using unique restriction enzymes and finally the RNA probes were prepared using IVT. The plasmid DNA templates for *Fgf8* and *Afp* (which were kindly provided by *Dr. Tristan Rodriguez* and *Dr. Anna-Katerina Hadjantonakis* respectively) have been sent in the form of a DNA spot on a piece of Whatman 3MM paper. For those probes at first the plasmid DNA templates were released from the paper and these DNA templates transformed with bacteria (see below). Afterwards the plasmid DNAs were purified using Midi-prep preparation then linearized using unique restriction enzymes and finally the RNA probes were prepared using IVT.

Bacterial transformation with plasmid DNA.

To transform competent bacteria with plasmid DNA were used the "*Subcloning Efficiency DH5a Competent cells"* (Invitrogen, Cat. No.1825-017). The plasmid DNA was added (concentration varies from 1ng-10ng) in a 1,5ml eppendorf tube which was contained 50μl of the bacteria and were incubated for 30 min on ice. Then the bacteria, were heat shocked by placed them on a water bath 42^{o}C for 20 sec. Under sterile conditions 950μl of SOC medium (Invitrogen, Cat. No. 15544-034) which is a medium for growing freshly transformed bacteria, were transferred in the tube and incubated at 37^{o}C at 225rpm incubator with shaking platform for 1 hour. After incubation, the bacteria under aseptic conditions were

spread on plates contained LB agar (Invitrogen, Cat. No. 22700025) and antibiotic and were grown so as to get individual colonies at 37^{o}C incubator overnight. The antibiotic that was used depends on the plasmid resistance. For all plasmids the ampicillin (Amp) was the antibiotic that was used (Sigma, Cat. No. A95-18-5G, 100mg/ml). The next day individual colonies were picked and then transferred in a tube which was contained 2.5ml LB growth (Invitrogen, Cat. No. 12780-052)/2.5μl Amp. The bacteria colonies were incubated at 37^{o}C at 225rpm incubator with a shaking platform overnight (12-16 hours). Finally the bacterial cultures were then used for re-growing them and 20μl (from 2.5 ml LB/Amp cultures) were added in flasks that were contained 50ml LB growth/50μl Amp, so as to be used for Midi-preparation.

DNA purification using Midi-Preparation.

The "*NucleoBond Xtra Midi, 50 preps*" plasmid purification kit from "*Machery-Nagel,* (Cat. No740410.50)." was used to purify the plasmid DNA. Each "*NucleoBond Xtra column*" contained a "*column filter*" and a "*column*" situated at the base of the syringe and this was the filter that would tap the DNA. This "*column*" contained silica resin beads and provides a high overall positive charge that permits the negatively charged phosphate backbone of plasmid DNA to bind with high specificity. The basic principle of this system is that the bactrerial cells were first lysed by an optimized set of buffers based on the NaOH/SDS lysis method. After equilibration of the "*NucleoBond Xtra column*", the entire lysate was loaded by gravity flow and simultaneously was cleared by the specially designed "*column filter*". The plasmid DNA was bound to the "*NucleoBond Xtra silica resin*" and after an efficient washes the plasmid DNA was eluted, precipitated, and easily dissolved in H_2O for further use. The bacterial cultures those were grown at 37^{o}C at 225 rpm, pellet by centrifugation at 5500g (rcf) for 15 min at 4°C and the supernatant was completely discarded. The bacterial pellet resuspended completely in 8ml resuspension buffer (RES) with RNaseA (60μg/ml) by pipetting the cells up and down. In the suspension was added 8ml of Lysis Buffer (LYS), mixed gently by inverting the tube 5 times and the mixture was incubated 5 min at RT. 12ml of Equilibration buffer (EQU) was applied onto the rim of the "column" and was allowed to empty by gravity flow. Then in the suspension was added 8ml of the Neutralization (NEU) buffer (the bacterial lysate appeared less viscous and more homogeneous) and then it was transferred to the equilibrated "column" and was allowed to empty by gravity flow. The "column filter" and the "column" were washed by added 5ml of

EQU buffer and then the "filter column" was discarded. The "column" was then washed by added 8ml of washing (WASH) buffer. To elude the plasmid DNA, 5ml of elution buffer (ELU) was added to the "column" and the DNA was then collected in a 50 ml centrifuge tube. For the precipitation of the plasmid DNA, 3.5ml of room temperature isopropanol (Sigma, Cat. No.19030-500ML) was added to the 5ml of eluted DNA, the mixture was let for 2 min at RT and then centrifuged at 15,000 rcf at 4^{o}C for 30 min. The supernatant was then removed carefully and the DNA pellet was washed twice using 70% ethanol (Merck, Cat. No.1009832500) in RNase-free H_2O and dried at RT for approximately 7 min. The DNA pellet was then dissolved in 100μl RNase-free H_2O. The concentration of the DNA was calculated using the spectrophotometer and finally the purified DNA stored at -20^{o}C until used.

Methodology for the restriction enzyme digestion for the linearization of the plasmid DNA template.

The DNA template that was purified using the Midi-prep method was then digested (linearized) to be used later for IVT. For each DNA template the unique restriction enzymes that were used are shown in the **Table II**. For final volume 100μl the concentrations that were used for the reaction were: 10mg DNA, 1X enzyme buffer, ddH_2O and enzyme 50units amount. The mixture was incubated at 37^{o}C overnight. To precipitate the digested DNA 10μl RNase free 3M Sodium Acetate pH 5.2 (Merck, Cat. No. 71196) and 250μl of RNase free 100% ethanol (Scharlau, Cat. No.ET006) were added to the mixture and incubated at -20^{o}C for 1 hour. Then the mixture was centrifuged at 14K rpm for 15 min at RT, the DNA pellet was then washed twice with 70% ethanol in RNase-free H_2O and it was left to air dry. To test the success of the digest, 1μl of the digested and 0.5μl of the undigested (control) DNA was loaded on 1% Agarose gel in 1X TAE gel and run at 120 V for 30 min.

***In vitro* transcription for making the RNA probe.**

Anti-sense Digoxigenin-labeled and Fluorescein-labeled RNA probes were synthesized by *in vitro* transcription (IVT) from the linearized plasmid template using RNA polymerases (T7, T3 or SP6) and a ribonucleotide mixture in which the UTPs are labeled either with Digoxigenin (DIG-11-UTP, Roche, Cat. No.11277073910) or Fluorescein

(Fluorescein-12-UTP, Roche, Cat. No. 11427857910). The transcription mixture (10μl reaction) was included 0.5μg of linearized template cDNA, 1μl transcription buffer (10X), 1μl DIG RNA labeling mix (Roche, Cat. No.11277073910), 0.5μl RNase Inhibitor (HT Biothechnology Ltd, Cat. RI01a- 40units/μl), 0.5μl RNA polymerase (SPC6: Roche, Cat. No.10810274001; T3: Roche, Cat. No.11031163001; T7 Roche, Cat. No. 10881767001) and RNase free ddH_2O. *In vitro* transcription was performed for 3 hours at 37^oC for T3 and T7 and at 40^oC for SP6 polymerases. The cDNA template was then digested by RNase-free DNaseI (1μl at 1 unit/μl, 15 min at 37°C, Roche, Cat. No.04716728001) and the RNA was precipitated by adding 10μl 4% LiCl (Fisher Scientific, Cat. No.L/2201/50, 250g), 89μl RNase-free H_2O and 300μl 100% ethanol and the mixture was incubated at -20^oC for 1hour. After centrifugation at 14k rpm for 20 min at 4^oC, the precipitated RNA was washed twice with 70% ethanol in RNase-free H_2O and was left to air dry. For RNA resuspension 55μl of RNase-free H_2O were added and incubated for -80^oC for 1 hour. To test the success of IVT 5μl of each of the RNA probes were run on RNase free 1X/TAE 1% agarose gel at 150V for 20-25 min. The RNA probes then stored at -80^oC until used. For Fluorescein-labeled RNA probe preparation the method that was used for *in vitro* transcription was the same but instead of digoxigenin labeling mix, was used Fluorescein RNA Labeling Mix (Roche, Cat. No. 11685619910).

Table II: Restriction enzymes and polymerases for *anti-sense* probes that were used for each gene.

Gene	Restriction Enzymes	Polymerase for *anti-sense* probe
AFP	XhoI	T3
Bmp4	AccI	T7
Bra	XbaI	T7
Cdx2	XhoI	T7
Cer	SalI	Sp6
Chrd	SacI	T3
Cripto	HindIII	T7
Elf5	SalI	T7
Eomes	EcoRI	T7
Esrrb	EcoRI	Sp6
Fgf8	HindIII	T3
Foxa2	HindIII	T7
FoxH1	SalI	T7
Gsc	SacI	T3
Hex	EcoRI	T7
Nodal	BamHI	T7
Noto	SmaI	Sp6
Shh	HindIII	T3
Snail	ClaI	T7
Spc4 (Pace)	SalI	T7
Wnt3	EcoRI	T3

3.3.2 One colour whole-mount RNA *in situ* hybridization.

(*Georgiades and Rossant 2006*)

<u>Day 1:</u> Rehydration, permeabilization, post-fixation, pre-hybridization, hybridization.

At first the *Ets2* type-II mutants and wt (controls) embryos rehydrated for 5 min at RT through a methanol series (100% methanol, 75% methanol, 50% methanol, 25% methanol in RNase-free PBT (1X RNase-free PBS with 0.1% Tween 20) for 5 min at RT and then washed twice for 10 min at RT in RNase-free PBT. The embryos were permeabilized by incubation at RT with RNase free RIPA solution (150mM RNase-free NaCl (Sigma, Cat.No. S3014), 1% Nonidet P-40 (Sigma, Cat. No. 18896-100ml), 0.5% Sodium deoxycholate (Sigma, Cat. No. D6750-25g), 0.1% SDS (Sigma, Cat. No. L3771-100G), 1mM EDTA (Fisher Scientific, Cat. No. D/0700/53-500g), 50mM Tris pH 8 (Fisher Scientific, Cat. No T/P630/60-1Kg) either for 30min (for E7.0 and E7.5-75 stage embryos) or for 20min for (for E6.75 stage embryos). Alternative, for permeabilization was also used 10μg/ml Proteinase K (Roche, Cat. No. 03115836001) in RNase-free PBT. The incubation with Proteinase K for E7.5-E7.75 stage embryos was 2:30 min at RT and for E6.4-E7.0 stages the time of incubation was 1:30 min at RT. To stop the reaction (and hence the permeabilization) the samples were washed three times for 5min at RT in RNase free PBT and post fixated in 0.2% Glutaraldehyde (Sigma, Cat. No. G6257) in 4% RNase-free pfa for 20min at RT. After fixation they were incubated in the prehybridization solution (DEPC-treated H_2O (Sigma, Cat. No. D5758-25ML), 50% Ultrapure formamide (Invitrogen, Cat. No.15515-026), 5XSSC RNase-free pH4.5 (3M NaCl, Fisher, Cat. No. BPE358-10; 0.3M Sodium Citrate Dihydrate, Fisher, Cat. No. BPE327-1), 50mg/ml tRNA (Roche, Cat. No. 10109495001), 50mg/ml Heparin (Sigma, Cat. No. H-3393), 1% RNase-free 10% SDS) for 5 hours in 67^{o}C hybridization oven. Finally, the embryos were incubated in the hybridization solution (prehybridization solution containing the appropriate amount of RNA digoxigenin-labeled probe of interest) in 67^{o}C hybridization oven overnight (for at least 14 hours).

<u>Day 2</u>: Post-hybridization washes, RNase step, pre-block and antibody incubation.

After overnight hybridization the embryos were washed three times with Solution I for 30 min at 67^{o}C. For 10ml total volume Solution I, were added: 5ml Formamide (FLUKA, Cat. No.47670-2.5L-F), 2,5ml 20X RNase free SSC pH4.5, 1,5ml RNase free H_2O and 1ml 10% SDS. Then they were washed three times with TNT solution (for 50ml total volume TNT solution were added: 44,5ml RNase-free ddH_2O, 5ml 5M NaCl (Fisher Scientific, Cat. No. BPE358-10), 0.5ml 1M TrisCl pH7.5 (Fisher Scientific, Cat. No.

T/P630/60), and 0.1% Tween 20) for 5 min at RT followed by incubation with RNaseA (Roche, Cat. No. 10109169001, 10mg/ml) in TNT solution at 37^{o}C for 1hour. The embryos were then washed three times with Solution II. For Solution II were added 5ml Formamide (FLUKA, Cat. No. 47670-2.5L-F), 1ml 20X RNase-free SSC pH4.5, 4ml RNase-free H_2O and 100μl 10% SDS at 67^{o}C. Then the embryos were incubated three times with MAB solution pH 7.5. The MAB solution was contained ddH_2O, 0.1M Maleic acid (Sigma, M0375), 2mM Levamisole (Sigma, L9756), 0.15M NaCl and 0.1% Tween20) for 5 min at RT. They were then incubated in pre-block solution containing MAB/Block (MAB solution and 1% Blocking reagent, Roche, Cat. No. 11096176001) with 0.1% Sheep Serum (Sigma, Cat. No. S2263) for 3 hours at RT and finally were incubated overnight with the antibody (1:1000, Anti-Digoxigenin-AP, Fab fragments, Roche, Cat. No. 11093274910) at 4^{o}C in the dark with rocking.

Day 3: Post-antibody washes.

The embryos were washed three times with MAB solution for 10 min at RT, then six times for 1 hour at RT and finally were left in MAB solution overnight at 4^{o}C with rocking.

Day 4: Visualization of the probe signal.

For the color reaction the embryos were prepared as followed: first they were incubated three times with NTMT solution for 10 min at RT. The NTMT was contained ddH_2O, 1M TrisCl pH 9.5, 1M $MgCl_2$ (Sigma, M2670), 200mM Levamisole and 0.1% Tween 20. Then were incubated in BM purple (which is an Alkaline Phosphate substrate producing a chromogenic reaction blue/purple color, Roche, Cat. No.11442074001) in the dark. The color development time was varied and this was depended on the probe (from 2 hours to 48h). The embryos after the color development were washed twice with PBT for 10 min at RT and then were fixed in 4% pfa. The embryos were documented as photos were taken using the inverted microscope Zeiss Axiovert 200M with AxioVision software.

3.3.3 Double colour whole-mount RNA *in situ* hybridization.

Day 1: Rehydration, permeabilization, post-fixation, pre-hybridization, hybridization.

At first the *Ets2* type-II mutants and wt (controls) embryos rehydrated for 5 min at RT through a methanol series (100% methanol, 75% methanol, 50% methanol, 25%

methanol in RNase-free PBT (1X RNase-free PBS with 0.1% Tween 20) for 5 min at RT and then washed twice for 10 min at RT in RNase-free PBT. The embryos were permeabilized by incubation at RT with RNase free RIPA solution (150mM RNase-free NaCl (Sigma, Cat.No. S3014), 1% Nonidet P-40 (Sigma, Cat. No. 18896-100ml), 0.5% Sodium deoxycholate (Sigma, Cat. No. D6750-25g), 0.1% SDS (Sigma, Cat. No. L3771-100G), 1mM EDTA (Fisher Scientific, Cat. No. D/0700/53-500g), 50mM Tris pH 8 (Fisher Scientific, Cat. No T/P630/60-1Kg) either for 30min (for E7.0 and E7.5-75 stage embryos) or for 20min for (for E6.75 stage embryos). Alternative, for permeabilization was also used 10μg/ml Proteinase K (Roche, Cat. No. 03115836001) in RNase-free PBT. The incubation with Proteinase K for E7.5-E7.75 stage embryos was 2:30 min at RT and for E6.4-E7.0 stages the time of incubation was 1:30 min at RT. To stop the reaction (and hence the permeabilization) the samples were washed three times for 5min at RT in RNase free PBT and post fixated in 0.2% Glutaraldehyde (Sigma, Cat. No. G6257) in 4% RNase-free pfa for 20min at RT. After fixation they were incubated in the prehybridization solution (DEPC-treated H_2O (Sigma, Cat. No. D5758-25ML), 50% Ultrapure formamide (Invitrogen, Cat. No.15515-026), 5XSSC RNase-free pH4.5 (3M NaCl, Fisher, Cat. No. BPE358-10; 0.3M Sodium Citrate Dihydrate, Fisher, Cat. No. BPE327-1), 50mg/ml tRNA (Roche, Cat. No. 10109495001), 50mg/ml Heparin (Sigma, Cat. No. H-3393), 1% RNase-free 10% SDS) for 5 hours in 67^{o}C hybridization oven. Finally, the embryos were incubated in the hybridization solution (prehybridization solution containing the appropriate amount of RNA digoxigenin-labeled probe of interest) in 67^{o}C hybridization oven overnight (for at least 14 hours). Moreover for <u>triple colour</u> whole-mount RNA *in situ* hybridization the embryos were incubated in the hybridization solution containing the appropriate amount of the three RNA probes. The one was fluorescein-labeled and the other two were digoxigenin-labeled RNA probes.

<u>Day 2</u>: Post-hybridization washes, RNase step, pre-block and antibody incubation.

After overnight hybridization the embryos were washed three times with Solution I for 30 min at 67^{o}C. For 10ml total volume Solution I, were added: 5ml Formamide (FLUKA, Cat. No.47670-2.5L-F), 2,5ml 20X RNase free SSC pH4.5, 1,5ml RNase free H_2O and 1ml 10% SDS. Then they were washed three times with TNT solution (for 50ml total volume TNT solution were added: 44,5ml RNase-free ddH_2O, 5ml 5M NaCl (Fisher Scientific, Cat. No. BPE358-10), 0.5ml 1M TrisCl pH7.5 (Fisher Scientific, Cat. No. T/P630/60), and 0.1% Tween 20) for 5 min at RT followed by incubation with RNaseA (Roche, Cat. No. 10109169001, 10mg/ml) in TNT solution at 37^{o}C for 1hour. The embryos

were then washed three times with Solution II. For Solution II were added 5ml Formamide (FLUKA, Cat. No. 47670-2.5L-F), 1ml 20X RNase-free SSC pH4.5, 4ml RNase-free H_2O and 100μl 10% SDS at 67^{o}C. Then the embryos were incubated three times with MAB solution pH 7.5. The MAB solution was contained ddH_2O, 0.1M Maleic acid (Sigma, M0375), 2mM Levamisole (Sigma, L9756), 0.15M NaCl and 0.1% Tween20) for 5 min at RT. They were then incubated in pre-block solution containing MAB/Block (MAB solution and 1% Blocking reagent, Roche, Cat. No. 11096176001) with 0.1% Sheep Serum (Sigma, Cat. No. S2263) for 3 hours at RT and finally were incubated overnight with the antibody (1:1000, Anti-Digoxigenin-AP, Fab fragments, Roche, Cat. No. 11093274910) at 4^{o}C in the dark with rocking.

<u>Day 3</u>: Post-antibody washes.

The embryos were washed three times with MAB solution for 10 min at RT, then six times for 1 hour at RT and finally were left in MAB solution overnight at 4^{o}C with rocking.

<u>Day 4:</u> Visualization of the RNA Fluorescein-labeled probe signal.

For the color reaction the embryos were prepared as followed: first they were incubated three times with NTMT solution for 10 min at RT. The NTMT was contained ddH_2O, 1M TrisCl pH 9.5, 1M $MgCl_2$ (Sigma, Cat. No. M2670), 200mM Levamisole and 0.1% Tween 20.. Then the embryos were incubated in TBS staining solution containing 1M TrisHCl pH9.5, 1M $MgCl_2$, 5M NaCl plus INT/BCIP (Alkaline Phosphates substrate producing red/orange color, Roche, Cat. No. 1681460) in the dark. The color development time for Fluorescein-labeled probes was varied and this was depended on the probe. The embryos were documented as photos were taken using the inverted microscope Zeiss Axiovert 200M with AxioVision software. After documentation they were then used for the development of the digoxigenin-labeled probes.

<u>Day 5:</u> Dehydration, Rehydration, pre-block and incubation with the second antibody.

The *Ets2* type-II mutants and wt (controls) embryos dehydrated and then rehydrated through a methanol series (100% methanol, 75% methanol, 50% methanol, 25% methanol in RNase-free PBT (1X RNase-free PBS with 0.1% Tween 20) for 5 min at RT for the removal of the orange colour from the embryos. Then they were washed three times in RNase-free PBT for 5 min at RT. To remove any alkaline phosphatases the embryos were incubated in RNase-free PBT for 1 hour at 70^{o}C (hybridization oven). After the alkaline phosphatases heat

inactivation the samples were washed three times with MAB solution pH 7.5 (ddH_2O, 1M Maleic acid, 200mM Levamisole, 5 M NaCl and 0.1% Tween 20) for 5 min at RT and then incubated in pre-block solution containing MAB/Block (MAB solution and 1% blocking reagent) with 0.1% Sheep Serum for 3 hours at RT. Finally the embryos were left overnight with the second antibody (Anti-Digoxigenin-AP, Fab fragments) at 4^{o}C in the dark with rocking.

<u>Day 6:</u> Post-antibody washes.

The embryos were washed three times with MAB solution for 10 min at RT, then six times for 1 hour at RT and finally were left in MAB solution overnight at 4^{o}C with rocking.

<u>Day 7:</u> Visualization of the RNA digoxigenin-labeled probes signal.

For the colour reaction the embryos were prepared as followed: first they were incubated three times with NTMT solution (ddH_2O, 1M TrisCl pH 9.5, 1M $MgCl_2$, 200mM Levamisole) for 10 min at RT and then were incubated in BM purple in the dark for the development of the digoxigenin-labeled probes. The BM purple removes a phosphate and turns the substrate purple. The embryos documented as photos were taken using the inverted microscope Zeiss Axiovert 200M with AxioVision software.

3.4 Histology.

For histology, the *Ets2* type-II mutants and wt (controls) embryos after dissection were fixed in 4% pfa in 1XPBS overnight at 4^{o}C. The embryos then were dehydrated for 2 min at 4^{o}C through an ethanol series (100% ethanol, 70%, 50% and 30% ethanol in ddH_2O), then were incubated twice in xylene (Fisher, Cat. No. X/0250/17) for 2 min at RT and finally embedded in paraffin wax (Fisher Scientific, Cat. No. P7385) overnight incubation in 62^{o}C paraffin wax). The embedded embryos were then orientated in the molds and left at RT overnight. Then the molds were stored at 4^{o}C until used. The molds were then pasted in the cassettes and placed in the microtome. The embedded embryos in paraffin wax were sectioned (cross sections) and the sections were placed on slides for further analysis. The thickness of sections was of 7 (microns) μm.

3.4.1 Hematoxylin and Eosin (H&E) staining.

Hematoxylin and Eosin staining was used for the selection based on morphology of embryo sections at the level of the primitive streak of the *Ets2* type-II mutant and wt (control). Slides with every 10^{th} embryo section were stained with Haematoxylin (which marks the nucleus) and Eosin (which marks the cytoplasm) so as to be able to choice the sections of the area of interest.

At first the embryo sections were deparaffinized as they incubated in xylene for 2min at RT. Then the embryo sections were rehydrated as they were incubated twice in 100% ethanol for 2 min at RT and through a methanol series (100% methanol, 75%, 50% and 30% methanol in ddH_2O) for 2min at RT. After rehydration they were washed in ddH_2O for 2 min at RT and were placed on haematoxylin solution (Sigma, Cat. No. GHS332) for 5 min at RT. The slides were rinsed under running tap water until the water was no longer colored (~5 min.) and then were incubated in 70% ethanol with 0.5% v/v of HCl for seconds at RT until the sections turned pink. Afterward the slides were rinsed under running tap water and incubated for 3 min in 0.5% eosin solution (Sigma, Cat. No. 318906). Then the slides were washed with in ddH_2O for 30 sec at RT dehydrated through a methanol series (30%, 50%, 75% methanol in ddH_2O, 100% methanol). Then the slides were incubated twice in 100% ethanol for 2 min at RT and then twice in xylene for 2min at RT. Finally the sections were mounted with DPX (Sigma, Cat. No. 44581) which was xylene-based mounting medium and the staining was visualized using the inverted microscope Zeiss Axiovert 200M with AxioVision software. The paraffin sections of interest that were selected based on H&E staining (from *Ets2* type-II mutant and wt embryos at the level of the PS), they placed on slides and analyzed using immunohistochemistry for the detection of E-cadherin (Cdh1) protein.

3.5 Immunohistochemistry

3.5.1 Fluorescent immunohistochemistry on embryo paraffin wax sections.

Ets2 type-II mutants and wt (controls) embryos were embedded in paraffin wax as described above (Histology section). For the detection of E-cadherin (Cdh1) protein embryo sections were incubated with the rabbit anti-E-cadherin antibody (Abcam, Cat. No. ab53033) at 1:100 dilution, followed by incubation with an anti-rabbit IgG secondary antibody

conjugated to Cy3 (Abcam, Cat. No. ab6939) at 1:100 dilution. The wax embedded sections (cross sections at the level of the PS) of *Ets2* type-II mutant embryos and wt embryos (controls) were first deparaffinized using xylene. The embryo sections were incubated twice for 2 min in Xylene at RT, and then were rehydrated for 2 min at RT through an ethanol series (100% ethanol, 70%, 50% and 30% ethanol in ddH_2O) for 2min at RT followed a microwave heat treatment with TriSodium Citrate pH6 (Sigma, Cat. No. S1804) for 10 min (Antigen Retrieval). The embryo sections were then blocked with 1% BSA (Albumin from bovine serum, Sigma, Cat. No. A9418) and incubated with the E-cadherin antibody (1μl antibody in 100μl blocking solution which was 1% BSA) at 4^{o}C overnight. Embryo sections were then incubated with the secondary antibody Cy3 for 2 hours at RT and counterstained with Hoechst (marks the nucleus). Finally the sections were washed for 10 min in 1% PBS and mounted with coverslips. (*Elia et al., 2011*) The immunostaining was visualized under fluorescence using a Zeiss Axio Imager.Z2 confocal microscope (E-cadherin was detected as red fluorescence and Hoechst as blue fluorescence). Finally the photos were analysed using the Zen 2010 software.

3.5.2 Whole-mount immunohistochemistry.

Ets2 type-II mutants and wt (controls) embryos at E7.5-E7.75 stage were used for whole-mount immunohistochemistry for the detection of the *Dolichos biflorus agglutinin* (DBA) lectin. DBA lectin which is specific for D-N-acetylgalactosamine was found to be expressed in VE cells but not in the DE cells (*Sherwood, Jitianu et al. 2007*). The embryos after dissection were washed twice with 1XPBS and then fixed in 4% pfa in 1XPBS O/N at 4^{o}C. Also, embryos that were already in 4% pfa in 1XPBS after *in situ* hybridization treatment were used for whole-mount immunohistochemistry for the detection of the DBA lectin. All embryos were at first washed three times in 1XPBS plus 0.1% Triton-X100 (Sigma, Cat. No. T8787) for 10min at RT, were permiabilized in 1XPBS plus 0.25% Triton-X100 for 30 min at RT and were washed three times in IXPBS plus 0.1% Triton-X100 for 10 min at RT. The embryos were then blocked with blocking solution containing 1% BSA in 1XPBS, plus 10% goat serum (Abcam, Cat. No. ab7481) and 0.1% Triton-X100 for 1 hour at RT (e.g. for 10ml blocking solution were added: 9ml 1% BSA in 1XPBS, 1ml goat serum and 10μl 0.1% Triton-X100). For the first antibody reaction the embryos were incubated with biotinylated DBA lectin (Sigma, Cat. No. L6533) in blocking solution without 0.1% Triton-X100 in dilution 1:3000, O/N at 4^{o}C. The next day the embryos were washed three times in

1XPBS plus 0.1% Triton-X100 for 10 min at RT. For the secondary antibody reaction they were incubated with Streptavidin Peroxidase (ready used from abcam, Abcam, Cat. No. ab64269) for 15 min at RT and then were washed three times in 1XPBS plus 0.1% Triton-X100 for 10 min at RT. Finally for the chromogen reaction the embryos were incubated in DAB [1ml DAB substrate with 20μl 3,3' Diaminobenzidine (DAB), Abcam, Cat. No. ab64238] and then washed with 1XPBS to stop the reaction. During the chromogen reaction the peroxidase reacts with the hydrogen peroxidase (DAB substrate contained 5% hydrogen peroxidase) to degrade it, which in turn reacts with the DAB and produces a dark brown colour.

3.6 Quantitative Real Time PCR.

Quantitative Real time PCR (qRT-PCR) is a method that used for the quantification of differences in mRNA expression levels. It's a sensitive method that allows exponential amplification of short cDNA sequences using a pair of primers of about 20 nucleotides length.

3.6.1 RNA isolation from embryos.

Ets2 type-II mutants and wt (controls) embryos were dissected at E6.7 stage. After dissection the embryos washed twice with IX PBS and placed in a 1,5ml eppendorf tubes. The "*NucleoSpin RNA XS*" kit from "*Macherey-Nagel*" (Cat. No. 740902.50) was used for RNA isolation as it allows an efficient RNA isolation/purification from very small samples. This kit was contained a column with a *micro silica membrane* of highest sensitivity allowing the purification of high concentrations of RNA and this make it suitable for qRT-PCR. Using the "*NucleoSpin XS RNA*" kit, the cells at first were lysed by incubation in solutions (RA1, RA2, MDB buffers) containing large amounts of chaotropic ions (they contain guanidinium thiocyanate) which inactivates RNases and creates the appropriate binding conditions which help the adsorption of RNA onto the silica membrane of the column. However, DNA which was also bound to the silica membrane was removed by an RNase-free rDNase solution which was directly applied onto the silica membrane of the column. Simple washing steps with two different buffers (RA2, RA3 buffers) were removed salts, metabolites and

macromolecular cellular components and finally the pure RNA was eluted with RNase-free H_2O. The RNA isolation using the "*NucleoSpin RNA XS*" kit was performed at room temperature. The embryos at first were lysed and homogenized by adding 200μl Buffer RA1 and 4μl TCEP (Tris (2-carboxyethyl) phosphate) buffer to the sample and vortex vigorously (2 x 5 seconds). Then 5μl of the Carrier RNA solution (poly(-A) RNA: poly(A) potassium salt, 20ng) was added to the lysate, mixed by vortexing (2 x 5 s) and spin down (1000 x g). The lysate was then filtered through "*NucleoSpin Filter*" by centrifugation for 30 s at 11,000 x g. The "*NucleoSpin Filter*" was discarded and then 200μl 70 %ethanol were added to the homogenized lysate and mixed by pipetting up and down (5 times). The lysate was then loaded to the "*NucleoSpin RNA XS Column*" and centrifuged for 30s at 11,000 x g. To dry the silica membrane of the column 100μl MDB (Membrane Desalting Buffer) were added and centrifuged at 11,000 x g for 30s. Then to digest the DNA 25μl of RNase-free rDNase were applied directly onto the center of the silica membrane of the column and the mixture was incubated at room temperature for 15 min. To wash and dry the silica membrane of the column at first were added 100μl Buffer RA2 (inactivation of the rDNAase) to the "*NucleoSpin RNA XS Column*", incubated for 2 min at RT and centrifuged for 30s at 11,000 x *g*. Then were added 400μl Buffer RA3 to the column and centrifuged for 30s at 11,000 x *g*, the flow through was then discard and the column was placed back into the collection tube. Finally 200μl Buffer RA3 (96%-100% ethanol) were added to the column and centrifuged for 2 min at 11,000 x g to dry the membrane. The RNA was eluted in 5μl RNase/DNase free H_2O and centrifuged for 30 s at 11,000 x g. The concentration of the RNA was calculated using the nanodrop and then it was stored at -80^{o}C until used. The concentration of the RNA that was used for reverse transcription was ~10ng.

3.6.2 Reverse transcription.

Reverse transcriptase was used to convert mRNA into cDNA using an oligo dT primer and the enzyme reverse transcriptase (AMV, Finnzymes- Thermo Scientific, Cat. No. F-570S). For reverse transcription 1.6μl oligo dT primers (50nM, Invitrogen, Cat. No. 18418012) were added in total RNA (16ng) that was isolated and incubated at 70^{o}C for 10 min. Then the samples were incubated on ice for 3 min and reverse transcribed. For total reaction 20μl were added: the appropriate volume of DEPC H_2O, 2μl dNTPs (10mM), 0,5μl RNase inhibitor (Invitrogen, Cat. No. 10777-019), 2μl enzyme buffer (1X) and 0,4μl enzyme

reverse transcriptase AMV (4000 units/ml stock). The mixture was then incubated at 42^{o}C for 40 min and the cDNA stored at -20^{o}C until used. (*Odiatis and Georgiades 2010*)

3.6.3 PCR reaction.

For quantitative Real Time-PCR (qRT-PCR) the primers for the housekeeping gene *Beta-actin* (internal gene control), as well as for *Ets2*, *Bmp4* and *Nodal* were designed using the "*Primer 3 Output*" software from cDNA sequences found in the NCBI Gene Database (Nucleotide) and are shown in Table III. Also the specificity of the primers was tested using a BLAST analysis against the genomic NCBI database. The anneal temperature for the each set of primers was designed to be 59^{o}C. The conditions for Real Time PCR reactions were: 50°C for 2 minutes, 95°C for 12 minutes; 39 cycles of 95°C for 20 seconds, 59°C 1 minute; 72°C for 30 seconds, then 72°C for 10 minutes. For this experiment was used cDNA from *Ets2* type-II mutants and wt (control) embryos at E6.7 stage. Each sample was done in triplicate for each gene. All PCR reactions were performed in a 10μl reaction volume, using 5μl SYBR Green Supermix (Applied Biosystems, Cat. No. 4309155), 0,5μl of 200nM of each specific primer and 1μl of diluted cDNA (1:10) from one embryo equivalent per reaction. During the reaction SYBR Green which is a DNA-binding dye binds to cDNA (the region of the cDNA in which the pair of primers binds) causing fluorescence of the dye. The Real Time PCR machine (iCycler iQ Real-Time PCR Detection System, Bio-rad) was detected the fluorescence and the software was calculate the Ct (Cycle threshold) values from the intensity of the fluorescence. The Ct is the number of cycles required for the fluorescent signal to cross the threshold. Ct is the cycle number at which the increase in fluorescence is exponential as the threshold is at the base of the linear phase. Ct levels are inversely proportional to the amount of target nucleic acid in the sample. The relative quantification of gene expression between *Ets2* type-II mutants and wt (control) embryos was analyzed by the $2^{-\Delta\Delta Ct}$ approximation method (*Livak and Schmittgen 2001*). For each sample (either the *Ets2* type-II mutants or wt embryos) the difference in Ct values for the genes of interest and the internal gene control (which was the *B-actin*) was calculated as the ΔCt value. Then, the subtraction of the ΔCt of the gene of interest of the wt embryo from the ΔCt of the same gene of the mutant embryo results to the ΔΔCt value. The $2^{-\Delta\Delta Ct}$ equation represents the relative quantity value (Fold change) of the gene of interest of the mutant embryo of that gene in the wt (control) embryo. Two values per gene from four separate mutant embryos (n=4) were

obtained to calculate the standard error of the mean (s.e.m). Statistical analysis was carried out using the one-tailed unpaired Student's t-test, found online at: http://faculty.vassar.edu/lowry/VassarStats.html. Differences were considered statistically significant for those with $P<0.001$

Table III: The primers that were designed for qRT-PCR.

Gene	Forward Primer	Reverse Primer
B-actin	5-gacggccaggtcatcactat-3	5-aaggaaggctggaaaagagc-3
Ets2	5-gggagttcaagcttgctgac-3	5-cccgaagtcttgtggatgat-3
Bmp4	5-cgttacctcaagggagtgga-3	5-atgcttgggactacgtttgg-3
Nodal	5- actttgctttgggaagctga-3	5- acctggaacttgaccctcct-3

Chapter 4

RESULTS

4.1 Results for specific aim 1: Establishment of a morphological and marker gene expression assay for distinguishing between *Ets2* Type-I and Type-II phenotypes.

Generation and identification of *Ets2*-/- embryos

Ets2-/- type-I and type-II embryos (that is, homozygous mutants for the *Ets2* null mutation) were generated by inter-crossing *Ets2-/+* (i.e. heterozygous) parental mice. Based in gross morphology, homozygous mutant embryos could be distinguished from their wt and heterozygous littermates, based on their smaller size and reduced accumulation of maternal blood around the implantation site during their isolation. Confirmation of their homozygosity was accomplished by PCR genotyping using either genomic DNA extracted from Richert's membrane (or EPC fragment) or from whole embryos after whole-mount RNA *in situ* hybridization or immunochemistry treatments. This was carried out as previously shown (*Yamamoto, Flannery et al. 1998; Georgiades and Rossant 2006*) using two sets of primers: one specific for the wild-type and the other for the mutant allele, producing a 220 or 200 base pair long fragments, respectively (data not shown).

Distinguishing between type-I and type-II phenotypes

It was important for the interpretation of the results to be able to clearly distinguish between these two phenotypes. It was previously reported that one way to distinguish type-I from type-II was the presence of a morphological distal VE thickening (apparent from pre-gastrulation stages, indicating failure of DVE to become AVE) and absence of PS in type-I, but not type-II mutants (*Georgiades and Rossant 2006*). This was confirmed here as shown by the presence of a distal VE thickening in type-I mutants (that is, mutants without a PS identified by whole mount RNA *in situ* hybridization for the PS marker *Bra*) at E6.7 and E7.5-E7.75 (*Fig.12a,b,e,f*). This VE thickening of type-I mutants was confirmed to be DVE that failed to anteriorize (that is, failed to become AVE) based on the distal localization of *Hex* expression (a DVE/AVE marker) (*Fig.12c,d*). In contrast, type-II mutants were confirmed to have a PS and an AVE, based on double-colour whole-mount *in situ* hybridization on the same embryo for *Bra* (PS marker) and *Cer1* (DVE/AVE and DE marker) (*Fig.19a-c*, see below). The absence of a thickened distal VE in type-II mutants (that is, mutants with a PS) was confirmed by the absence of this morphology in all mutants that express PS markers such as *Bra* or *Cripto* at E6.7 or E7.5 (*Fig.13a,c,d; Fig.19d*).

Type-I mutants lack anterior PS derivatives

Since type-I mutants lack a PS and mesoderm (a major PS derivative), it was important to confirm that they also lack the other major PS derivatives DE, node and anterior axial mesendoderm (AME). This was found to be the case based on examination of type-I mutants at E7.75 that were subjected to double-colour whole-mount *in situ* hybridization for *Bra* (PS marker) and *Shh* (node and AME marker) and DBA lectin staining (indirect marker for DE formation). DBA lectin specifically stains all VE, but not DE, mesoderm or epiblast cells. Therefore, when DE cells intercalate into the epiblast associated VE to form the DE layer, the initially closely packed VE cells (which are marked by continuous DBA positivity) become dispersed in this part of the VE (generating patchy DBA positivity) so as to be able to accommodate the newly formed DE cells. VE dispersal does not occur in the EXE-associated VE, where DE does not form (and so there is continuous DBA positivity) (*Sherwood, Jitianu et al. 2007*). It is shown here that type-I mutant embryos (that is, mutants negative for *Bra* expression) also lack expression of Shh (suggesting absence of node and AME) and display continuous DBA lectin positivity (indicative of absence of DE formation) (*Fig.12e,f*) in type-I mutants is consistent with the absence of GFP positivity from the VE of E7.75 type-I chimaeras (see *Fig.9c,d in 'Aims' section above*).

Figure 12: *Ets2* type-I phenotype that distinguish it from that of type-II.

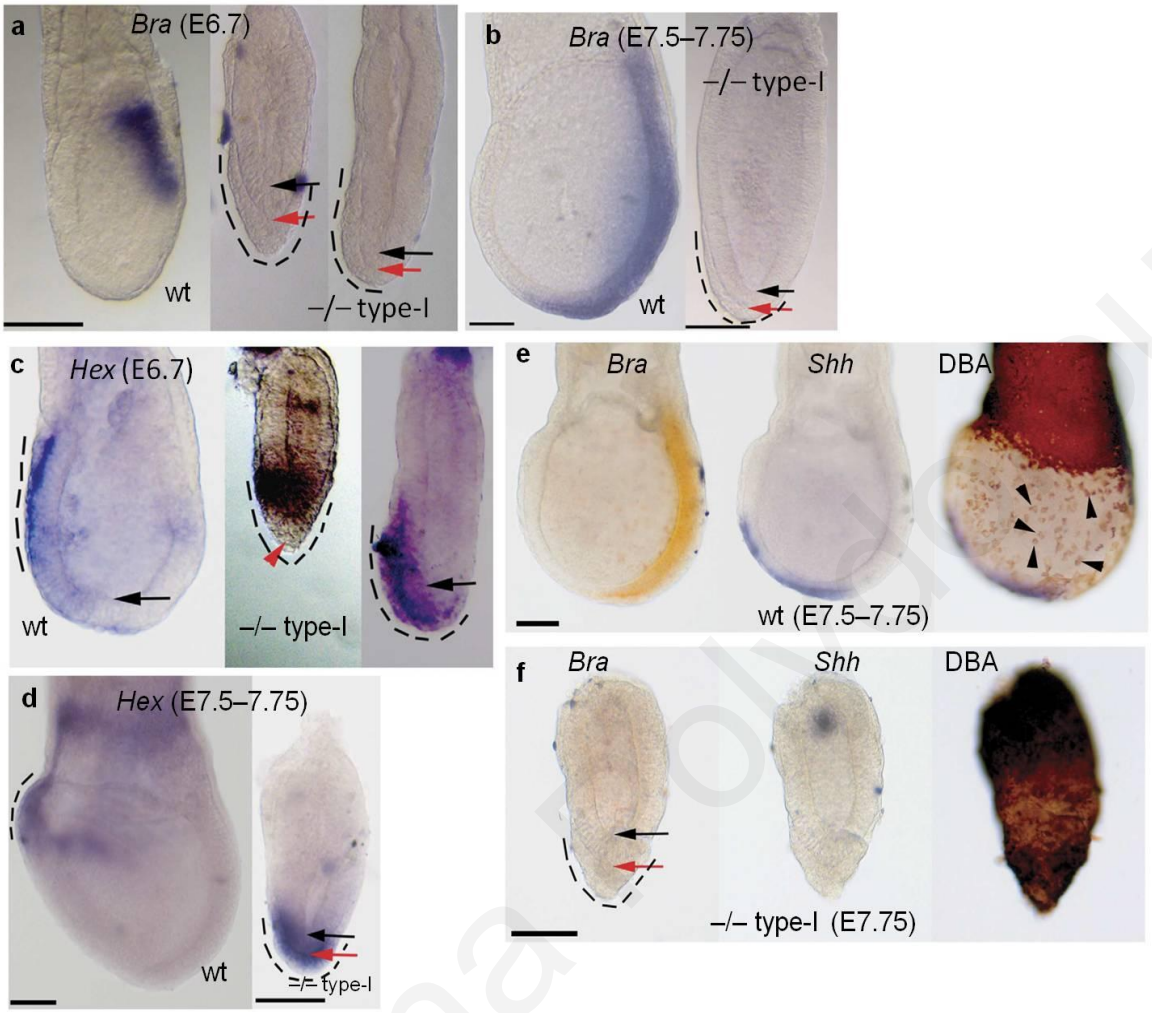

Bra expression of type-I mutants and controls at E6.7 (**a**) and E7.5–7.75 (**b**). Note the absence of *Bra* expression and a DVE thickening, which always includes a region at the distal tip of the epiblast. **(c,d)** *Hex* expression in controls and type-I mutants at E6.7 **(c)** and E7.5–7.75 stages **(d).** Note the *Hex* positivity at the distal tip of the epiblast. **(e)** Double *in situ* hybridization with *Bra* (orange) and *Shh* (blue), followed by DBA staining (brown) of the same embryo in E7.5–7.75 controls **(e)** and type-I mutants **(f).** Note that type-I mutants (that is, mutants without *Bra* expression) do not express *Shh* and display continuous DBA positivity, indicative of failure to form DE. Black and red arrows depict the luminal side and outer side of distal tip epiblast, respectively. Dotted lines depict the localization of DVE/AVE along the anterior-posterior axis. Black arrowheads depict VE cells that experienced spreading, while red arrowheads depict regions of Richert's membrane left attached to the embryo. Scale bars, 100 μm.

4.2 Results for specific aim 2: Primitive streak development in *Ets2* type-II mutant embryos.

The PS of type-II mutants is abnormally short.

The first aim here was to confirm the existence and identify the extent of the PS elongation defect in type-II mutants. Using whole-mount RNA *in situ* hybridization, the expression pattern of *Bra* (a PS and newly formed mesoderm marker; *Herrmann et al., 1991*), *Cripto* (marker of PS and entire mesoderm up to E7.0, which then becomes downregulated from the mesoderm by E7.5 stage; (*Ding, Yang et al. 1998; Arnold and Robertson 2009)* and *Chordin* (*Chrd;* marker of anterior PS from the early streak stage onwards; (*Bachiller, Klingensmith et al. 2000; Dunn, Vincent et al. 2004*) was examined in *Ets2* type-II mutants at E7.5-E7.75, a stage when the PS in controls has fully extended to the distal tip of the embryo. It was found (*Fig.13*) that the PS of these mutants is short at varying degrees and in all cases fails to reach the distal tip, based on the pattern of *Bra* (n=11), *Cripto* (n=3) and *Chr* (n=3) expression. Moreover, the presence of *Cripto* expression in the mesoderm of the mutants suggests that their mesoderm is specified, at least to some degree (*Fig.13c,d*). Interestingly in some mutants, *Bra* and *Cripto* expression, in addition to being confined to the PS, it was also found to be ectopically localized in the anterior epiblast (*Fig.13d; Fig.16d*). This phenotype is further dealt later.

The PS of type-II mutants is abnormally patterned and these mutants lack an allantois and amnion.

The second aim here was to investigate the failure of posterior PS derivative formation and patterning of the PS along its anterior-posterior (A-P) axis in type-II mutants. at E7.5-E7.75 stage. The above-mentioned absence of anatomical allantois and amnion in the mutants (*Fig.8b,d,f*) was confirmed here by examining the expression of *Bmp4,* which at E7.75 stage marks the posterior PS, the base of allantois, the chorion and amnion (Winnier, Blessing et al. 1995) and the expression of *Cdx2* (which marks the entire PS and base of allantois; (*Chawengsaksophak, de Graaff et al. 2004*) using whole-mount RNA *in situ* hybridization analysis. *Bmp4* (n=3; *Fig.13e*) and *Cdx2* (n=3; *Fig.13f*) expression at this stage was absent from *Ets2* type-II mutant embryos. Based on these results the A-P patterning of the PS is defective and there is no formation of chorion, amnion and allantois.

Type-II mutants fail to complete epithelial to mesenchymal transition (EMT) at their PS *via* failure to downregulate E-cadherin in a *Snail*-dependent way.

The third aim here was to examine whether the failure of intraembryonic mesoderm to migrate away from the PS in type-II mutants (see above), is due to defective epithelial to mesenchymal transition (EMT). To address this fluorescent immunohistochemistry for the expression of e-cadherin (Cdh1) protein in paraffin embedded embryo sections, 7μm thick, at the level of the PS (perpendicular to the long axis of the embryo) of the *Ets2* type-II mutants embryos at E7.75 was carried out. E-cadherin is an epithelial marker that mediates adhesive interactions between epithelial cells by being a component of adherent junctions and is expressed in the PS cells that do not undergo EMT. The loss of these epithelial adhesive interactions, as marked by the downregulation of E-cadherin expression, is necessary for the loosening of PS epiblast cells from the rest of the epiblast, so as to be able to migrate away from the PS region and become localized as mesoderm cells between the PS epiblast and the VE (*Arnold, Hofmann et al. 2008*). Although epiblast cells in the PS of E7.75 mutants lose their elongated (epithelial) shape (*Figs. 8c,d, 14b*), a process indicative of EMT initiation, they fail to downregulate the levels of Cdh1 (E-cadherin) protein (n=2; *Fig.14b*). This result indicates that although intraembryonic mesoderm forms in these mutants, its EMT is incomplete, thus providing an explanation why these mesodermal cells fail to migrate away from the streak.

To explore the molecular basis of this EMT defect, the expression of *Eomes* and *Snail* was investigated in *Ets2* type-II mutant embryos at E6.7 and E7.75 using whole-mount RNA *in situ* hybridization. It was previously shown that the transcriptional repressor *Snail* binds directly to e-cadherin promoter and represses it. *Snail* is expressed in the epiblast cells undergoing EMT, as well as in the mesoderm cells that migrate away from the PS epiblast and it is required for normal EMT at the PS by downregulating e-cadherin (*Carver, Jiang et al. 2001*). Also, *Eomes*, which is expressed in PS epiblast and newly formed mesoderm, is required in the epiblast for correct EMT at the PS, by downregulating e-cadherin (*Arnold, Hofmann et al. 2008*). It is shown here that *Eomes* expression at E6.7 stage is absent (n=3; *Fig.15a*) from the PS of *Ets2* type-II mutant embryos, but by E7.75 it is expressed in their PS (n=5; *Fig.15b*) (not in the EXE- *see below*), indicating a delay in the onset of its expression. On the other hand, *Snail* expression was absent from the PS of the mutants at E6.7 stage (n=3; *Fig.15c*) and barely detectable at E7.75 (n=5; *Fig.15d*). These data suggest that the failure of PS EMT in type-II mutants is dependent on *Snail*, but not *Eomes* expression in the PS.

Figure 13: ***Ets2*** **type-II mutants display defective PS development.**

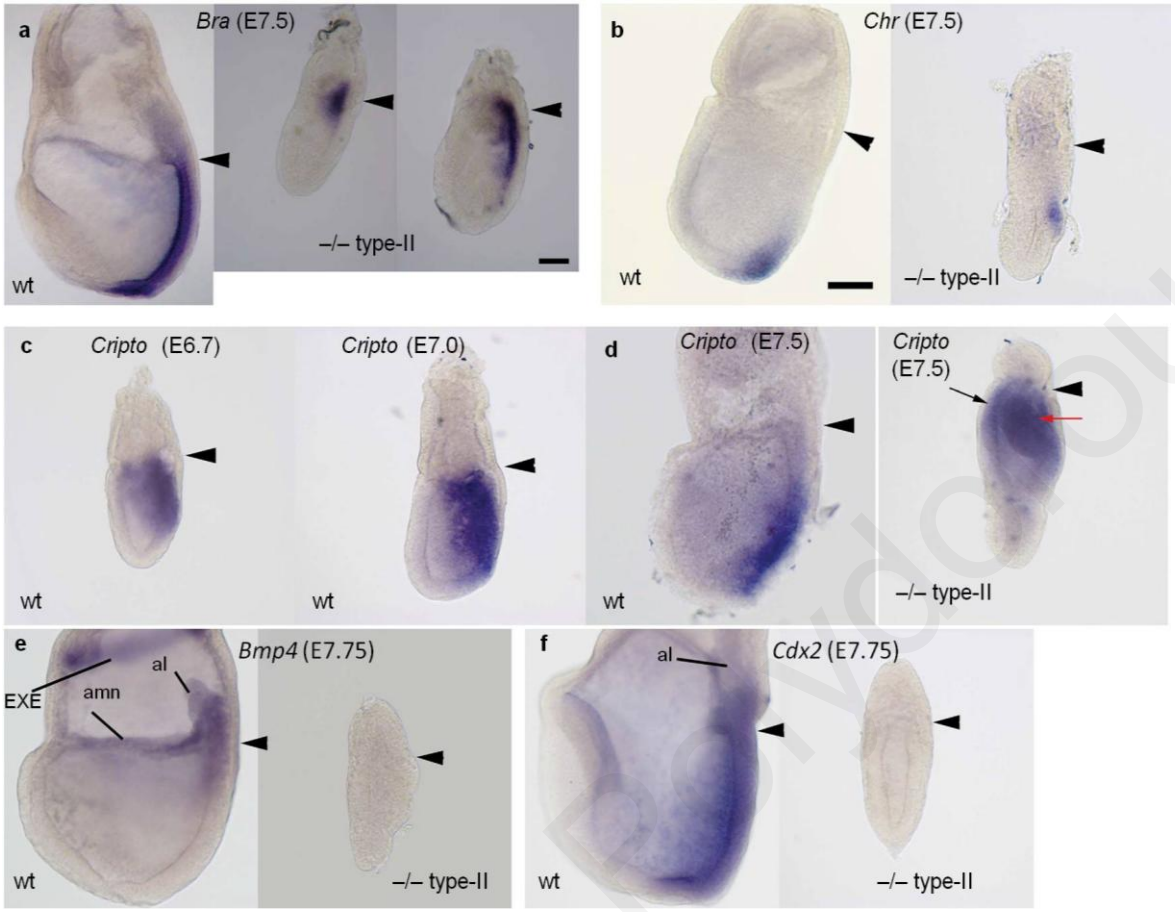

(**a,b**) *Bra* and *Chrd* expression at E7.5 control (wt, left panels in **a** and **b**) and mutant embryos (-/-, right panels in **a** and **b**), showing failure of PS elongation. At E7.5 stage in control (wt) embryos *Bra* expression marks the PS and the node (**a**, left panel). Note that in *Ets2* type-II mutants *Bra* expression remains short and never reaches the distal tip of the embryo (**a**, right panel). *Chordin* (*Chrd*) expression in control (wt) embryos marks the anterior PS (**b**, left panel). In *Ets2* type-II mutant embryos *Chrd* expression remains in the short PS (**b**, right panel) (**c,d**) *Cripto* expression (PS and intraembryonic mesoderm marker) in control (wt) embryos at E6.7, E7.0 and E7.5 and in an E7.5 *Ets2* type-II mutant embryos. In mutants *Cripto* is expressed in PS/mesoderm but its expression remains in the proximal epiblast (**d**, second embryo from the left). Based on *Cripto* expression the PS is able to produce mesoderm but it remains proximal in *Ets2* type-II mutant embryos. **(e,f)** *Ets2* type-II mutant embryos shown a defective anterior-posterior (A-P) patterning based on *Bmp4* and *Cdx2* expression. Normally at E7.5 stage *Bmp4* (**e**, wt) start being expressed in the posterior PS (base of allantois, chorion and amnion) and *Cdx2* (**f**, wt) in the entire PS. In the mutant embryos their expression is absent in these regions at E7.5-E7.75 stage (**e,f** right images -/- type-II), indicating a defective anterior-posterior patterning of the PS. There is an absence of

Bmp4 expression (**e,** right panel -/- type-II) and hence there is no formation of the chorion, amnion and allantois in *Ets2* type-II mutants at E7.75 stage. Also, *Cdx2* expression (**f,** right panel -/- type-II) is absent in mutants at E7.75 stage.

All embryos are of the same magnification. Black arrowheads depict the embryonic-extraembryonic junction at the posterior side of the embryo. All embryos were subjected to whole-mount *in situ* hybridization. All embryos are of the same magnification. Scale bar in **a** and **b** is 10μm.

Figure 14: The EMT in *Ets2* type-II mutants is incomplete.

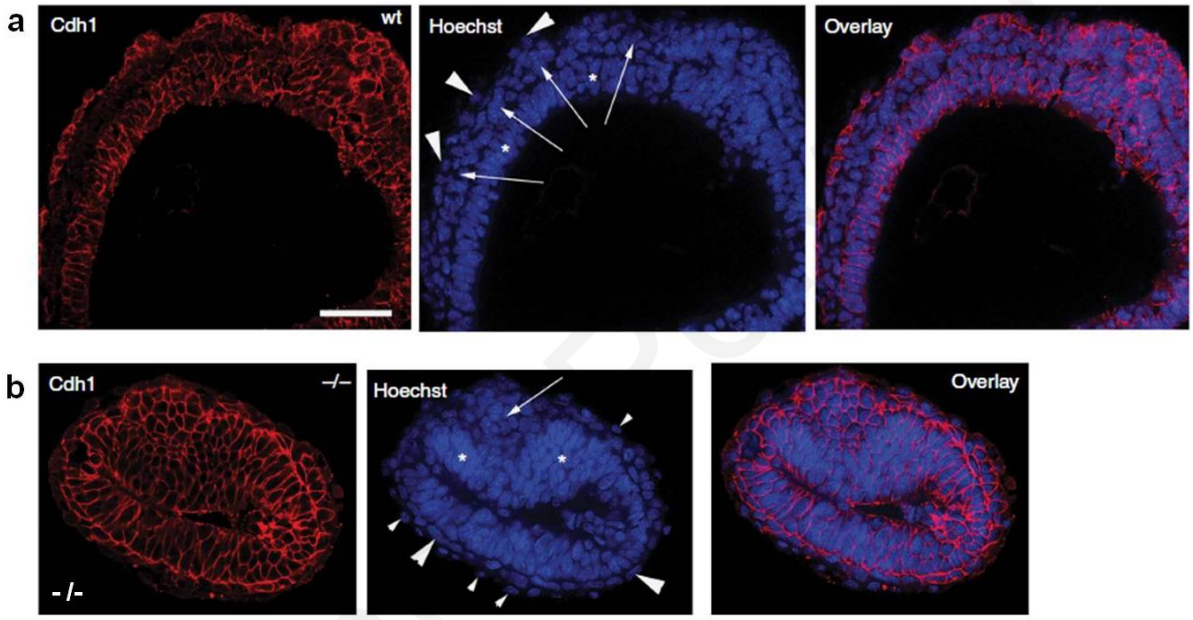

Fluorescent views of embryo sections at the level of PS/mesoderm at E7.75 from control (**a**) and type-II mutant embryo (**b**), showing E-cadherin (Cdh1) protein localization (red fluorescence) and nuclei (blue fluorescence). In controls, Cdh1 positivity marks the epiblast (asterisks in a) and the outermost layer (endoderm; white arrowheads in **a**), but not the epiblast-derived mesoderm cells (white arrows in **a**). In the mutant, although Cdh1 positivity also marks the epiblast and endoderm (asterisks and large white arrowheads in **b**, respectively), it fails to become downregulated from the mesoderm (white arrow in **b**). Note that cells of Richert's membrane (normally Cdh1 negative) are present in the mutant (small arrowheads in g), because they were not removed. All sections are of the same magnification and the scale bar is 5μm.

<u>Figure 15:</u> Defective expression of *Eomes* and *Snail* in *Ets2* type-II mutant embryos at E6.7 and E7.5-E7.75.

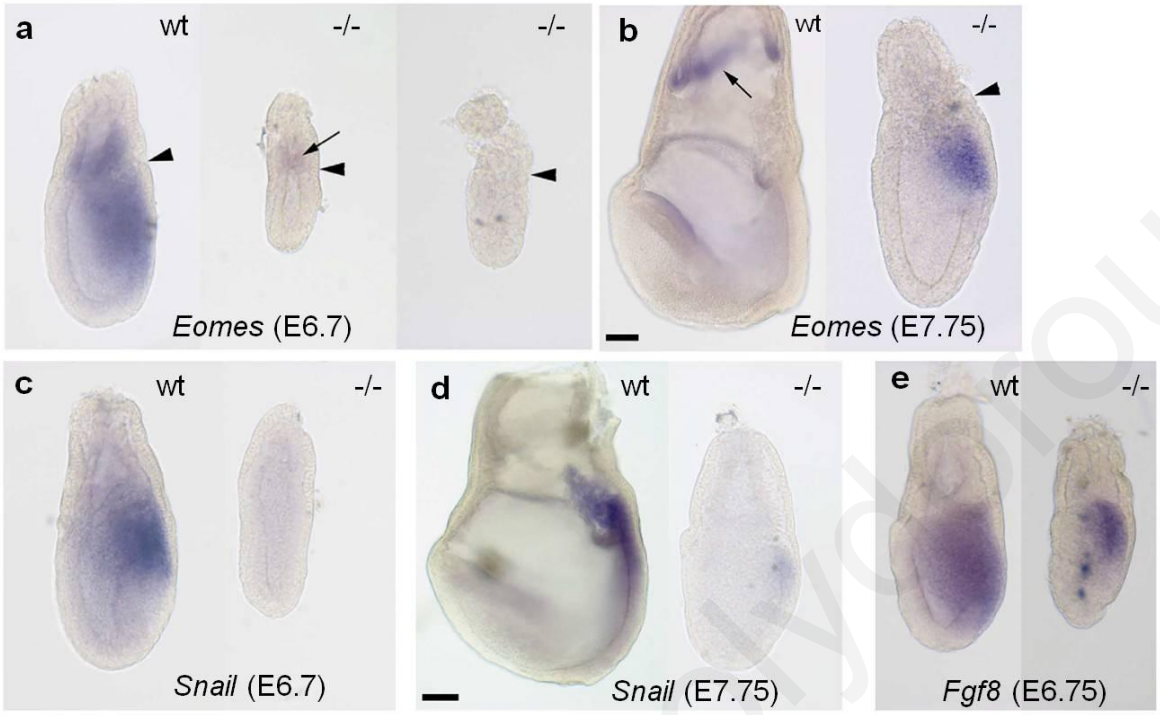

(a,b) *Eomes* expression at E6.7 **(a)** and E7.75 **(b)** in controls (left images) and mutants (middle and right images). *Eomes* expression at E6.7 is expressed faintly in the EXE and its expression is absent from the epiblast. By E7.75 stage in control embryo (left embryo in b) and in *Ets2* type-II mutant embryo (right panel in b) is expressed in the chorion but its expression in the mutants is restricted to the posterior PS-epiblast/mesoderm and is absent from the EXE. (**c,d**) *Snail* is expressed in the PS of E6.7 and E7.75 controls (left images in c and d, respectively), but is downregulated in the mutants (right images in d and e, respectively). **(e)** *Fgf8* is expressed at normal levels (as in controls) in the short PS of E6.7 mutants (right image). All embryos were subjected to whole-mount *in situ* hybridization In all embryos, the posterior is to the right. Arrowheads show the embryonic–extraembryonic junction. All embryos are of the same magnification, except the left images in panels b and d. Scale bars, 10 μm.

4.3 Results for specific aim 3: Anterior primitive streak derivatives development in *Ets2* type-II mutants.

Since morphological examination of *Ets2* type-II mutants showed absence of a morphologically recognizable node (an anterior PS derivative) and investigation of *Ets2* type-II chimaera data suggested reduced or absent definitive endoderm (DE) formation (another anterior PS derivative) (see above), the aims here were to: (a) Examine whether node specification occurs in these mutants and to confirm that node absence is a feature of the type-II phenotype. (b) Investigate the development of axial anterior mesendoderm (AME; another anterior PS derivative – see above), and if it is defective to confirm that it is a feature of the type-II phenotype. (c) Identify defects in DE formation and confirm that they belong to the type-II phenotype.

Ets2 type-II mutants lack a node and display defective node specification.

The first aim in this section was to examine whether node specification occurs in type-II mutants. This is because a morphologically recognizable node (an anterior PS derivative – see above) was not observed in *Ets2* type-II mutants by E7.75 based on sectioning and chimaera analysis (*Fig.8b,d,i*). During normal development, a morphologically recognizable node appears by E7.75 (early head-fold stage). The mouse node is a unique structure and it consists of a two-layered columnar epithelium at the distal tip of the embryo, between the anterior end of the PS and the posterior end of AME. The morphologically recognizable node is marked by the expression of *Noto, Foxa2* and *Nodal*. (*Blum, Gaunt et al. 1992; Davidson and Tam 2000; Kinder, Tsang et al. 2001; Abdelkhalek, Beckers et al. 2004; Yamanaka, Tamplin et al. 2007*). To investigate in more detail the specification of the node in type-II mutants, the expression of the node markers *Noto* and *Nodal* (*Brennan, Norris et al. 2002; Abdelkhalek, Beckers et al. 2004*) was examined at E7.5-7.75 using whole mount RNA *in situ* hybridization. It is shown here that these gene markers are not expressed anywhere in the mutants (n=4/4 for *Noto*; n=2/4 for *Nodal*) *with Nodal* expression being barely detectable in the PS region (n=2/4) (*Fig.16a,b*). This indicates that node specification is defective in these mutants and suggests that they fail to form a node because node precursor cells fail to become specified to differentiate into this structure.

Because type-I mutants fail to form a node as a consequence of absence of PS formation (see above), it was important to confirm that the absence of a node is also a feature of the type-II phenotype and that it is independent of the variability in the length of their

abnormally short PS (see above). To examine this, E7.5-E7.75 controls and type-II mutants (that is mutants with a PS) were subjected to double colour whole-mount RNA *in situ* hybridization analysis for the simultaneous detection of *Bra* (marker of the entire PS and node at this stage) and *Foxa2* (marker of the anterior PS at early stages and of the node when it forms) (*Herrmann 1991; Dufort, Schwartz et al. 1998*). In these experiments, the node could be defined molecularly as a region at the distal tip of the embryo that co-expresses *Bra* and *Foxa2* (*Fig. 17a*). It was found that in *Ets2* type-II mutants (that is, mutants with *Bra* expression) at E7.5 stage there was an absence of *Bra-Foxa2* co-expression at the distal tip irrespective of the variability in PS length (n=4; *Fig.17c,e*), confirming that absence of node is also a feature of the type-II phenotype.

***Ets2* type-II mutants lack any signs of axial anterior mesendoderm (AME).**

The AME forms shortly after E7.5, where it is localized immediately anterior to the node and consists of an anterior half (called the prechordal plate) and a posterior half (head process or anterior notochord) (*Kinder, Tsang et al. 2001; Robb and Tam 2004; Lewis, Khoo et al. 2007; Tam and Loebel 2007; Yamanaka, Tamplin et al. 2007*) To begin to assess whether type-II mutants form an AME, whole mount RNA *in situ* hybridization experiments on E7.75 type-II mutants were carried out to examine the expression of gene expression markers of the AME such as *Foxa2* and *Shh* (at E7.75, both of these mark the node and the entire AME, whilst *Foxa2* marks the anterior PS at earlier stages) and *Bra* (marks the entire PS, node and anterior notochord, but not the prechordal plate of the AME) (*Herrmann 1991; Ding, Yang et al. 1998; Kinder, Tsang et al. 2001; Anderson, Lawrence et al. 2002; Dunn, Vincent et al. 2004; Robb and Tam 2004; Yamanaka, Tamplin et al. 2007*). It was found that *Shh* is not expressed in the mutants (n=3; *Fig. 16e*) and that *Bra* (n=3; *Fig. 16d*) and *Foxa2* (n=4; *Fig.16c*) expression is absent from the distal/anterior half of the *Ets2* type-II mutant embryos. These results therefore suggest that AME fails to form in these mutants.

To confirm that this AME defect is part of the type-II phenotype (because type-I mutants also lack AME due to absence of a PS – see above) double colour whole-mount RNA *in situ* hybridization analysis in the same embryo at E7.75 was employed for the simultaneous detection of *Bra* (marker of the entire PS; *Herrmann 1991*) and *Shh expression* (AME and node marker). It is shown here that mutants with a PS (that is, type-II mutants based on the presence of *Bra* expression) lack *Shh* expression irrespective of PS length (n=4;

Fig.17d,f). This confirms that this AME defect is a feature of the type-II phenotype and is independent of the extent of the abnormally short PS in these mutants.

Figure 16: Absence of node and AME formation in *Ets2* type-II mutants.

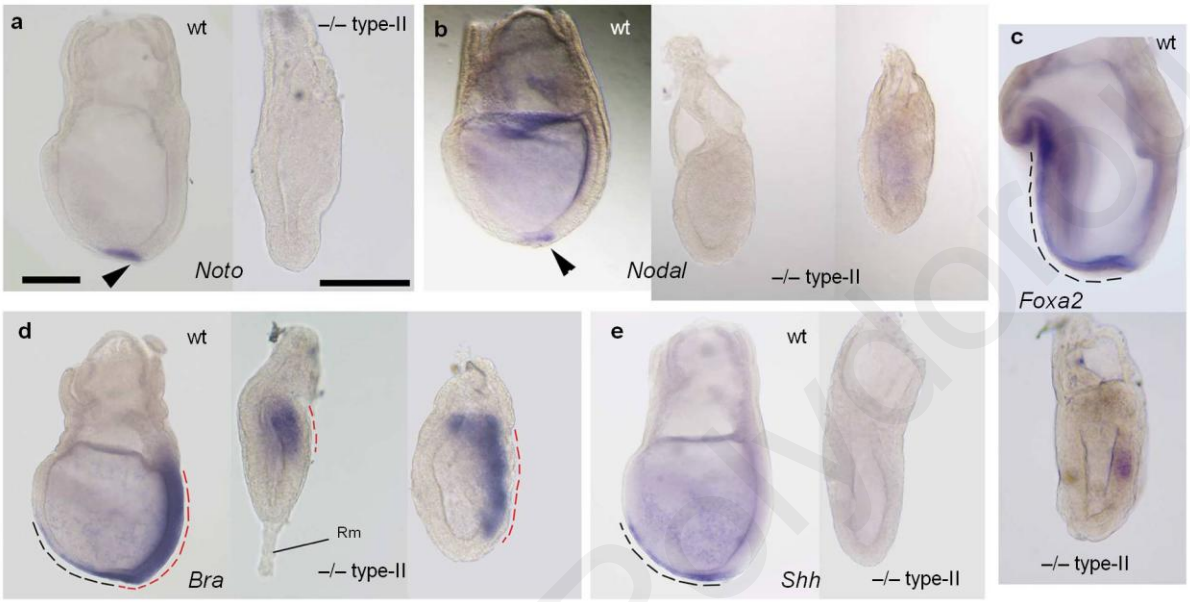

(a,b) Absence of node markers *Noto* and *Nodal* (arrowheads in controls) from E7.5-E7.75 mutants. **(c–e)** Absence of anterior and distal expression of *Foxa2* (node and AME marker; dotted lines in **c**), *Bra* (PS and node/head process marker; black and red dotted lines in **d**, respectively) and *Shh* (node and AME marker; dotted lines in **e**) in E7.75 mutants. All panels show whole-mount RNA *in situ* hybridizations, with the posterior embryo side being on the right. All whole-mount control (wt) embryos are of the same magnification, as are all mutant ones. Rm, Richert's membrane. Scale bar, 20 μm.

<u>Figure 17:</u> Node and AME development in *Ets2* type-II mutants

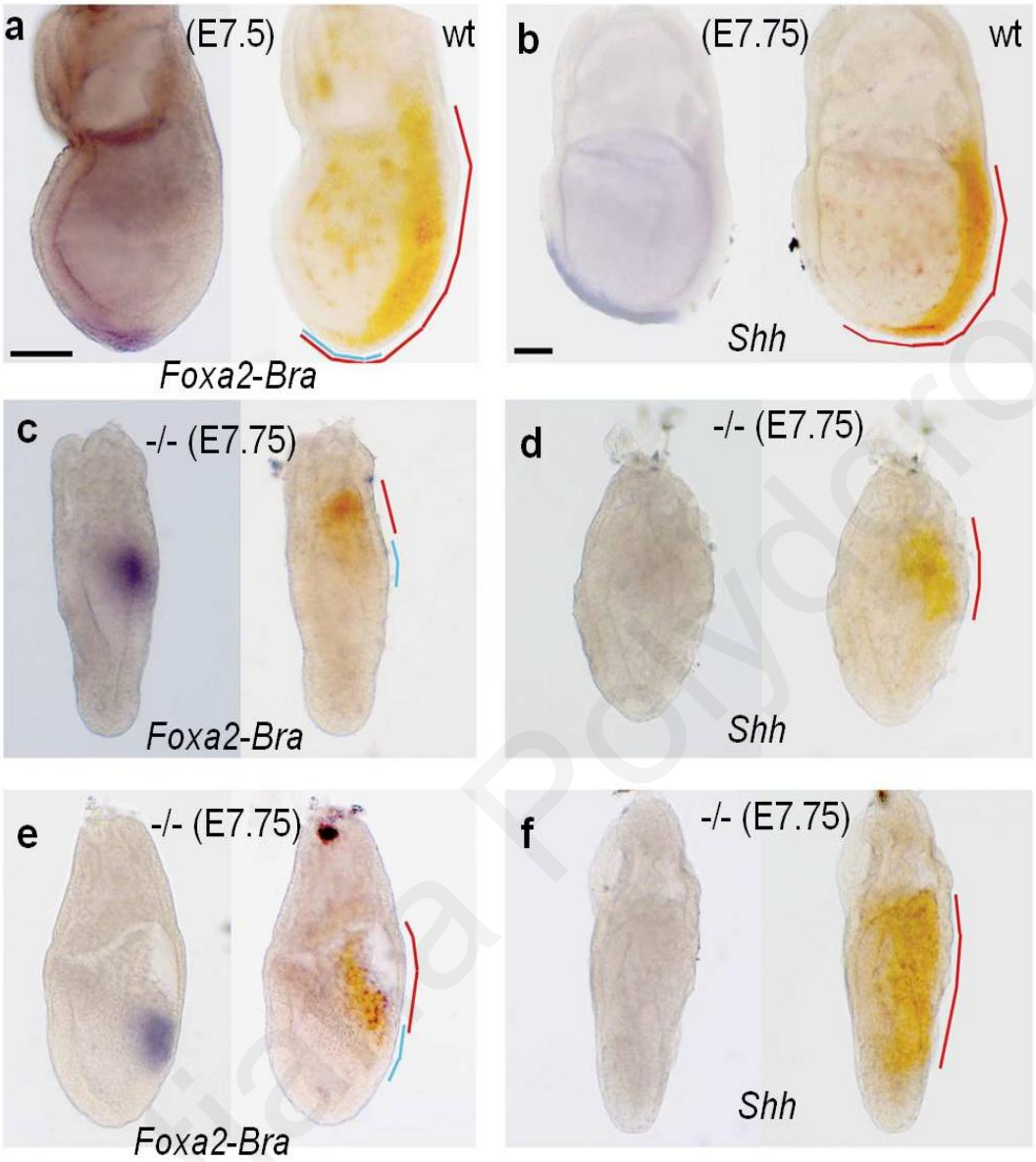

(a,c,e) Double-colour *in situ* hybridization with *Foxa2* (blue) and *Bra* (orange) in control E7.5 embryos **(a)** and E7.75 mutants **(c,e).** In controls, the node is a region at the distal tip of the embryo that can be defined by the complete overlap between *Foxa2* and *Bra* expression (overlap between blue and red lines in **a**). In the mutants, there is no distal *Foxa2* or *Bra* expression or any significant overlap between their expression patterns, irrespective of whether the PS is only about 1/5th **(c)** or about half the proximo-distal length of the posterior epiblast **(e). (b,d,f)** Double-colour *in situ* hybridization with *Shh* (blue signal) and *Bra* (yellow/orange signal) in wild-type E7.75 embryos **(b)** and E7.75 type-II mutants **(d,f)**. Note the absence of *Shh* expression in mutants with short **(d)** or longer **(f)** PS. The posterior side in all embryos is on the right. In all the panels, each pair of images is of the same embryo, with the left image photographed last, after alcohol-mediated disappearance of *Bra* expression and

completion of *Foxa2/Shh* colour detection procedures. Red and blue lines represent the anterior-posterior extent of *Bra* and *Foxa2* expression, respectively. Panels a and c–f are of the same magnification; Scale bar, 100 μm.

Definitive endoderm (DE) development and anterior visceral endoderm (AVE) localization in *Ets2* type-II mutant embryos.

The main aims here were to: (a) investigate DE development in type-II mutants and (b) explore the localization of anterior visceral endoderm (AVE) in these mutants. The first aim was based on the GFP localization in type-II chimaeras made from aggregating *Ets2* +/+ GFP-positive ES cells with GFP-negative 4N *Ets2* -/- embryos (see above). Specifically, a minority (n=2/6) of these chimaeras failed to show GFP positivity in their VE by E7.75 and the remaining majority of these (n=4/6) showed reduced GFP positivity in their VE (*Fig.8i,k*). This suggested that DE formation in type-II mutants fails in a minority and is reduced in most of these mutants. The second aim was based on the observation that some type-II mutants show ectopic expression of PS markers in the anterior-proximal epiblast (see above), suggesting that their AVE (which was previously shown to suppresses posterior epiblast character including PS marker gene expression) may not be completely anteriorized.

The DE is one of the three embryonic germ layers, which together with the other two (mesoderm and ectoderm) gives rise to the cells of the entire foetus. The DE appears at about 8 to 10 hr after the onset of gastrulation (~E7.0) and is derived from the anterior part of the PS (*Lawson, Meneses et al. 1991; Tam and Beddington 1992*). By the completion of gastrulation the DE constitutes a squamous epithelium covering the embryo, but is absent from the extraembryonic region (*Lewis and Tam, 2006*). Cells that are fated to become DE (DE progenitors) appear in the anterior PS region from mid-PS to late-PS stages (*Lawson, Meneses et al. 1991;* (*Kinder, Loebel et al. 2001; Kinder, Tsang et al. 2001)* and initially undergo (epithelial to mesenchymal transition) EMT to become flattened mesenchymal cells situated between the epiblast and the adjacent VE. They then intercalate within the VE layer whilst at the same time becoming epithelial (*Tam and Loebel 2007; Kwon, Viotti et al. 2008; Burtscher and Lickert 2009*).

To explore DE formation and AVE localization in *Ets2* type-II mutants, *Hex* and *Cerberus1 (Cer1)* expression was examined first using whole mount RNA *in situ* hybridization during the E7.0-E7.75 period in these mutants. *Hex* and *Cer1,* both mark the (AVE at all these stages and they are also expressed in the newly formed DE (in the distal

region of the embryo) at around E7.0, with *Cer1* expression remaining in the anterior DE up to E7.5-7.75, a stage when it is situated in the anterior half of the embryo (*Thomas, Brown et al. 1998; Kinder, Tsang et al. 2001*).

It was found that at E7.0 and E7.5-7.75 *Hex* is expressed in the AVE in all cases in *Ets2* type-II mutants (*Fig.18a,b*). Moreover *Hex* expression was absent from the DE in the majority of cases (n=5/6 at E7.0 and n=5/9 at E7.5) (*Fig.18a,b*) and its expression was weak in the DE in the remaining cases (n=1/6 at E7.0 and n=4/9 at E7.5) (*Fig.18a,b and 20e black asteriscs*). Similarly, *Cer1* expression is localized in the AVE in all E7.5-7.75 mutants that were examined (*Figs.18c,d;19c;20a-c*), but its expression in DE was absent from some mutants (n=5/11) and present in others (n=6/11) (*Fig.18c,d, black asterisks*). Regarding DE formation based on absence or presence of *Hex/Cer1* expression, these results were regarded as insufficient because they mainly mark anterior DE and absence of their expression does not necessarily mean absence of DE formation, as a DE forms in *Hex*-/- embryos, which also lack *Cer1* expression formation (*Martinez Barbera, Clements et al. 2000*). However, these findings are informative regarding the extent of AVE anteriorization in type-II mutants based on *Hex/Cer1* expression pattern. Specifically, although all type-II mutants form an AVE (that is, their AVE is not localized, partly or completely at the distal tip) it was noticed that its anterior edge fails to closely approach the anterior embryonic-extraembryonic junction (that is, their AVE fails to anteriorize completely). This was shown from the expression of *Hex* or *Cer1* at E6.7 (n=3/4; *Fig.19a,b*), *Hex* at E7.0 (n=4/6; *Fig.18a*) and *Hex* (n=8/9; *Fig.18b*) or *Cer1* (n=9/11; *Fig.18c,d*) at E7.75 *Ets2* type-II mutant embryos. This AVE defect could explain the ectopic expression of *Bra* and *Cripto* expression from the anterior epiblast in 37% (n=7/19) of E7.75 type-II mutants (*Figs 13a,c and 20g,h*). As the AVE normally inhibits posterior epiblast character (*Kimura et al., 2000*) in the anterior epiblast, this is consistent with the finding that the AVE in 44% (n=8/18) of E7.75 *Ets2* type-II mutants fails to reach the region situated underneath the anterior-most 40% of the anterior epiblast, based on *Hex* and *Cer1* AVE expression patterns. To confirm that this AVE anteriorization defect belongs to the type-II phenotype and is unrelated to the developmental stage (based on the extent of PS elongation) of the mutants, simultaneous examination of *Bra* and *Cer1* expression in the same embryo was carried out. This was confirmed, as shown by the result that the majority (n=3/4) of E7.75 mutants which possessed a PS (and hence being type-II mutants) fail to completely anteriorize their AVE, irrespective of the variability in PS length (*Fig.20a-c*).

In view of the relatively non-informative results of *Hex/Cer1* expression regarding DE formation (see above), this process was further examined in *Ets2* type-II mutant embryos

with RNA *in situ* hybridization for the expression of *Gsc*. *Gsc* is an anterior PS epiblast and anterior DE marker from around E7.0 and by E7.5-7.75 its expression becomes downregulated from DE and is restricted to the prechordal plate (part of AME) (*Lewis et al., 2007*). It is shown that *Gsc* is not expressed in a minority of E7.5-7.75 type-II mutants (n=1/4) (*Fig.18e; 5th embryo from the left*), but is expressed in the majority of these mutants in the DE and anterior epiblast (n=3/4) (*Fig.18e*). To confirm that *Gsc* expression was extended to the outermost layer of the *Ets2* type-II mutant embryos (thereby signifying DE expression as opposed to anterior PS expression only), these mutants were then embedded in paraffin and sectioned at the level of the anterior DE. From these (n=2) it is shown that *Gsc* expression extends to the outermost layer, indicating DE formation in these mutants (*Fig.18f,g*). This suggests that the majority of type-II mutants form a DE and is consistent with the pattern of GFP positivity in type-II chimaeras (see above).

Figure 18: Definitive endoderm marker gene expression in *Ets2* type-II mutants.

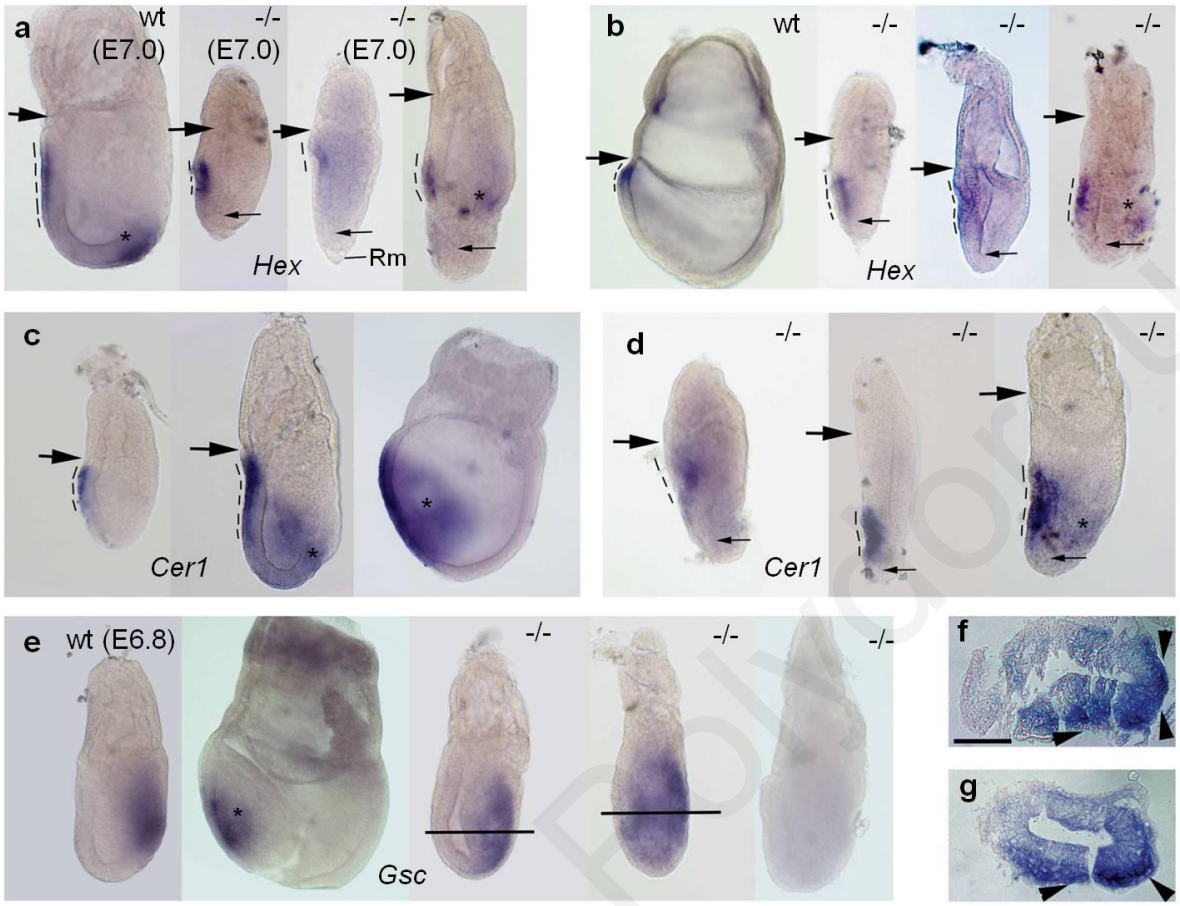

(a,b) *Hex* expression (AVE and anterior DE marker, dotted lines and asterisk, respectively) in E7.0 **(a)** and E7.5–7.75 **(b)** controls and mutants. Note that some, but not all, mutants possess DE, while some fail to completely anteriorize AVE localization. **(c,d)** *Cer1* expression (AVE and anterior DE marker; dotted lines and asterisk, respectively) in controls at E6.7, E7.0 and E7.75 **(c)** and in E7.75 mutants **(d).** Note that in some mutants DE forms and that AVE localization fails to anteriorize completely. **(e)** *Gsc* expression (anterior DE marker depicted by an asterisk) in wt at E6.8 and at E7.5–7.75 (first and second panels from the left, respectively) and in E7.5-E7.75 mutants (last three left hand side images). Note that some mutants show DE formation. **(f,g)** Cross-sections of the mutants shown in e (third and fourth images from the left, respectively), taken from where the black lines are, showing expression in the anterior epiblast and in the posterio-lateral outermost layer (DE cells), indicated by arrowheads. All panels except f and g show whole-mount *in situ* hybridizations, with the posterior embryo side being on the right. Large and small arrows depict the embryonic–extraembryonic junction and the luminal surface of distal tip epiblast, respectively. Black asterisks mark DE cells. Rm, Richert's membrane. Scale bar, 20 μm. Sections in f and g are of the same magnification with scale bar, 50 μm (f).

<u>Figure 19:</u> AVE failed to anteriorize in *Ets2* type-II mutant embryos.

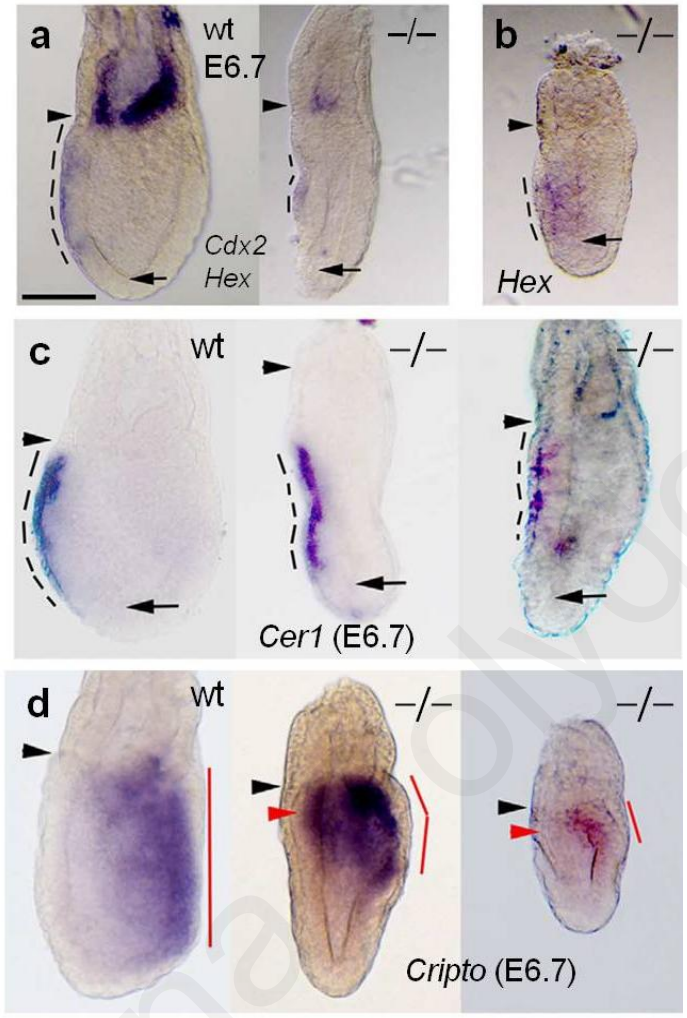

(a–c) Expression of *Hex/Cdx2*: simultaneous detection of both genes **(a),** only *Hex* **(b)** and only *Cer1* **(c)** at E6.7. Note the failure of AVE (*Hex/Cer1* positivity) to closely approach the anterior embryonic–extraembryonic junction in the most mutants. **(d)** *Cripto* expression in E6.7 mutants showing a short PS in all and ectopic expression in anterior epiblast in some. Dotted lines mark the antero-posterior extent of AVE and red lines that of the PS. All images in panels a–d are of the same magnification and were subjected to whole-mount *in situ* hybridization. Scale bar, 100 μm (a).

In view of the fact that *Gsc* expression is a marker of anterior DE and does not normally remain in the DE by E7.75 (see above), DE development in type-II mutants was also investigated by examining the pattern of the 'global' DE markers (albeit indirect ones – see below) DBA lectin binding and *Afp* expression. Although DBA lectin specifically stains all VE, but not DE, mesoderm or epiblast cells (*Sherwood, Jitianu et al. 2007*), it can be used as an indirect marker of DE formation. This is because when DE cells intercalate into the epiblast-associated VE to form the DE layer, the initially closely packed VE cells become dispersed in this part of the VE, but not in the EXE-associated VE where DE does not form (*Kwon, Viotti et al. 2008*). During normal development, patchy-DBA lectin positivity marks the VE into which DE forms (epiblast-associated VE by E7.5), whereas the opposite (continuous/non-patchy DBA lectin) marks VE signal (EXE-associated VE by E7.5). *Gata4* and *Afp* are initially expressed throughout the VE and downregulation of their expression from epiblast-associated VE is an indirect indication of DE formation because it occurs in those VE cells that experience spreading as a result of DE formation (*Kwon, Viotti et al. 2008; McKnight, Hou et al. 2010*). Therefore, to examine DE formation in type-II mutants epiblast-associated VE spreading was first assessed using whole-mount DBA lectin staining in E7.75 type-II mutants these were also previously subjected to RNA *in situ* hybridization with the PS markers *Bra* or *Cripto*, to confirm that they are type-II mutants). These experiments showed that VE spreading (patchy- DBA positivity within the epiblast-associated VE) and hence DE formation, occurred in the majority (n=12/14; 86%) (*Fig.20b,c,e,f,h*), but not in a minority (n=2/14; 14%) of type- II mutants (that is, mutants with a PS) (*Fig.20g*). However, in these mutants with DE formation (based on presence of patchy DBE staining), patchy DBA staining was not evident in the most proximal epiblast-associated VE (n=12/12; *Fig.20a-g)*, indicating reduced DE formation in all of them. In *Ets2* type-II mutant embryos *Afp* (n=3) and *Gata4* (n=4) expression is restricted within the proximal epiblast-associated VE at E7.5 indicating reduced DE formation consistent with DBA lectin staining results (*Fig.21a,b*).

Taken together, these results (and the type-II chimaera data –see above) indicate that in the majority of type-II mutants the AVE fails to completely anteriorize (providing an explanation for the ectopic PS marker gene expression in some of these) and that although the DE forms in most of them, its formation is reduced in that it fails to also form in the mutant chimaeras (*Fig.8j,k*). Moreover there is no correlation between PS length and DBA-based on DE detection, as mutants with similar PS lengths may or may not display DE formation (*Fig.20* proximal embryonic region). These findings also confirm that these AVE

and DE defects belong to the type-II phenotype and they are independent of the developmental stage reached based on the extent of PS length. Moreover, although non-AVE (that is, putative DE) *Cer1/Hex* expression in these mutants was always associated with patchy DBA positivity (n=4/4; *Fig. 20a-c,e*), such DBA staining was not always observed in mutants lacking non-AVE *Cer1/Hex* expression (n=2/4; *Fig. 20d,e*), confirming that assessing absence of DE formation based on absence of *Hex/Cer1* expression is not reliable in the context of the type-II phenotype.

<u>Figure 20:</u> Marker gene expression and DBA staining in *Ets2* type-II mutants.

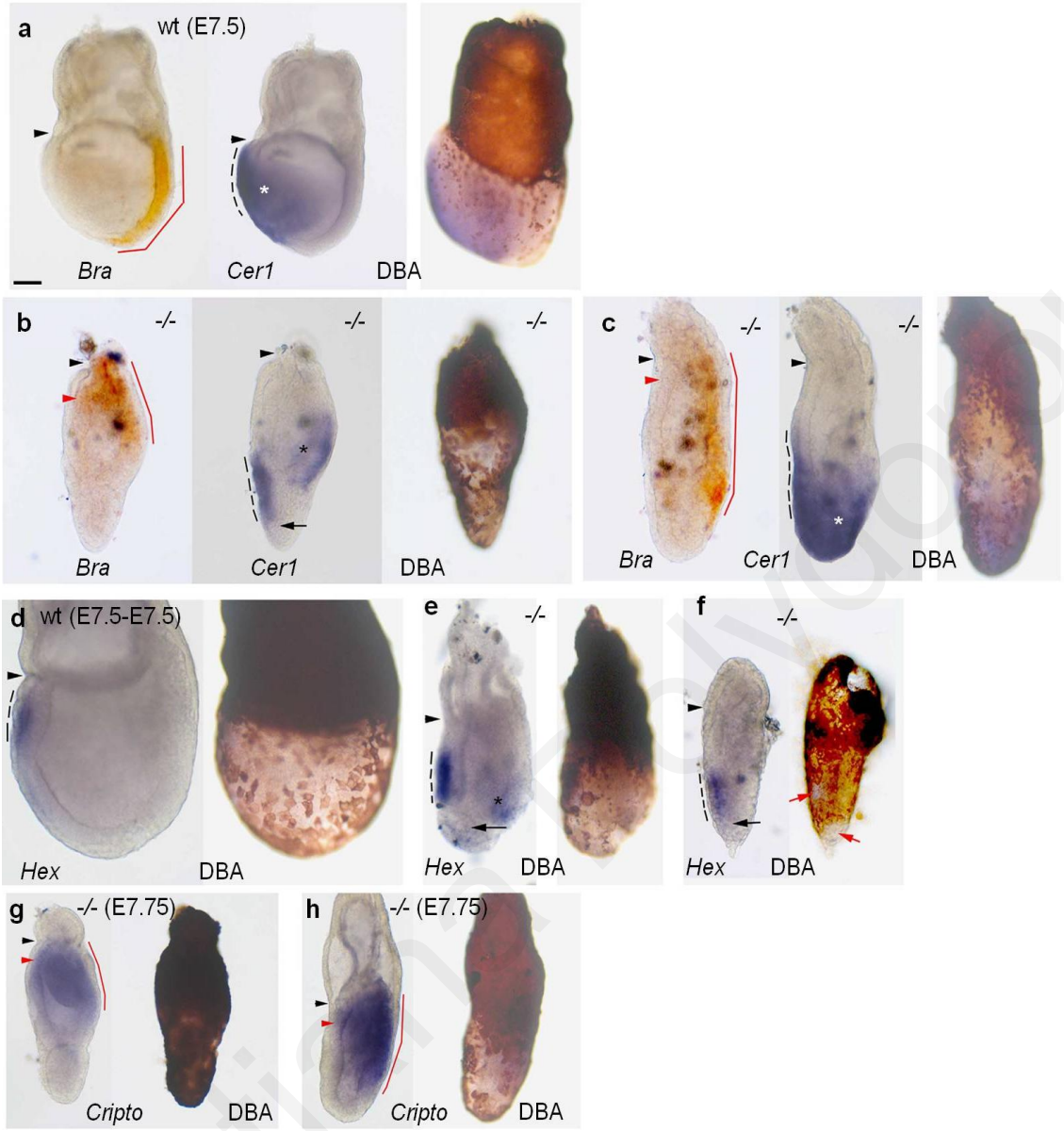

(a–b) Double-colour *in situ* hybridization with *Bra* (orange) and *Cer1* (blue), followed by DBA staining (brown) of the same embryo in E7.5-E7.75 controls **(a)** and E7.75 type-II mutants **(b,c).** Mutants failed to completely anteriorize their AVE (AVE expression of *Cer1* in b and c) and can form DE (non-AVE expression of *Cer1*; asterisks in b and c and patchy DBA positivity in a and b). When AVE fails to reach the anterior 40% of anterior epiblast, there is ectopic expression of *Bra* in anterior epiblast **(b)** and when it doesn't *Bra* expression remains posterior **(c)**. **(d,e)** showing *Hex* expression and DBA staining: patchy DBA staining (right image in e and red arrows in right image of f) was associated with the presence **(e)** or absence (left image in f) of non-AVE (DE) *Hex* expression. **(g,h)** E7.75 mutants showing *Cripto* expression and DBA staining: some do not form DE (continuous DBA positivity in g), while others do (patchy DBA staining in h). In all, posterior is to the right. Black and red

arrowheads depict the anterior embryonic-extraembryonic junction and proximo-anterior epiblast, respectively. Arrows mark the distal tip of the epiblast. Dotted lines mark the antero-posterior extent of AVE, red lines that of the PS and asterisks the DE. All images are of the same magnification. Scale bar, 100 μm

Figure 21: ***Afp*** **and** ***Gata4*****expression in** ***Ets2*** **type-II mutants.**

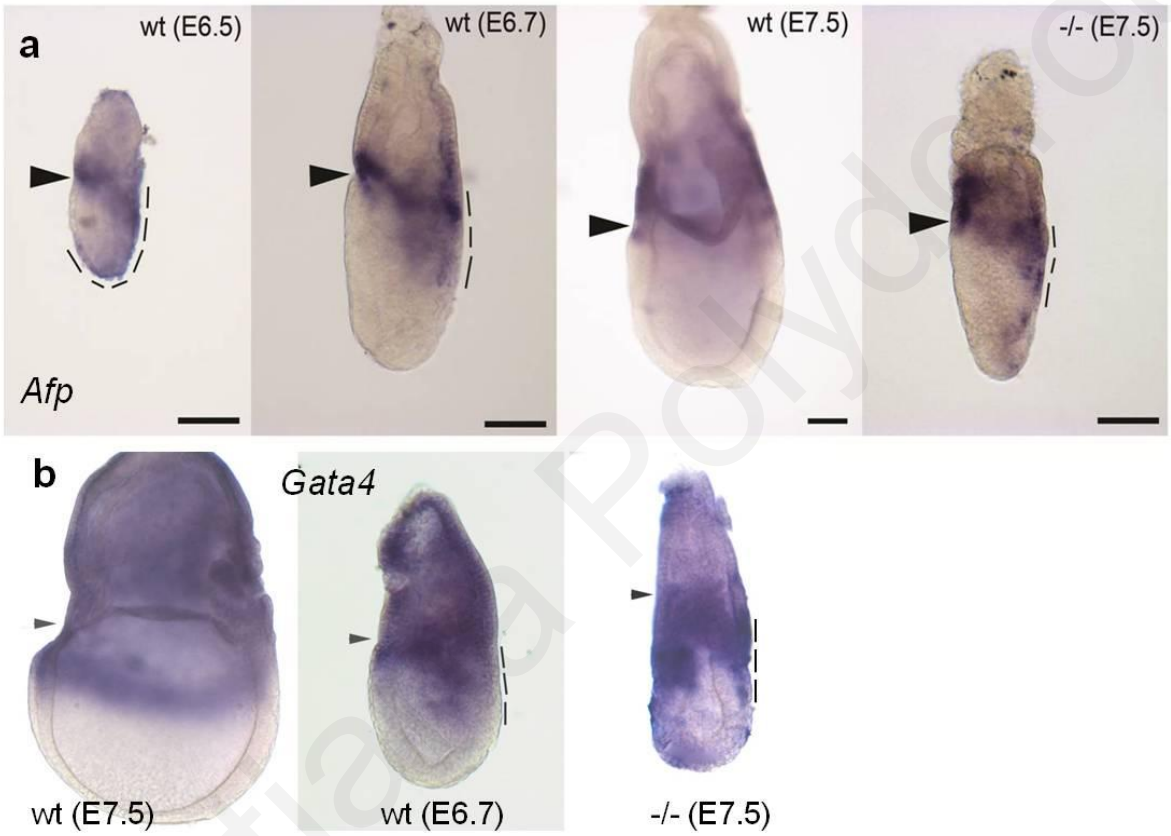

(a) The VE-specific gene *Afp* expression in controls at E6.5 (left embryo), E6.7 (second embryo from the left) and E7.5 (third embryo from the left) and in a mutant at E7.5 (fourth embryo from the left). *Afp* in controls at E6.5 and E6.7 (stages prior to DE intercalation within the epiblast-associated VE) is expressed in this VE (dotted lines) where it becomes restricted to its posterior side by E6.7. Note that by E7.5 in controls, when DE intercalation has already started, this epiblast-associated VE expression is no longer detectable. In the E7.5 mutant however, *Afp* expression fails to become downregulated from the posterior epiblast-associated VE (dotted lines the fourth embryo from the left) indicating reduced DE formation. **(b)** *Gata4* expression in controls at E7.5, E6.7 (second embryo form the left) and in mutant at E7.5 (third embryo from the left). In the E7.5 mutant *Gata4* expression fails to become downregulated from the posterior epiblast-associated VE (dotted lines) indicating

reduced DE formation in *Ets2* type-II mutant emrbyos. All embryos are whole mount *in situ* hybridizations, with the posterior side being on the right and arrowheads depicting the embryonic-extraembryonic junction. The third and fourth embryos from the left in **a** are of the same magnification. Scale bar is 100μm.

4.4 Results for specific aim 4: Regulatory gene expression in the epiblast of type-II mutants.

The main aim here was based on the results of the previous sections, which showed that type-II mutants fail to completely elongate their primitive streak (PS), they lack the anterior PS derivatives node and axial anterior mesendoderm (AME), show reduction or lack of definitive endoderm (DE; the other major anterior PS derivative) formation and their intraembryonic mesoderm fails to migrate away from the PS because there is incomplete epithelial to mesnechymal transition (EMT) due to failure of E-cadherin downregulation from the newly formed mesoderm cells via a *Snail*-dependent pathway. The aim here was to identify putative upstream epiblast-derived genetic pathways that could be responsible for mediating these gastrulation processes. The genes whose expression was tested here were *Nodal*, *Foxh1* and *Wnt3*.

Nodal is a member of the TGF-β family of secreted signaling molecules and is derived from a secreted precursor, which is cleaved by two secreted proteases of the subtilisin-like proprotein convertase (SPC) family called Furin and PACE4 (*Beck, Le Good et al. 2002*). Furin is first expressed throughout the primitive endoderm of the implanting blastocyst but in response to *Nodal* signaling between E4.5–5.0 stage becomes restricted to the VE and extraembryonic ectoderm (EXE), whereas PACE4 (or Spc4) is exclusively expressed in polar trophectoderm and its derivatives (EXE and then chorion) at all stages between E4.5 to 7.5 (*Beck, Le Good et al. 2002; Mesnard, Guzman-Ayala et al. 2006*). At E5.5, *Nodal* expression is detected throughout the epiblast and the entire VE. By the early streak stage (E6.5) its expression is localized to the PS the entire VE, by mid-streak stage (E6.75-E7.0) its expression is restricted to the PS and by the late streak stage (E7.5-E7.75) to the node (the peripheral cells of the node) (*Conlon, Lyons et al. 1994*). Nodal signaling in the epiblast is required for the establishment of the anterior-posterior (A-P) and left-right (L-R) axis of the embryo and for the specification of the anterior PS derivatives (*Brennan, Lu et al. 2001*). It has been previously shown that embryos with an epiblast-specific null mutation for

Nodal do not form a PS or mesoderm indicating that *Nodal* expression in the epiblast is required for PS, mesoderm and distal VE (DVE)/anterior VE (AVE) formation (*Beddington and Robertson 1999;* (*Lu, Brennan et al. 2001; Yamamoto, Meno et al. 2001; Vincent, Dunn et al. 2003)*. Furthermore epiblast *Nodal* expression maintains EXE character by maintaining the expression of *Bmp4* and *Eomes* (*Brennan et al., 2001*). Importantly, high levels of Nodal signaling/expression within the PS are required for PS elongation and anterior PS derivative formation (*Yamamoto, Meno et al. 2001; Vincent, Dunn et al. 2003*; *Dunn, Vincent et al. 2004; Shen 2007*). Investigation of Nodal expression in type-II mutants was first carried out by whole-mount *in situ* hybridization during the early PS stage (at E6.7). It was found here that *Nodal* expression levels in E6.7 type-II mutants become significantly downregulated (n=4/5) (*Fig.22a*). To confirm and quantify this downregulation of *Nodal* levels quantitative real time PCR (qRT-PCR) for *Nodal* expression was performed on E6.7 type-II mutants. As judged by qRT-PCR, the reduction in *Nodal* levels was about 60% (n=4 from four E6.7 mutants) (*Fig.25*). These findings therefore provide a molecular explanation (that is, abnormally low levels of *Nodal* expression and hence reduced Nodal signaling in the epiblast) for the defects in PS elongation and anterior PS derivatives (DE, node and AME) seen in *Ets2* type-II mutant embryos.

To begin to understand the upstream genetic pathways that could influence *Nodal* levels in the epiblast in the context of the type-II phenotype, the expression of *Foxh1* was examined first. The winged-helix transcription factor *FoxH1* is expressed throughout the epiblast and associated VE and is required in the epiblast for maintaining *Nodal* levels there via direct binding to *Nodal* enhancer sequences (*Hoodless et al. 2001; Yamamoto et al. 2001*). Using whole-mount RNA *in situ* hybridization followed by sectioning of these embryos, it is shown here that *Foxh1* expression in E6.7 (early PS stage) type-II mutants appears normal in the epiblast, but is absent from the VE (n=4; *Fig.22b*). These results indicate that *Foxh1* expression in the epiblast is not likely involved in regulating *Nodal* expression in type-II mutants.

To further explore epiblast-derived factors that could explain the reduced *Nodal* expression and failure of intraembryonic mesoderm EMT in type-II mutants, the expression of *Wnt3* was investigated. *Wnt3* codes for a secreted signaling molecule whose expression is first detected in the posterior VE at around E5.5 stage also appears in the proximal/posterior epiblast around E6.0 and by the early PS stage becomes restricted to the PS (*Liu et al., 1999; Rivera-Perez and Magnuson, 2005; Tortelote et al., 2012*). *Wnt3* knockout embryos do not

initiate gastrulation, as they do not form a PS or mesoderm (*Liu, Wakamiya et al. 1999; Yamamoto, Meno et al. 2001*). Addition of Wnt3 protein to E5.75 epiblast explants resulted in induction *Nodal* and of PS gene expression such as *Bra* (*Ben-Haim, Lu et al. 2006*). Moreover, *Wnt3* expression is required *in vivo* for the maintenance of epiblast *Nodal* expression in a largely Foxh1-independent way (*Ben-Haim, Lu et al. 2006*). Importantly, epiblast-specific deletion of *Wnt3* showed that this gene is required in posterior VE for gastrulation initiation, whereas its epiblast/PS expression is required for the correct progression of gastrulation after PS initiation (*Tortelote, Hernandez-Hernandez et al. 2013*). Strikingly, the post-PS initiation gastrulation defects that result from *Wnt3* deletion in the epiblast are very similar to those seen here in type-II mutants, especially in relation to the failure of intraembryonic mesoderm to migrate away from the PS and defective development of anterior PS derivatives (*Tortelote, Hernandez-Hernandez et al. 2013*). Regarding the role of Wnt3 in mesoderm migration, previous work with embryoid bodies [three-dimensional aggregates of embryonic stem (ES) cells] cultured under conditions that result in spontaneous mesoderm formation showed that *Wnt3* promotes mesoderm EMT by upregulating *Snail* expression which in turn downregulates e-cadherin (*ten Berge, Koole et al. 2008*). Taken together, these previous studies indicate that Wnt3 is required for the maintenance of *Nodal* expression in the epiblast and suggest that *Wnt3* expression in the epiblast is also required for the promotion of mesoderm EMT by induction of *Snail* expression. In view of these, the expression of *Wnt3* was examined here in *Ets2* type-II mutant embryos at E6.7, a stage when it is normally expressed in the PS, using whole-mount RNA *in situ* hybridization The results show that *Wnt3* expression is absent from type-II mutants (n=4; *Fig. 22c*).

<u>Figure 22:</u> Defective *Nodal, FoxH1* and *Wnt3* expression in *Ets2* type-II mutant embryos at E6.7.

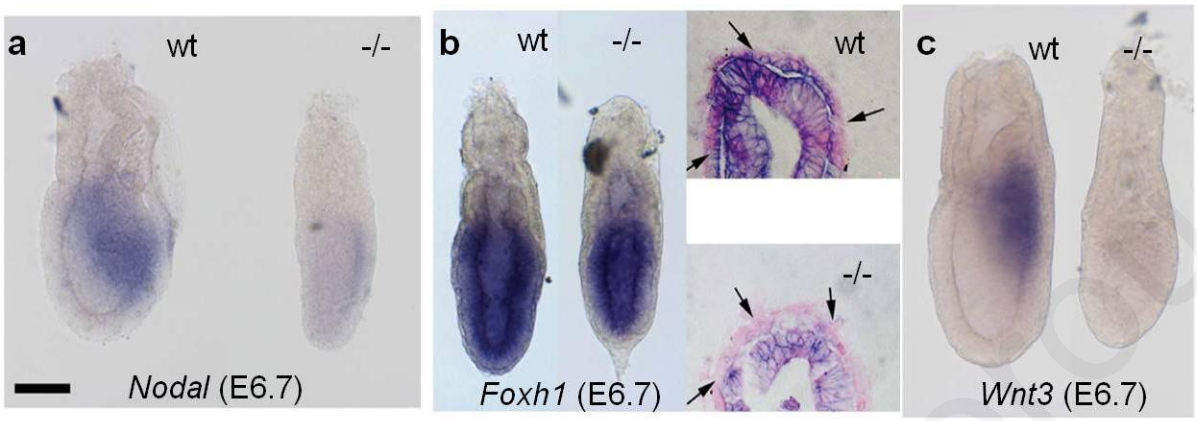

Nodal expression at E6.7 in controls (embryos on the left of each panel) and mutants embryos on the right of each panel). By E6.7 after the initiation of gastrulation and hence the formation of PS the expression levels of *Nodal* are dramatically downregulated in mutant embryos (right panel in a). **(b)** *Foxh1* (epiblast and VE marker) at E6.7 is expressed in control (left panel) and *Ets2* type-II mutant embryos its expression is restricted to the epiblast and is absent from the VE (right embryo). The absence of *Foxh1* from the VE was confirmed in embryo cross-sections as shown in right panel (black arrows denote the VE layer). **(c)** *Wnt3* is expressed in the PS of controls (left), but not that of mutants (right). The black arrowheads show the embryonic-extraembryonic junction. All the embryos were subjected with whole mount *in situ* hybridization and are of the same magnification. Scale bar in a 10μm.

4.5 Results for specific aim 5: Trophoblast gene expression in *Ets2* type-II mutant embryos.

The main aim here was to provide a molecular explanation about how *Ets2* in trophoblast mediates gastrulation progression in the epiblast by examining the expression of various trophoblast-specific genes that could be downstream of *Ets2* in this tissue. Previous experiments using trophoblast stem (TS) cells, the *in vitro* equivalent of extraembryonic ectoderm (EXE) trophoblast, showed that *Ets2* is required for TS cell self-renewal and for maintaining the expression of several TS/EXE genes including *Bmp4, Cdx2, Eomes, Esrrb* and *Pace4* (*Wen, Tynan et al. 2007; Odiatis and Georgiades 2010*) *Cdx2* is exclusively expressed in the EXE before and during gastrulation and by E7.75 its expression is restricted to the PS and extraembryonic mesoderm. Importantly, *Cdx2* is required for TS cell self-renewal (*Niwa, Toyooka et al. 2005*) and in these cells, it maintains the expression of *Bmp4 (Murohashi, Nakamura et al. 2010)* and *Elf5* (*Niwa, Toyooka et al. 2005*) by binding to their promoters (*Ng, Dean et al. 2008*). *Elf5* is exclusively expressed in the EXE and its derivatives and is also needed for EXE maintenance and TS self-renewal (*Donnison, Beaton et al. 2005*). In TS cells, *Elf5* maintains the expression of *Cdx2 and Eomes* expression, through direct activation of their promoters (*Donnison et al., 2005*; *Ng et al., 2008*). *Esrrb,* an EXE and chorion marker, plays an important role in early placentation (*Pettersson et al. 1996;(Tremblay, Kunath et al. 2001),* is expressed in the undifferentiated TS cells *(Tanaka, Kunath et al. 1998*) and is required for TS cells self-renewal (*(Tremblay, Kunath et al. 2001)*. Another EXE marker, *Pace4* (*Spc4*) is exclusively expressed in the EXE and its derivatives (*Beck, Le Good et al. 2002; Mesnard, Guzman-Ayala et al. 2006*). *Bmp4* codes for a secreted signaling molecule required for gastrulation initiation, as shown in a subset of *Bmp4* null mice (*Winnier, Blessing et al. 1995; Fujiwara, Dehart et al. 2002*), which is expressed exclusively in the EXE before and during gastrulation (at E5.5 and E6.75). By E7.5 *Bmp4* expression is restricted to the posterior PS, extraembryonic mesoderm (the base of allantois) and chorion. The phenotype of a different subset of *Bmp4* null embryos combined with results from chimaera analysis showed that absence of *Bmp4* in trophoblast causes reduced extraembryonic mesoderm formation (small to no allantois) and absence of primordial germ cells (*Zhao et al., 2003*). Importantly, addition of *Bmp4*, but not *Nodal*, proteins to pregastrulation naked epiblasts is sufficient for induction of *Wnt3* expression in the latter, whereas Nodal in the epiblast is required for maintaining *Bmp4* expression in the EXE (*Brennan, Lu et al. 2001; Ben-Haim, Lu et al. 2006*).

In view of the above, the EXE expression of *Cdx2, Elf5, Essrb, Pace4* and *Bmp4* was examined in type-II mutants at E6.7 (and for some also at E7.5-7.75) using whole-mount RNA *in situ* hybridization. The findings of these experiments are as follows. (a) *Bmp4* expression is extensively downregulated in E6.7 mutants (n=3; *Fig.24b*) and is absent or abnormally low in E7.5–7.75 mutants (n=3; *Fig.13e*). This *Bmp4* downregulation as judged by qRT-PCR data (n=4, from four E6.7 mutants) was about 80% (*Fig.25*). (b) *Cdx2* was found to be faintly expressed (n=2/3; *Fig.13f; Fig.23d*) or absent (n=1/3) (*Fig.23d*). Since in two of these the *in situ* hybridization involved the simultaneous detection of *Cdx2* and *Bra* (a PS marker) in the same embryo, the presence of *Bra* expression in both cases confirms that defective EXE gene expression is also part of the type-II phenotype (*Fig.23d*). Moreover, by E7.75 *Cdx2* expression is undetectable (n=3) in type-II mutants (*Fig.13f*). (c) *Esrrb* expression was found to be either be undetectable (n=1/3; *Fig.23a, 3rd embryo from the left*) or extremely low (n=2/3; *Fig.23a, middle image*) in type-II mutant embryos at E6.7 (d) *Pace4* expression was also found to be absent in all E6.7 type-II mutants analysed (n=3; *Fig.23e*). (e) Similarly, *Elf5* expression is absent from the EXE of type-II mutant embryos at E6.7 (n=3*; Fig.23c*). Taken together, the results shown here indicate that the trophoblast of type-II mutants lacks EXE character (e.g. lack *Cdx2* and *Elf5* expression) and EXE signaling capability (downregulation of *Bmp4* expression) from at least the early PS stage (E6.7) onwards. Together with previous work (see above in this section), they provide a molecular explanation as to how the expression of *Ets2* in trophoblast mediates the progression of gastrulation in the epiblast after PS initiation (see Discussion).

<u>Figure 23:</u> Trophoblast gene markers expression in *Ets2* type-II mutant embryos.

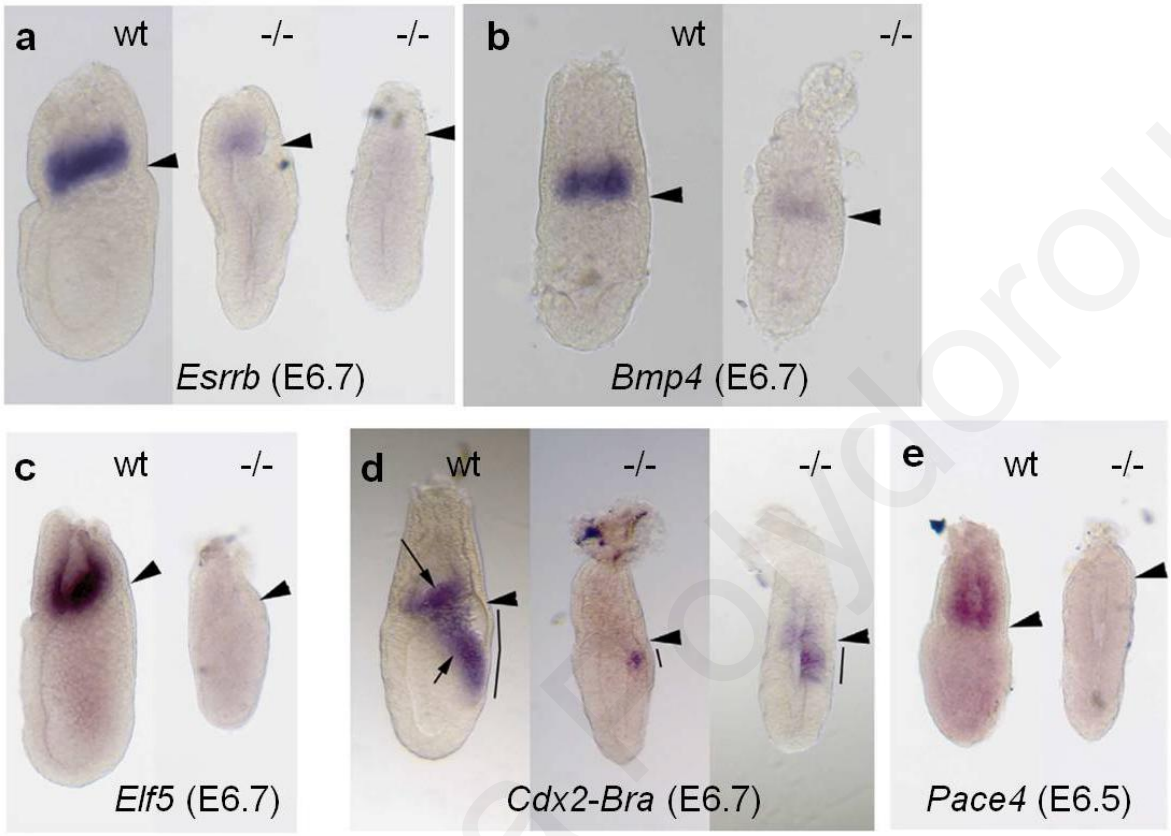

(a) *Esrrb* expression in E6.7 control (left embryo) and mutants showing weak or no expression in the EXE of mutants (middle and right embryos, respectively). **(b)** *Bmp4* expression in control embryo (left image) and in *Ets2* type-II mutant embryo (right image). Note that *Bmp4* expression in mutants was very weak in the EXE. **(c)** *Elf5* expression in E6.7 control (left embryo) and mutants, showing weak or no expression in the EXE of mutants (middle and right embryos, respectively). (**d**) Simultaneous detection of *Cdx2* (EXE marker) and *Bra* (PS marker) expression at E6.7 in control (left embryo) and mutant embryos (right panels) showing either a weak (middle panel in d) or absence (third panel from the left in d) of *Cdx2* expression. **(e)** *Pace4* expression in mutants (right image in e) is undetectable. In all, posterior is to the right. Arrowheads depict the embryonic–extraembryonic junction and asterisks signify Richert's membrane that was not removed. All embryos are of the same magnification. Scale bars, 10 μm.

4.6 Results for specific aim 6: Pre-gastrulation examination of type-I and type-II mutants.

The aims here were based on the findings that (a) *Ets2* type-I mutants lack EXE character (e.g *Cdx2* expression) and *Bmp4* expression from their trophoblast (from pregastrulation stages (at least E5.5) and their epiblast lacks *Wnt3* and exhibits low *Nodal* expression at the early PS stage (*Georgiades and Rossant 2006*), and (b) *Ets2* type-II mutants also lack these as well as exhibiting low *Nodal* expression from at least E6.7 (early PS stage) onwards (results of this work -see above). Therefore, the question addressed here was whether type-II mutants differ from type-I mutants in these parameters at any stages prior to E6.7.

To begin to address this, double-colour whole-mount RNA *in situ* hybridization examining the expression of three genes simultaneously was carried out at pregastrulation stages (E6.3 or E6.4; gastrulation normally starts at E6.5 with the formation of the PS) for both type-I (presence of distal VE thickening) and type-II (absence of distal VE thickening) mutants. The genes tested were *Wnt3* (posterior epiblast marker), *Bmp4* (EXE signaling capability marker) and *Elf5* (EXE/TS cell self-renewal marker). It was found that although E6.3 type-I mutants do not express any of these (*Fig.24b,d*), type-II mutants do express all of these at apparently normal levels (n=3) (*Fig.24b,c*). Regarding *Nodal* expression at E6.4, it is shown here that it is expressed at normal levels in type-II mutants (n=4; *Fig.24a*). These findings can explain why type-II mutants initiate a PS, whereas type-I ones do not (see Discussion) and indicate that type-II mutants loose EXE character/*Wnt3* expression and downregulate *Nodal* expression sometime between E6.3/4 and E6.7.

Figure 24: ***Nodal, Wnt3, Elf5*** **and** ***Bmp4*** **expression in pre-gastrulation stages in** ***Ets2*** **type-II and type-I mutant embryos.**

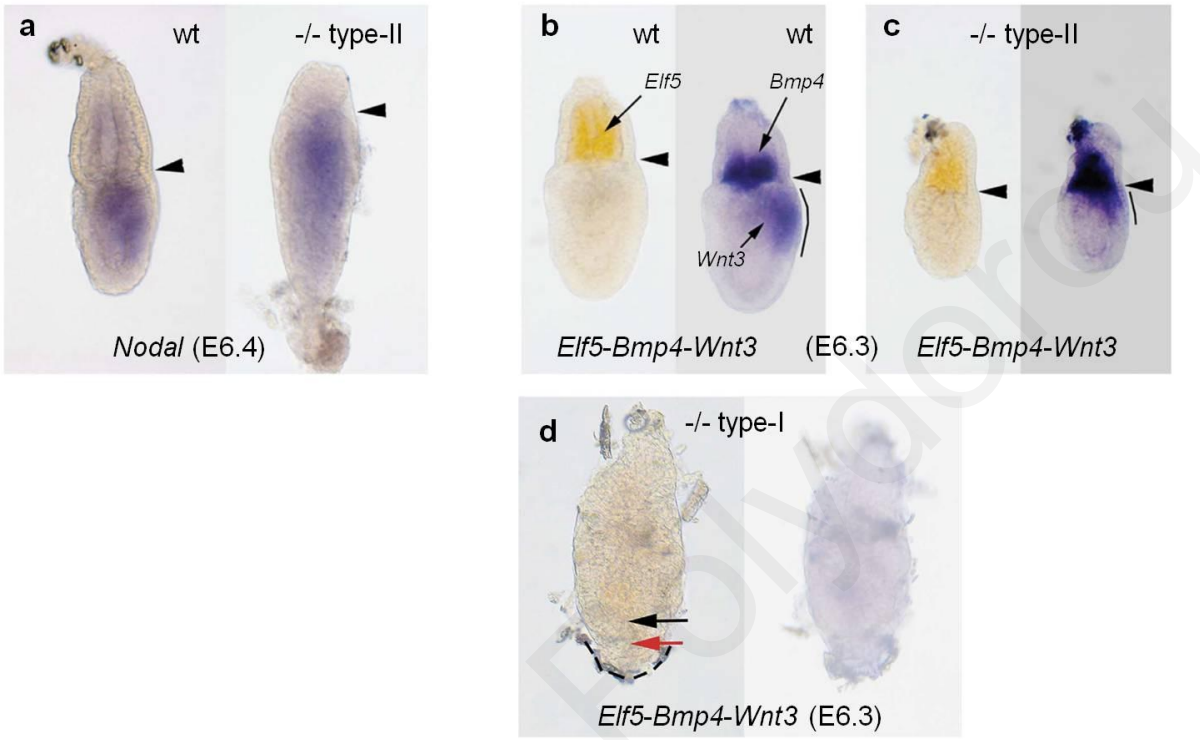

(a) *Nodal* expression in E6.4 controls (left) and *Ets2* type-II mutants (right) showing normal expression levels. (**b-c**) Triple colour whole-mount *in situ* hybridizations were used for *Elf5* (orange colour) and *Bmp4 and Wnt3* (purple colour) expression domains marked in the same embryo. In all panels the right image was taken after *Elf5*, but before *Bmp4* and *Wnt3 in situ* hybridization. (**b**) Control embryos showing the expression of *Elf5* (EXE marker, left panel) and *Bmp4* (EXE marker) and *Wnt3* (posterior epiblast and associated VE marker) at E6.4 stage. (**c**) *Ets2* type-II mutant embryo expressing *Elf5* (orange colour, left panel in b) and *Bmp4* (EXE) and *Wnt3* (posterior epiblast) expression (right panel in b). (**c**) *Wnt3* is expressed in the PS of E6.7 control (left embryo in c), but is absent from the *Ets2* type-II mutant embryo (right embryo in c). **(d)** Double-colour *in situ* hybridization for the expression of *Elf5* (orange), *Bmp4* (blue) and *Wnt3* (blue) at E6.3 in type-I mutants. There is no expression of those genes in the type-I mutants.

The dotted black lines in d showed the abnormally thickened DVE in type-I mutant embryos. The black arrowheads show the embryonic-extraembryonic junction. All the embryos are of the same magnification 10μm.

Figure 25: Real-time PCR (qRT–PCR) gene expression level quantification in E6.7 *Ets2* type-II mutant embryos.

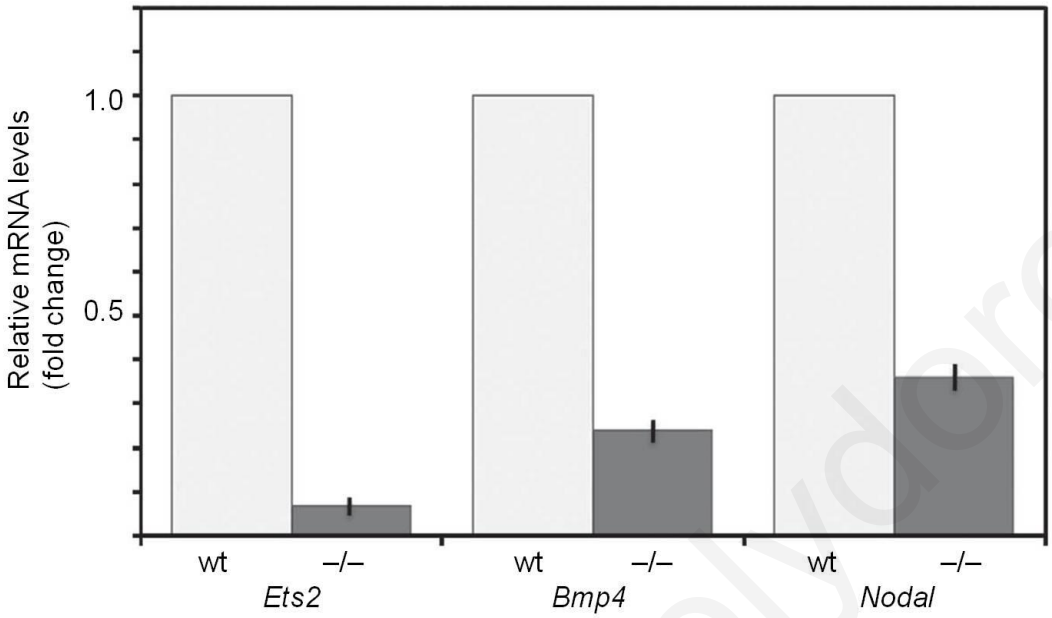

The graph shows the mean values of fold change for *Ets2, Bmp4* and *Nodal* mRNA levels in E6.7 mutants (dark grey columns) relative to those of E6.7 wild-type (wt) control embryos (light-grey columns). Both control and mutant values were relative to those of the internal control gene *beta-actin*, with mutant values representing the fold change relative to that of controls, which was converted to 1. For each gene (n=4; 2 values per embryo from 4 mutants), the mean values in the mutants were 0.07, 0.24 and 0.36 for *Ets2, Bmp4* and *Nodal*, respectively. The s.e.m. is shown by error bars (black lines) and all mutant values represent statistically significant fold changes ($P<0.001$), using the one tailed unpaired Student's t-test.

Chapter 5

DISCUSSION

The main finding of this work is that it demonstrates for the first time that trophoblast signaling in embryo patterning is not only required for primitive streak (PS) and mesoderm formation (that is, gastrulation initiation) *(Donnison, Beaton et al. 2005; Rodriguez, Srinivas et al. 2005; Georgiades and Rossant 2006; Mesnard, Guzman-Ayala et al. 2006*), but also for gastrulation progression after PS initiation and establishes the transcription factor Ets2 as the first gene product required in trophoblast for this novel trophoblastic influence. The gastrulation events that depend on this novel *Ets2*-dependent trophoblast signaling take place between PS initiation (E6.5) and E7.75 (that is, just before the beginning somitogenesis) and include correct gene expression in the early PS, PS elongation, completion of intraembryonic mesoderm epithelial to mesenchymal transition (EMT) and the development of the anterior PS derivatives node, axial anterior mesendoderm (AME) and definitive endoderm (DE). The results of this study also provide evidence (a) for a model about the genetic pathways involved regarding how *Ets2* in trophoblast mediates these gastrulation events within the epiblast (see below), (b) about the timing for the requirement of this *Ets2*-mediated trophoblastic influence (see below).

The results of this work were mainly derived from the study of *Ets2*-/- conceptuses belonging to the type-II phenotype. *Ets2*-/- embryos display two main phenotypes, type-I and type-II (*Georgiades and Rossant 2006*) and both die before mid-gestation, at around E9.0 (*Yamamoto, Flannery et al. 1998; Georgiades and Rossant 2006*). These conceptuses (both type-I and type-II phenotypes), represent an *in vivo* mammalian system for investigating trophoblast-mediated influences on early mouse embryo development. This is because: (a) *Ets2* is exclusively expressed in trophoblast, but not in the other major extraembryonic tissue visceral endoderm (VE) or the epiblast, prior to and during gastrulation, although it appears in the PS by E7.75 (*Yamamoto et al., 1998; Georgiades and Rossant, 2006*). (b) *Ets2*-/- embryos die before mid-gestation (*Yamamoto, Flannery et al. 1998; Georgiades and Rossant 2006*). (c) Chimaeras generated by the aggregation of *Ets2*+/+ tetraploid (4N) embryos (whose cells give rise only to the major extraembryonic tissues trophoblast and VE) with *Ets2* -/- embryonic stem (ES) cells (which exclusively form the epiblast and all its derivatives) resulted in embryos that developed normally and could survive to term (*Yamamoto et al., 1998*). (d) *Ets2*-/- conceptuses also develop normally and survive to term provided they are subjected to *lentivirus*-mediated trophoblast-specific *Ets2* expression from the blastocyst stage (*Yamamoto et al., 1998; Okada et al., 2007*). (e) Chimaeras made in the opposite direction to those just mentioned, that is, aggregation chimaeras using *Ets2*-/- 4N

embryos and *Ets2*+/+ ES cells, phenocopy either the type-I phenotype (no PS formation and absence of AVE), the so-called '*Ets2* type-I chimaera' subset (*Georgiades and Rossant 2006*), or phenocopy the type-II phenotype (defective gastrulation after PS initiation), the so-called '*Ets2* type-II chimaeras' (Georgiades – see 'AIMS' section above)

For this study it was important to distinguish the type-I from the type-II phenotypes of *Ets2-/-* conceptuses because the crosses used here produced both and because this work was predominantly concerned with the type-II phenotype. This work therefore first confirmed the main differences between these two phenotypes. As shown previously, the main embryonic defects of type-I mutants were the absence of gastrulation initiation failure of distal VE (DVE) to shift anteriorly to form AVE so that the entire DVE remains thickened at the distal embryonic tip (based on *Hex* and *Cer* expression which were found to be expressed in the distal tip of the embryo and mark the DVE) (*Georgiades and Rossant 2006*). On the other hand, *Ets2* type-II mutants initiate gastrulation by the early PS stage and form an AVE, thereby having a thin distal tip VE (*Georgiades and Rossant 2006*). These differences were confirmed here in the sense that at gastrulation stages type-II mutants (that is mutants that express PS markers such as *Bra*) do not possess a thick DVE, whereas type-I mutants (that is mutants that do not express PS marker genes) do possess a thick DVE. This thick DVE in type-I mutants was further confirmed here to represent DVE that failed to become AVE, as shown by the distal expression pattern of *Hex* expression (which is a DVE/AVE marker) even at the E7.75 stage, consistent with previous findings (*Georgiades and Rossant, 2006*). These results demonstrate that during gastrulation, one can distinguish type-II from type-I mutants based on morphology (for example, no DVE thickening in type-II mutants) or PS marker gene expression (for example, *Bra* expression in type-II mutants).

Before embarking on the examination of the type-II phenotype (the main topic of this work), this study also examined the following unknown aspects of the type-I phenotype. First, because type-I mutants fail to form a PS or mesoderm (*Georgiades and Rossant 2006*) they would be expected to also lack the other main PS derivatives, node, AME and DE. However, this was not previously explored and was addressed here. Indeed, this study showed that E7.75 type-I mutants (that is mutants without *Bra* expression) also lack node/AME (based on the absence of expression of the node/AME marker *Shh*), as well as DE (as judged by the non-patchy DBA staining pattern throughout their VE). Second, although by the early PS stage type-I mutants are devoid of any PS marker gene expression (i.e. they lack posterior epiblast character) and that of several TS cell self-renewal genes from their EXE such as *Elf5*, it was unknown whether they also lack posterior epiblast character (e.g.

Wnt3 expression) and *Elf5* expression at pregastrulation stages. It is shown here that they also lack these at pregastrulation stages (E6.3). These results therefore: (a) Suggest that type-I mutants (i.e. mutants that fail to form a PS and mesoderm) also lack other PS derivatives (e.g. node, AME and DE) as a secondary consequence of absence of PS formation. (b) Indicate that the defective posterior epiblast character of type-I mutants is not only present by the early PS stage, but also from before PS initiation.

The data here show that *Ets2* is required in trophoblast for the migration of intraembryonic mesoderm away from the PS by mediating the completion of its EMT via a mechanism that involves downregulation of e-cadherin. Evidence is provided suggesting that this trophoblast-mediated mesoderm EMT depends of PS *Snail* expression. This is because *Ets2* type-II mutants showed the following defects: (a) At E7.75 PS mesoderm cells accumulate at the PS with absence of mesenchymal cells posteriorly and anteriorly. (b) Although the PS cells of type-II mutants transform from a columnar to a round shape (indicative of EMT initiation), they fail to become mesenchymal thereby failing to complete their EMT, a process necessary for their migration. (c) e-cadherin, whose downregulation in PS epiblast cells is necessary for their EMT (*Burdsal, Damsky et al. 1993; Zohn, Li et al. 2006*), fails to become downregulated in E7.75 type-II mutants, thereby providing a molecular description of this EMT failure. (d) The expression of *Snail*, which is normally required in the PS for mesoderm EMT via downregulation of E-cadherin, *(Carver, Jiang et al. 2001*) is absent or greatly downregulated in the PS of *Ets2 type-II* mutants at both E6.7 and E7.5. (e) *Cripto*, which is a marker of PS and mesoderm (*Ding, Yang et al. 1998*), is expressed in the round cells that accumulate at the PS of E7.75 type-II mutants, confirming that they represent specified mesoderm.

The findings of this work indicate that in addition to the absence of intraembryonic mesenchymal cells (that is, differentiated intraembryonic mesoderm), type-II mutants also show defective extraembryonic mesoderm development: absence of allantoic mesoderm and reduced formation yolk-sac mesoderm. These results are based on morphological observations and on the absence of expression of *Bmp4* and *Cdx2* (markers of some extraembryonic tissues including the allantois) *(Lawson, Meneses et al. 1991; Winnier, Blessing et al. 1995; Fujiwara, Dehart et al. 2002; Chawengsaksophak, de Graaff et al. 2004*) in the extraembryonic region of these mutants at E7.75. The reason for these extraembryonic mesoderm defects is unclear but they could be related to the above-mentioned mesoderm EMT defect, since both the allantois and yolk-sac mesoderm is derived from the posterior PS, with the former forming early and the latter at a later stage *(Lawson,*

Meneses et al. 1991; Tam and Behringer 1997; Kinder, Tsang et al. 1999; Kinder, Loebel et al. 2001; Robb and Tam 2004)

This work also shows that *Ets2* in trophoblast mediates other fundamental gastrulation events within the epiblast in addition to PS mesoderm EMT. These are PS elongation, formation/specification of node and AME (anterior PS derivatives), as well as the appearance or complete formation of DE (the other major derivative of the anterior PS). Importantly, evidence is presented that these gastrulation events depend on the maintenance of high *Nodal* expression levels in the PS and/or posterior epiblast from around E6.5 onwards. This is based on the following findings: (a) The PS of type-II mutants, as judged by the expression of the PS markers *Bra* and *Cripto* fails to fully extend anteriorly to reach the distal tip of the embryo in all cases examined. (b) E7.5–7.75 type-II mutants lack a morphological node, as well as the expression of the node markers *Noto* (*Abdelkhalek, Beckers et al. 2004*), and *Nodal*, which at this stage is normally not expressed in the PS, but only the peripheral crown cells of the node (*Davidson and Tam 2000; Rob and Tam 2004; Blum et al 2004*) and whose expression in the node is required for node formation (*Beddington and Robertson 1999*). Although co-expression of *Foxa2* and *Bra* at the distal tip of the E7.5 embryo is another molecular marker of the node (*Kinder, Tsang et al. 2001; Burtscher and Lickert 2009*), this expression pattern was not detected in E7.5-E7.75 type-II mutants. These node data, taken together, indicate not only absence of a morphological node, but also failed node cell specification in type-II mutants. AME, which is an axial structure anterior to the node (*Kinder, Tsang et al. 2001*), is incorrectly specified and may be absent from E7.75 type-II mutants based on absence from the anterior half of the embryo of the expression of *Bra*, which marks the entire PS, node and posterior AME by E7.75 (*Herrmann 1999*), as well as that of *Foxa2* and *Shh*, which are markers of node and entire AME by E7.75 (*Kinder, Tsang et al. 2001;* (*Dunn, Vincent et al. 2004*). (d) The DE layer, which normally forms by intercalation of the PS-derived DE cells within the VE layer whose cells spread to allow this intercalation (*Kwon, Viotti et al. 2008; Burtscher and Lickert 2009; McKnight, Hou et al. 2010*) was either absent (in a minority) or present, but at reduced levels in the majority of E7.75 type-II mutants. This is because: (d1) In a minority of these mutants *Gsc* expression, a marker of anterior PS and anterior DE between E6.7 and E7.5 (*Lewis et al., 2006*) was absent, suggesting absence of DE. (d2) DBA lectin staining pattern, a global VE marker not present in DE or epiblast cells (*Tam et al., 1993; Sherwood et al., 2007*) was non-patchy in the VE of a minority of E7.5-7.75 type-II mutants, indicating absence of VE spreading and hence no DE formation. (d3) A patchy DBA lectin staining pattern was

detected in the epiblast-associated VE of most E7.5-7.75 type-II mutants, indicating DE formation, but in the proximal epiblast associated VE this staining was non-patchy, indicating an overall reduced DE formation. (d4) This reduced DE formation in the majority of type-II mutants was confirmed by *Afp* expression, which normally marks the entire epiblast-associated VE and becomes downregulated from those VE cells that experience spreading due to DE intercalation (Kwon, Viotti et al. 2008; Burtscher and Lickert 2009; McKnight, Hou et al. 2010), as *Afp* expression was downregulated in the epiblast-associated VE of type-II mutants except from its most proximal part. (e) *Nodal*, whose high level expression/signaling in the epiblast is required for PS elongation and anterior PS derivative formation (*Carver, Jiang et al. 2001; Dunn, Vincent et al. 2004; Shen 2007*) was expressed at extremely low levels in the PS/epiblast of E6.7 type-II mutants, but at apparently normal levels in their pregastrulation (E6.4) counterparts.

Regarding the localization of AVE, this study demonstrates that *Ets2* in trophoblast is also required for the complete anteriorization of AVE (that is, its localization reaching the most anterior region of the anterior epiblast half), a process probably necessary for the exclusion of posterior epiblast character (e.g. *Bra* and *Cripto* expression) from the anterior-proximal epiblast. This is based on the following. First, *Hex* and *Cer1* expression, which normally exclusively marks the DVE/AVE at E6.7 or earlier, but also the anterior DE after E6.7 (*Thomas et al., 1998; Kinder et al., 2001*), shows that although the AVE forms in all type-II mutants (that is, the AVE does not extend to the distal tip), it fails to reach the anterior-most part of the epiblast in most of them. Second, as the AVE normally inhibits posterior epiblast character from anterior epiblast (*Kimura, Yoshinaga et al. 2000*), this AVE defect could explain the ectopic expression of *Bra* and *Cripto* in the proximal anterior epiblast in 37% of E7.75 type-II mutants. This is because a similar prercentage (44%) of E7.75 type-II mutants fail to show extension of the anterior edge of the AVE into the anterior-most 40% of the anterior epiblast, based on *Hex* and *Cer1* expression patterns. The molecular and cellular basis of this AVE defect is not known, although it could be related to the absence of *Foxh1* expression in the VE, but not the epiblast, of E6.7 type-II mutants, as *Foxh1* is required in the VE, but not in the epiblast, for correct positioning of the AVE (*Yamamoto, Meno et al. 2001*). Further experiments are needed to explore this.

This study provides a molecular explanation within the epiblast that could explain the major gastrulation defects seen in type-II mutants (that is, PS elongation defect, absence of intraembryonic migration due to incomplete mesoderm EMT and failure of anterior PS derivative development). Specifically, the results of this study, combined with previous

findings, suggest that Ets2-mediated trophoblast signaling mediates all these aspects of gastrulation progression by maintaining *Wnt3* expression in posterior epiblast and/or the PS from around E6.5 onwards, which in turn maintains high expression of *Nodal* in the epiblast (for the mediation of PS elongation and anterior PS derivative development –see above) and induces Snail expression in the PS for mesoderm EMT. This scenario is based on the following: (a) *Wnt3* deletion specifically in the epiblast showed that Wnt3 is required in this tissue (but not in the VE) for gastrulation progression after PS initiation in processes that are very similar to those affected in type-II mutants including mesoderm migration away from the PS, PS elongation and anterior PS derivative development (*Tortelote, Hernandez-Hernandez et al. 2013*). (b) *In vivo Wnt3* maintains high levels of *Nodal* expression in the epiblast in a *Foxh1*-independent way (*Ben-Haim, Lu et al. 2006*) (c) *Ex vivo*, *Wnt3* is sufficient for maintaining *Nodal* expression in epiblast explants (*Ben-Haim, Lu et al. 2006*). (d) Experiments with ES cell-derived embryoid bodies showed that *Wnt3* mediates mesoderm EMT by downregulating e-cadherin via upregulation of *Snail* expression (*ten Berge, Koole et al. 2008*). (e) In E6.7 type-II mutants, the low level expression of *Nodal* and the absence of *Snail* expression in their PS/posterior epiblast are associated with absence of *Wnt3* expression (this study). (e) *Nodal* and *Wnt3* expression in type-II mutants is apparently normal at pregastrulation stages (E6.3/E6.4) (this study).

Based on the above, the data presented here together with previous findings suggest that Ets2 in trophoblast mediates the aforementioned gastulation processes by maintaining *Wnt3* expression in the posterior epiblast and/or PS. One obvious question arises: How could the transcription factor Ets2 in trophoblast maintain *Wnt3* expression in the epiblast? An answer could be that *Ets2* in trophoblast is required for maintaining EXE character and the expression of the secreted signaling protein Bmp4, an EXE expressed gene prior to and during the initial stages of gastrulation, via maintaining the EXE expression of *Cdx2*. Evidence in support of this assertion is as follows: (a) *Ets2* in TS cells (the *in vitro* equivalent of EXE) is required for their self-renewal by maintaining the expression of *Cdx2* as it binds directly to its promoter (*Wen, Tynan et al. 2007; Odiatis and Georgiades 2010*) (b) *Cdx2* is required for TS cell self-renewal (*Niwa, Toyooka et al. 2005*) and maintains the expression of *Bmp4* (*Murohashi et al., 2010*) and *Elf5* (*Niwa, Toyooka et al. 2005*) by binding to their promoters in these cells (*Ng et al., 2008; Murohashi et al., 2010*). Moreover it was shown that *Elf5* in TS cells is needed for their self-renewal (*Donnison, Beaton et al. 2005*) and for the maintenance of *Cdx2* and *Eomes* expression, through direct activation of their promoters. (c) *Bmp4*, but not *Nodal*, is sufficient for maintaining *Wnt3* expression in epiblast explants

(*Ben-Haim et al., 2006*). (d) In the EXE of *Ets2* type-II mutants at E6.7, there is an absence or great reduction in the expression levels of *Bmp4* and of the TS cell self-renewal genes *Cdx2, Elf5, Eomes* and *Esrrb* (this study). (e) However, the EXE of type-II mutants at pregastrulation stages (E6.3) shows normal EXE character and *Bmp4* signaling capability, as it expresses *Bmp4* and *Elf5* (this study). This model of how *Ets2* in trophoblast could mediate gastrulation progression within the epiblast is shown diagrammatically (*Fig. 27*).

It must be noted that although this work shows for the first time that trophoblast signaling is required for the progression of gastrulation by mediating gastrulation processes that take place from the time of PS initiation until just before the onset of somitogenesis, previous studies have shown that trophoblast signalling is also required for correct PS development during the early somite stages. This came from the examination and chimaera analysis of a phenotypic subset of *Bmp4* -/- mutant embryos in which gastrulation proceeded normally before somite stages, but by the early somite stage there was abnormal mesodermal cell accumulation at the posterior PS, there was no allantois and the node morphology was abnormal (the ventral surface of the node was flat rather than concave) (*Lawson et al., 1999; Fujiwara et al., 2002*). It was shown that at the early somite stage, *Bmp4* is needed in trophoblast for mesoderm migration away from the posterior PS and this could explain the absence allantois formation in these mutants. Trophoblast-derived *Bmp4* was also responsible for correct node morphology, but it was not clear whether this phenotype was due to defective gastrulation or due to processes within the node, as all node cells correctly formed (*Winnier et al., 1995; Kinder et al., 1999*; *Lawson et al., 1999; Fujiwara et al., 2002*). Interestingly, a different phenotypic subset of *Bmp4*-/- conceptuses was reported to show 'absence of an organized PS' by E7.5 (*Winnier et al., 1995*), suggesting a gastrulation progression defect, chimaera analysis of this subset to exclude a causative role for PS-derived *Bmp4* (*Bmp4* is also expressed in the PS by E7.5) has not been done.

An important question regarding *Ets2*-/- conceptuses is: Why do some of these mutants display the type-I phenotype (that is, no gastrulation initiation due to absence of PS formation) whilst others the type-II phenotype (that is, failure of gastrulation progression after PS initiation)? The answer to this is not known, but this study together with published work on the type-I phenotype (*Georgiades and Rossant, 2006*), suggest an answer, which is as follows. Due to the outbred genetic background (ICR) of *Ets2*-/- conceptuses, there is variability in the response of EXE trophoblast to the loss of *Ets2* in this tissue, so that some (type-I phenotype) loose EXE character and *Bmp4* expression early (from E5.5) and others from around the E6.4-E6.7 period (type-II phenotype). As a result, the early loss of these

trophoblast aspects leads to absence of PS initiation, whereas a later loss leads to PS formation with failure of gastrulation progression. Evidence in support of this is as follows. First, *ex vivo* surgical ablation of EXE trophoblast at E5.5 results in absence of PS formation, whereas when this ablation is done at E6.0, a PS forms (*Georgiades and Rossant 2006*). Second, *Ets2* type-I mutants lack EXE character (*Cdx2* expression) and *Bmp4* expression from at least E5.5 (*Georgiades and Rossant, 2006*). Third, *Ets2 t*ype-II mutants possess EXE character (*Elf5* expression) and *Bmp4* expression at E6.3, but loose both by E6.7 (this study).

Figure 26: Model of *Ets2* action during gastrulation propagation.

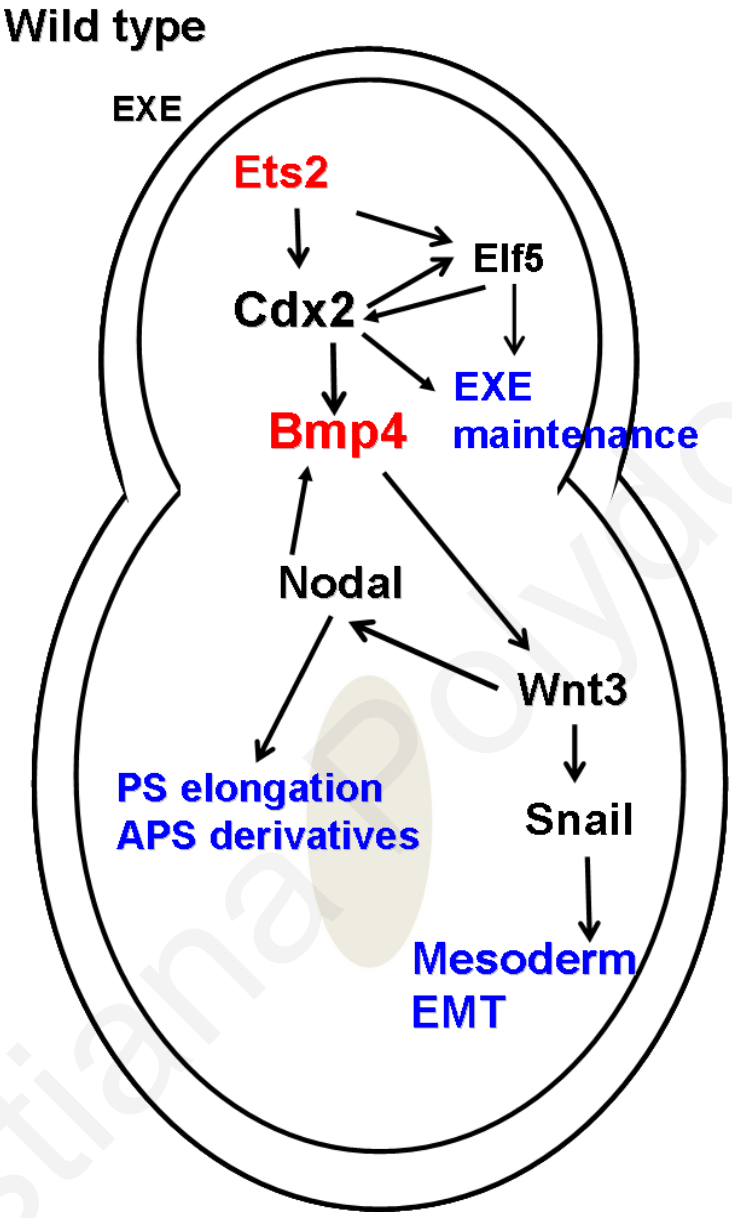

Within the EXE, *Ets2* maintains *Bmp4* expression and EXE character by directly maintaining the expression of *Cdx2*. *Cdx2* in turn conserves the expression of *Bmp4* and *Elf5* with the latter directly reinforcing *Cdx2* expression. Subsequently, EXE-derived *Bmp4* signaling maintains epiblast *Wnt3* expression, which in turn is responsible for two processes. The first is the maintenance of high epiblast *Nodal* expression levels for the mediation of PS elongation and anterior PS derivative development and the second is the induction of *Snail* expression in the PS for completion of mesoderm EMT to allow mesoderm migration.

Future directions

Here in this study we have established new roles for EXE trophoblast signaling which is required for gastrulation propagation soon after PS initiation. More experiments are needed to identify the exact time by which this requirement is needed or how the absence of the *Ets2* in the EXE could be involved in neurulation which took place after gastrulation. At first it will be very interesting to find the exact time by which the EXE trophoblast signaling is required for these processes during gastrulation. To investigate this wild-type (ICR) E6.25, E6.3 and E6.5 mouse conceptuses will be isolated alive using fine-needle micromanipulations followed by culture in rat serum. These conceptuses will be intact (controls) or EXE-ablated. For EXE ablation, conceptuses will be cut along the embryonic-extraembryonic junction using finely pulled glass rods. The EXE ablated embryos will be analyzed then using whole mount RNA *in situ* hybridization for the gene expression of marker genes that their expression in type-II mutants was defective so as to be able to identify whether EXE trophoblast ablations phenocopy the type-II phenotype. Also, it will be useful to find out if the *Bmp4* will rescue the type-II phenotype. This signaling molecule was shown in this study that is unable to maintain *Wnt3* expression which in turn maintains *Nodal* expression in the epiblast, leading to the defects seen during gastrulation propagation in the *Ets2* type-II mutant embryos. Overexpression of *Bmp4 lenti-virus* mediated expression in *Ets2* type-II mutant embryos from blastocyst stage onwards will show if this gene could rescue the type-II phenotype (O*kada, Y., Y. Ueshin, et al. 2007*). Finally it will be exciting to address the neural development in these mutants. In this study we showed that there is no formation of the node and AME in type-II mutant embryos, which in later stages these structures involved in the formation of forebrain, midbrain, hindbrain, and spinal cord and also the AME underlies the neural tissue and is required for its maintenance. So using whole-mount RNA *in situ* hybridization will be analyzed the expression of specification and formation marker genes of these neural structures. This will be of great interest as will underlie for the first time the possible involvement of the EXE trophoblast during neurulation.

References

Abdelkhalek, H. B., A. Beckers, et al. (2004). "The mouse homeobox gene Not is required for caudal notochord development and affected by the truncate mutation." Genes Dev **18**(14): 1725-1736.

Acampora, D., A. Annino, et al. (2005). "Otx genes in the evolution of the vertebrate brain." Brain Res Bull **66**(4-6): 410-420.

Alberts B, Johnson A, Lewis J, et al. (2002) Molecular Biology of the Cell. *4th* edition. Book.

Anderson, R. M., A. R. Lawrence, et al. (2002). "Chordin and noggin promote organizing centers of forebrain development in the mouse." Development **129**(21): 4975-4987.

Ang, S. L., R. A. Conlon, et al. (1994). "Positive and negative signals from mesoderm regulate the expression of mouse Otx2 in ectoderm explants." Development **120**(10): 2979-2989.

Ang, S. L. and J. Rossant (1994). "HNF-3 beta is essential for node and notochord formation in mouse development." Cell **78**(4): 561-574.

Arkell, R. M. and P. P. Tam (2012). "Initiating head development in mouse embryos: integrating signalling and transcriptional activity." Open Biol **2**(3): 120030.

Arnold, S. J., U. K. Hofmann, et al. (2008). "Pivotal roles for eomesodermin during axis formation, epithelium-to-mesenchyme transition and endoderm specification in the mouse." Development **135**(3): 501-511.

Arnold, S. J. and E. J. Robertson (2009). "Making a commitment: cell lineage allocation and axis patterning in the early mouse embryo." Nat Rev Mol Cell Biol **10**(2): 91-103.

Ashe, H. L. and J. Briscoe (2006). "The interpretation of morphogen gradients." Development **133**(3): 385-394.

Bachiller, D., J. Klingensmith, et al. (2000). "The organizer factors Chordin and Noggin are required for mouse forebrain development." Nature **403**(6770): 658-661.

Beck, S., J. A. Le Good, et al. (2002). "Extraembryonic proteases regulate Nodal signalling during gastrulation." Nat Cell Biol **4**(12): 981-985.

Beckers, A., L. Alten, et al. (2007). "The mouse homeobox gene Noto regulates node morphogenesis, notochordal ciliogenesis, and left right patterning." Proc Natl Acad Sci U S A **104**(40): 15765-15770.

Beddington, R. S. (1994). "Induction of a second neural axis by the mouse node." Development **120**(3): 613-620.

Ben-Haim, N., C. Lu, et al. (2006). "The nodal precursor acting via activin receptors induces mesoderm by maintaining a source of its convertases and BMP4." Dev Cell **11**(3): 313-323.

Bielinska, M., N. Narita, et al. (1999). "Distinct roles for visceral endoderm during embryonic mouse development." Int J Dev Biol **43**(3): 183-205.

Blum, M., P. Andre, et al. (2007). "Ciliation and gene expression distinguish between node and posterior notochord in the mammalian embryo." Differentiation **75**(2): 133-146.

Blum, M., S. J. Gaunt, et al. (1992). "Gastrulation in the mouse: the role of the homeobox gene goosecoid." Cell **69**(7): 1097-1106.

Boucher, D. M. and R. A. Pedersen (1996). "Induction and differentiation of extra-embryonic mesoderm in the mouse." Reprod Fertil Dev **8**(4): 765-777.

Brennan, J., C. C. Lu, et al. (2001). "Nodal signalling in the epiblast patterns the early mouse embryo." Nature **411**(6840): 965-969.

Brennan, J., D. P. Norris, et al. (2002). "Nodal activity in the node governs left-right asymmetry." Genes Dev **16**(18): 2339-2344.

Brunner, D., K. Ducker, et al. (1994). "The ETS domain protein pointed-P2 is a target of MAP kinase in the sevenless signal transduction pathway." Nature **370**(6488): 386-389.

Burdsal, C. A., C. H. Damsky, et al. (1993). "The role of E-cadherin and integrins in mesoderm differentiation and migration at the mammalian primitive streak." Development **118**(3): 829-844.

Burtscher, I. and H. Lickert (2009). "Foxa2 regulates polarity and epithelialization in the endoderm germ layer of the mouse embryo." Development **136**(6): 1029-1038.

Camus, A., B. P. Davidson, et al. (2000). "The morphogenetic role of midline mesendoderm and ectoderm in the development of the forebrain and the midbrain of the mouse embryo." Development **127**(9): 1799-1813.

Carver, E. A., R. Jiang, et al. (2001). "The mouse snail gene encodes a key regulator of the epithelial-mesenchymal transition." Mol Cell Biol **21**(23): 8184-8188.

Chawengsaksophak, K., W. de Graaff, et al. (2004). "Cdx2 is essential for axial elongation in mouse development." Proc Natl Acad Sci U S A **101**(20): 7641-7645.

Chiang, C., Y. Litingtung, et al. (1996). "Cyclopia and defective axial patterning in mice lacking Sonic hedgehog gene function." Nature **383**(6599): 407-413.

Chu, J., J. Ding, et al. (2005). "Non-cell-autonomous role for Cripto in axial midline formation during vertebrate embryogenesis." Development **132**(24): 5539-5551.

Ciruna, B. G. and J. Rossant (1999). "Expression of the T-box gene Eomesodermin during early mouse development." Mech Dev **81**(1-2): 199-203.

Conlon, F. L., K. M. Lyons, et al. (1994). "A primary requirement for nodal in the formation and maintenance of the primitive streak in the mouse." Development **120**(7): 1919-1928.

Copp, A. J., N. D. Greene, et al. (2003). "The genetic basis of mammalian neurulation." Nat Rev Genet **4**(10): 784-793.

Davidson, B. P. and P. P. Tam (2000). "The node of the mouse embryo." Curr Biol **10**(17): R617-619.

Ding, J., L. Yang, et al. (1998). "Cripto is required for correct orientation of the anterior-posterior axis in the mouse embryo." Nature **395**(6703): 702-707.

Donnison, M., A. Beaton, et al. (2005). "Loss of the extraembryonic ectoderm in Elf5 mutants leads to defects in embryonic patterning." Development **132**(10): 2299-2308.

Dufort, D., L. Schwartz, et al. (1998). "The transcription factor HNF3beta is required in visceral endoderm for normal primitive streak morphogenesis." Development **125**(16): 3015-3025.

Dunn, N. R., S. D. Vincent, et al. (2004). "Combinatorial activities of Smad2 and Smad3 regulate mesoderm formation and patterning in the mouse embryo." Development **131**(8): 1717-1728.

Fujiwara, T., D. B. Dehart, et al. (2002). "Distinct requirements for extra-embryonic and embryonic bone morphogenetic protein 4 in the formation of the node and primitive streak and coordination of left-right asymmetry in the mouse." Development **129**(20): 4685-4696.

Georgiades, P., A. C. Ferguson-Smith, et al. (2002). "Comparative developmental anatomy of the murine and human definitive placentae." Placenta **23**(1): 3-19.

Georgiades, P. and J. Rossant (2006). "Ets2 is necessary in trophoblast for normal embryonic anteroposterior axis development." Development **133**(6): 1059-1068.

Grapin-Botton, A. and D. A. Melton (2000). "Endoderm development: from patterning to organogenesis." Trends Genet **16**(3): 124-130.

Hay, E. D. (2005). "The mesenchymal cell, its role in the embryo, and the remarkable signaling mechanisms that create it." Dev Dyn **233**(3): 706-720.

Herrmann, B. G. (1991). "Expression pattern of the Brachyury gene in whole-mount TWis/TWis mutant embryos." Development **113**(3): 913-917.

Hoodless, P. A., M. Pye, et al. (2001). "FoxH1 (Fast) functions to specify the anterior primitive streak in the mouse." Genes Dev **15**(10): 1257-1271.

Kalluri, R. and R. A. Weinberg (2009). "The basics of epithelial-mesenchymal transition." J Clin Invest **119**(6): 1420-1428.

Kelly, O. G., K. I. Pinson, et al. (2004). "The Wnt co-receptors Lrp5 and Lrp6 are essential for gastrulation in mice." Development **131**(12): 2803-2815.

Kidder, B. L. and S. Palmer (2010). "Examination of transcriptional networks reveals an important role for TCFAP2C, SMARCA4, and EOMES in trophoblast stem cell maintenance." Genome Res **20**(4): 458-472.

Kilpatrick, L. M., I. Kola, et al. (1999). "Transcription factors Ets1, Ets2, and Elf1 exhibit differential localization in human endometrium across the menstrual cycle and alternate isoforms in cultured endometrial cells." Biol Reprod **61**(1): 120-126.

Kimura, C., K. Yoshinaga, et al. (2000). "Visceral endoderm mediates forebrain development by suppressing posteriorizing signals." Dev Biol **225**(2): 304-321.

Kinder, S. J., D. A. Loebel, et al. (2001). "Allocation and early differentiation of cardiovascular progenitors in the mouse embryo." Trends Cardiovasc Med **11**(5): 177-184.

Kinder, S. J., T. E. Tsang, et al. (1999). "The orderly allocation of mesodermal cells to the extraembryonic structures and the anteroposterior axis during gastrulation of the mouse embryo." Development **126**(21): 4691-4701.

Kinder, S. J., T. E. Tsang, et al. (2001). "The organizer of the mouse gastrula is composed of a dynamic population of progenitor cells for the axial mesoderm." Development **128**(18): 3623-3634.

Kwon, G. S., M. Viotti, et al. (2008). "The endoderm of the mouse embryo arises by dynamic widespread intercalation of embryonic and extraembryonic lineages." Dev Cell **15**(4): 509-520.

Lawson, K. A., J. J. Meneses, et al. (1991). "Clonal analysis of epiblast fate during germ layer formation in the mouse embryo." Development **113**(3): 891-911.

Lawson, K. A. and R. A. Pedersen (1987). "Cell fate, morphogenetic movement and population kinetics of embryonic endoderm at the time of germ layer formation in the mouse." Development **101**(3): 627-652.

Lee, J. D. and K. V. Anderson (2008). "Morphogenesis of the node and notochord: the cellular basis for the establishment and maintenance of left-right asymmetry in the mouse." Dev Dyn **237**(12): 3464-3476.

Leprince, D., A. Gegonne, et al. (1983). "A putative second cell-derived oncogene of the avian leukaemia retrovirus E26." Nature **306**(5941): 395-397.

Lewis, S. L., P. L. Khoo, et al. (2007). "Genetic interaction of Gsc and Dkk1 in head morphogenesis of the mouse." Mech Dev **124**(2): 157-165.

Liu, P., M. Wakamiya, et al. (1999). "Requirement for Wnt3 in vertebrate axis formation." Nat Genet **22**(4): 361-365.

Livak, K. J. and T. D. Schmittgen (2001). "Analysis of relative gene expression data using real-time quantitative PCR and the 2(-Delta Delta C(T)) Method." Methods **25**(4): 402-408.

Lu, C. C., J. Brennan, et al. (2001). "From fertilization to gastrulation: axis formation in the mouse embryo." Curr Opin Genet Dev **11**(4): 384-392.

Maroulakou, I. G. and D. B. Bowe (2000). "Expression and function of Ets transcription factors in mammalian development: a regulatory network." Oncogene **19**(55): 6432-6442.

Maroulakou, I. G., T. S. Papas, et al. (1994). "Differential expression of ets-1 and ets-2 proto-oncogenes during murine embryogenesis." Oncogene **9**(6): 1551-1565.

Martinez Barbera, J. P., M. Clements, et al. (2000). "The homeobox gene Hex is required in definitive endodermal tissues for normal forebrain, liver and thyroid formation." Development **127**(11): 2433-2445.

McKnight, K. D., J. Hou, et al. (2010). "Foxh1 and Foxa2 are not required for formation of the midgut and hindgut definitive endoderm." Dev Biol **337**(2): 471-481.

Mesnard, D., M. Guzman-Ayala, et al. (2006). "Nodal specifies embryonic visceral endoderm and sustains pluripotent cells in the epiblast before overt axial patterning." Development **133**(13): 2497-2505.

Murohashi, M., T. Nakamura, et al. (2010). "An FGF4-FRS2alpha-Cdx2 axis in trophoblast stem cells induces Bmp4 to regulate proper growth of early mouse embryos." Stem Cells **28**(1): 113-121.

Nagy A., Manipulating the mouse embryo. 2003 Book.

Ng, R. K., W. Dean, et al. (2008). "Epigenetic restriction of embryonic cell lineage fate by methylation of Elf5." Nat Cell Biol **10**(11): 1280-1290.

Niwa, H., Y. Toyooka, et al. (2005). "Interaction between Oct3/4 and Cdx2 determines trophectoderm differentiation." Cell **123**(5): 917-929.

Norris, D. P., J. Brennan, et al. (2002). "The Foxh1-dependent autoregulatory enhancer controls the level of Nodal signals in the mouse embryo." Development **129**(14): 3455-3468.

Odiatis, C. and P. Georgiades (2010). "New insights for Ets2 function in trophoblast using lentivirus-mediated gene knockdown in trophoblast stem cells." Placenta **31**(7): 630-640.

Okada, Y., Y. Ueshin, et al. (2007). "Complementation of placental defects and embryonic lethality by trophoblast-specific lentiviral gene transfer." Nat Biotechnol **25**(2): 233-237.

Papas, T. S., R. J. Fisher, et al. (1989). "The ets family of genes: molecular biology and functional implications." Curr Top Microbiol Immunol **149**: 143-147.

Perea-Gomez, A., M. Rhinn, et al. (2001). "Role of the anterior visceral endoderm in restricting posterior signals in the mouse embryo." Int J Dev Biol **45**(1): 311-320.

Perea-Gomez, A., F. D. Vella, et al. (2002). "Nodal antagonists in the anterior visceral endoderm prevent the formation of multiple primitive streaks." Dev Cell **3**(5): 745-756.

Pfister, S., K. A. Steiner, et al. (2007). "Gene expression pattern and progression of embryogenesis in the immediate post-implantation period of mouse development." Gene Expr Patterns **7**(5): 558-573.

Rivera-Perez, J. A., J. Mager, et al. (2003). "Dynamic morphogenetic events characterize the mouse visceral endoderm." Dev Biol **261**(2): 470-487.

Robb, L. and P. P. Tam (2004). "Gastrula organiser and embryonic patterning in the mouse." Semin Cell Dev Biol **15**(5): 543-554.

Rodriguez, T. A., S. Srinivas, et al. (2005). "Induction and migration of the anterior visceral endoderm is regulated by the extra-embryonic ectoderm." Development **132**(11): 2513-2520.

Rossant, J. and P. P. Tam (2009). "Blastocyst lineage formation, early embryonic asymmetries and axis patterning in the mouse." Development **136**(5): 701-713.

Saijoh, Y., H. Adachi, et al. (2000). "Left-right asymmetric expression of lefty2 and nodal is induced by a signaling pathway that includes the transcription factor FAST2." Mol Cell **5**(1): 35-47.

Sharrocks, A. D. (2001). "The ETS-domain transcription factor family." Nat Rev Mol Cell Biol **2**(11): 827-837.

Sharrocks, A. D., A. L. Brown, et al. (1997). "The ETS-domain transcription factor family." Int J Biochem Cell Biol **29**(12): 1371-1387.

Shawlot, W., J. M. Deng, et al. (1998). "Expression of the mouse cerberus-related gene, Cerr1, suggests a role in anterior neural induction and somitogenesis." Proc Natl Acad Sci U S A **95**(11): 6198-6203.

Shen, M. M. (2007). "Nodal signaling: developmental roles and regulation." Development **134**(6): 1023-1034.

Sherwood, R. I., C. Jitianu, et al. (2007). "Prospective isolation and global gene expression analysis of definitive and visceral endoderm." Dev Biol **304**(2): 541-555.

Shook, D. and R. Keller (2003). "Mechanisms, mechanics and function of epithelial-mesenchymal transitions in early development." Mech Dev **120**(11): 1351-1383.

Srinivas, S., T. Rodriguez, et al. (2004). "Active cell migration drives the unilateral movements of the anterior visceral endoderm." Development **131**(5): 1157-1164.

Stern (2004). Gastrulation From Cells to Embryo. Cold Spring Harbor, New York, Cold Spring Harbor Laboratory Press.

Stuckey, D. W., A. Di Gregorio, et al. (2011). "Correct patterning of the primitive streak requires the anterior visceral endoderm." PLoS One **6**(3): e17620.

Sulik, K., D. B. Dehart, et al. (1994). "Morphogenesis of the murine node and notochordal plate." Dev Dyn **201**(3): 260-278.

Sun, X., E. N. Meyers, et al. (1999). "Targeted disruption of Fgf8 causes failure of cell migration in the gastrulating mouse embryo." Genes Dev **13**(14): 1834-1846.

Takaoka, K. and H. Hamada (2012). "Cell fate decisions and axis determination in the early mouse embryo." Development **139**(1): 3-14.

Tam, P. P. and R. S. Beddington (1992). "Establishment and organization of germ layers in the gastrulating mouse embryo." Ciba Found Symp **165**: 27-41; discussion 42-29.

Tam, P. P. and R. R. Behringer (1997). "Mouse gastrulation: the formation of a mammalian body plan." Mech Dev **68**(1-2): 3-25.

Tam, P. P. and D. A. Loebel (2007). "Gene function in mouse embryogenesis: get set for gastrulation." Nat Rev Genet **8**(5): 368-381.

Tam, P. P., E. A. Williams, et al. (1993). "Gastrulation in the mouse embryo: ultrastructural and molecular aspects of germ layer morphogenesis." Microsc Res Tech **26**(4): 301-328.

Tanaka, S., T. Kunath, et al. (1998). "Promotion of trophoblast stem cell proliferation by FGF4." Science **282**(5396): 2072-2075.

ten Berge, D., W. Koole, et al. (2008). "Wnt signaling mediates self-organization and axis formation in embryoid bodies." Cell Stem Cell **3**(5): 508-518.

Thomas, P. and R. Beddington (1996). "Anterior primitive endoderm may be responsible for patterning the anterior neural plate in the mouse embryo." Curr Biol **6**(11): 1487-1496.

Thomas, P. Q., A. Brown, et al. (1998). "Hex: a homeobox gene revealing peri-implantation asymmetry in the mouse embryo and an early transient marker of endothelial cell precursors." Development **125**(1): 85-94.

Tortelote, G. G., J. M. Hernandez-Hernandez, et al. (2013). "Wnt3 function in the epiblast is required for the maintenance but not the initiation of gastrulation in mice." Dev Biol **374**(1): 164-173.

Tremblay, G. B., T. Kunath, et al. (2001). "Diethylstilbestrol regulates trophoblast stem cell differentiation as a ligand of orphan nuclear receptor ERR beta." Genes Dev **15**(7): 833-838.

Vincent, S. D., N. R. Dunn, et al. (2003). "Cell fate decisions within the mouse organizer are governed by graded Nodal signals." Genes Dev **17**(13): 1646-1662.

Wasylyk, B., J. Hagman, et al. (1998). "Ets transcription factors: nuclear effectors of the Ras-MAP-kinase signaling pathway." Trends Biochem Sci **23**(6): 213-216.

Wasylyk, B., S. L. Hahn, et al. (1993). "The Ets family of transcription factors." Eur J Biochem **211**(1-2): 7-18.

Wasylyk, C. and B. Wasylyk (1993). "Oncogenic conversion of Ets affects redox regulation in-vivo and in-vitro." Nucleic Acids Res **21**(3): 523-529.

Weinstein, D. C., A. Ruiz i Altaba, et al. (1994). "The winged-helix transcription factor HNF-3 beta is required for notochord development in the mouse embryo." Cell **78**(4): 575-588.

Weisberg, E., G. E. Winnier, et al. (1998). "A mouse homologue of FAST-1 transduces TGF beta superfamily signals and is expressed during early embryogenesis." Mech Dev **79**(1-2): 17-27.

Wen, F., J. A. Tynan, et al. (2007). "Ets2 is required for trophoblast stem cell self-renewal." Dev Biol **312**(1): 284-299.

Williams, M., C. Burdsal, et al. (2012). "Mouse primitive streak forms in situ by initiation of epithelial to mesenchymal transition without migration of a cell population." Dev Dyn **241**(2): 270-283.

Winnier, G., M. Blessing, et al. (1995). "Bone morphogenetic protein-4 is required for mesoderm formation and patterning in the mouse." Genes Dev **9**(17): 2105-2116.

Yamamoto, H., M. L. Flannery, et al. (1998). "Defective trophoblast function in mice with a targeted mutation of Ets2." Genes Dev **12**(9): 1315-1326.

Yamamoto, M., C. Meno, et al. (2001). "The transcription factor FoxH1 (FAST) mediates Nodal signaling during anterior-posterior patterning and node formation in the mouse." Genes Dev **15**(10): 1242-1256.

Yamanaka, Y., O. J. Tamplin, et al. (2007). "Live imaging and genetic analysis of mouse notochord formation reveals regional morphogenetic mechanisms." Dev Cell **13**(6): 884-896.

Zohn, I. E., Y. Li, et al. (2006). "p38 and a p38-interacting protein are critical for downregulation of E-cadherin during mouse gastrulation." Cell **125**(5): 957-969.

Publication

Polydorou, C. & Georgiades, P. *Ets2*-dependent trophoblast signalling is required for gastrulation progression after primitive streak initiation. Nat. Commun. 4:1658 doi: 10.1038/ncomms2646 (2013).